



Ahmet Refah Torun

## **Advanced manufacturing technology for 3D profiled woven preforms**

Dissertation



# **Advanced Manufacturing Technology for 3D Profiled Woven Preforms**

Von der Fakultät Maschinenwesen  
der

Technischen Universität Dresden

zur

Erlangung des akademischen Grades

Doktoringenieur (Dr.-Ing.)

angenommene Dissertation

M. Sc. Dipl.-Wirt. Ing. Ahmet Refah Torun

geb. am 26.10.1979 in Adana, Türkei

Tag der Einreichung: 29.04.2011

Tag der Verteidigung: 04.07.2011

Gutachter:

Prof. Dr.-Ing. habil. Dipl.-Wirt. Ing. Chokri Cherif

Prof. Dr.-Ing. Frank Ficker



## Acknowledgments

I owe my deepest gratitude to my supervisor, Prof. Dr.-Ing. habil. Dipl.-Wirt. Ing. Chokri Cherif, whose encouragement, supervision and support from the very beginning enabled this dissertation. I appreciate his vast knowledge and skills in many areas. His insight, invaluable ideas and comments have had a significant contribution to find my way both in research and in life.

I want to express my sincere gratitude to Prof. Dr.-Ing. Frank Ficker, for accepting to referee this dissertation.

I am indebted to Prof. Dr.-Ing. habil. Hartmut Rödel for his friendly support during my studies.

I am heartily thankful to Prof. Dr. Hiroyuki Hamada for his invaluable advices. He and Dr. Asami Nakai have given me great motivation and support during my research activities at the Kyoto Institute of Technology.

Meeting Prof. Dr. Ali Demir is one of the best things that happened to me. He is a great role model as a scientist and human. In such a hard time when everyone was gone away, he gave me encouragement to continue which have practically saved my life. He had convinced me in 2002 to start doing research without being affected by mental, cultural or geographical borders. In all those years, he provided me with direction and became more of a mentor than a professor.

I would like to express my sincere appreciation to Dr.-Ing. Gerald Hoffmann. He was officially research group leader but he was more like a father for me. Gerald has deep knowledge and interest both in technical challenges and psychology. He provided excellent guidance and still high amount of freedom to solve the problems, which was the most valuable learning process.

It was a great chance to cooperate with Dr.-Ing Andreas Mühl. He is an excellent researcher with a positive personality. I am very thankful for his advices and encouragement.

I appreciate the cooperation and friendship of Adil Mountasir at TU Dresden and Özgür Demircan at Kyoto Institute of Technology. I wish, together we will make significant contributions to engineering research.

I am grateful to Müslüm Kaplan and Recep Türkay Kocaman for their friendship and continuing help. My cousin Mehmet Berat Gök has always been beside me with his support in various subjects.

I would like to thank sincerely Mr. Dominique Maes and Mr. Luc Coenegracht of the company Van de Wiele for their continuous support and for their friendly approach.

I would like to express my sincere gratitude to German Research Foundation for the financial support of the collaborative research activities SFB 639, in particular the subprojects A3 and A4.

I am so much indebted to my parents Fatma Torun and Adil Torun. They do not really accept verbal or written sentences as an expression of my gratitude. For them research is the best way to serve humanity and to pray to God. They give me only one way to thank them: I have to continue and improve my research, encourage and support younger scientist. Promise, I will do my best!

To Kiyoko who can change nightmares into beautiful dreams...

Dresden, 29.04.2011

Ahmet Refah Torun

## Table of Contents

Symbols and Abbreviations .....	iii
Chapter 1 - Introduction .....	1
Chapter 2 - State of the Art and Aim.....	3
2.1 Composite Structures .....	3
2.1.1 Manufacturing Aspects .....	5
2.1.2 Advantages of Fiber Reinforcements.....	6
2.1.3 Matrices .....	9
2.2 Textile Preforms .....	10
2.3 Spacer Fabrics .....	14
2.3.1 Conventional Spacer Fabrics.....	14
2.3.2 Spacer Fabrics with Fabric Cross-links.....	16
2.4 Composite Stiffener Structures.....	19
2.5 Hybrid Yarns.....	20
2.6 Aim of the Thesis.....	22
Chapter 3 - Mathematical Treatment of 3D Woven Structures .....	24
3.1 Representation of Multi-layer Woven Fabrics.....	25
3.2 Alternative Ways of Weave Representation .....	27
3.3 Conclusion.....	38
Chapter 4 - Weaveability of Commingled Hybrid Yarns.....	40
4.1 Experimental .....	42
4.1.1 Materials .....	42
4.1.2 Testing Procedure.....	43
4.2 Results and Discussion .....	44
4.2.1 Commingled Yarn Structure.....	44
4.2.2 Commingled Yarn Friction Properties .....	47

---

4.2.3	Yarn Mechanical Properties .....	48
4.2.4	UD-Composite Properties .....	55
4.3	Conclusion.....	60
Chapter 5 - Mechanical Characterization of 2D Woven Preforms and Composite Panels from GF/PP Hybrid Yarn .....		62
5.1	Experimental .....	63
5.1.1	Materials .....	63
5.1.2	Testing procedure .....	63
5.2	Results and Discussions .....	64
5.3	Conclusion.....	70
Chapter 6 - Principals of Spacer Fabric Production.....		71
6.1	Terry Weaving Technology.....	71
6.2	U-shaped Spacer Fabrics.....	74
6.3	X-shaped Spacer Fabrics .....	78
6.4	V-shaped Spacer Fabrics .....	80
Chapter 7 - Production Principals of Complex Spacer Structures and Stiffeners .....		85
7.1	Variations of X-shaped Spacer Fabrics .....	86
7.2	Preforms for Panels with Integrated Stiffeners .....	87
Chapter 8 - Modifications and Realization of Spacer Fabric Weaving Technology... ..		94
8.1	Terry Weaving Mechanism.....	94
8.2	Linear Take-up System with Cutting and Laying Mechanism .....	96
8.3	Spacer Fabric Production .....	98
Chapter 9 – Conclusion and Outlook.....		101
Appendix: Advantage of Sandwich Materials.....		104
List of Figures .....		106
List of Tables .....		110
Bibliography.....		111

## Symbols and Abbreviations

Symbol	Dimension	Designation
[Q]	GPa	Stiffness matrix
[Q']	GPa	Reduced stiffness matrix
{ $\epsilon$ }	–	Strain tensor
{ $\sigma$ }	GPa	Stress tensor
2D	–	Two dimensional
3D	–	Three dimensional
A	mm <sup>2</sup>	Cross-sectional area of element
A <sub>1</sub>	mm <sup>2</sup>	Interface area
A <sub>2</sub>	mm <sup>2</sup>	New interface area
ASTM	–	American society for testing and materials
B	–	Base fabrics
B.C.	–	Before Christ
c	–	Number of lines
C	–	Connection section of floating yarns to fabric
CAD	–	Computer aided design
CAM	–	Computer aided manufacturing
CCD	–	Charge coupled device



Symbol	Dimension	Designation
D	mm	Fiber diameter
d	mm	Smaller fiber diameter
$d_{av}$	mm	Average yarn diameter
DIN	–	Deutsches Institut für Normung (German Institute for Standardization)
$D_r$	–	Damage factor of twist angle
E	GPa	Tensile modulus
e.g.	–	Exempli gratia (for example)
$E_1$	GPa	Tensile modulus of element 1
$E_2$	GPa	Tensile modulus of element 2
$E_L$	GPa	Tensile modulus in fiber direction (longitudinal)
$E_{Lf}$	GPa	Tensile modulus of fiber (longitudinal)
$E_m$	GPa	Tensile modulus of matrix
$E_{m1}$	GPa	Tensile modulus of matrix element 1
$E_{m2}$	GPa	Tensile modulus of matrix element 2
EN	–	European standards
$E_{r1}$	GPa	Tensile modulus of reinforcement element 1
$E_{r2}$	GPa	Tensile modulus of reinforcement element 2
$E_{re}$	GPa	Tensile modulus reduced after twisting

---

Symbol	Dimension	Designation
$E_T$	GPa	Transverse modulus
$E_{Tf}$	GPa	Transverse modulus of fibers
$E_x$	GPa	Modulus in the arbitrary x direction
$E_y$	GPa	Modulus in the arbitrary y direction
$E_z$	GPa	Tensile modulus before twisting
F	–	Floating warp yarns
$G_{12}$	GPa	In-plane shear modulus
$G_{12f}$	GPa	In-plane shear modulus of fiber
GF	–	Glass fiber
$G_m$	GPa	Shear modulus of matrix
H	cm	Distance between the horizontal position and the maximum height of eyelet
I	mm <sup>4</sup>	Second moment of area
ILK	–	Institute of Lightweight Engineering and Plastic Technology at Dresden University of Technology
ISO	–	International organization for standardization
ITM	–	Institute of Textile Machinery and High Performance Material Technology at Dresden University of Technology
IWM	–	Institute of Machine Tools and Control Engineering at Dresden University of Technology

Symbol	Dimension	Designation
k	N/mm	Overall spring stiffness
$k_1$	N/mm	Spring stiffness of element 1
$k_2$	N/mm	Spring stiffness of element 2
L	mm	Fiber length
$L_1$	mm	Length of element 1
$L_2$	mm	Length of element 2
$L_i$	–	Representative length of element I
M	Nmm	Moment
N	–	Number of fibers
n	–	Number of warp yarns
$n_{new}$	–	New number of fibers
NC	–	Number of cycles for warp yarns to pass through the heddle frames
OD	%	Over-delivery
OPP	–	Overall possibilities of patterns
PEEK	–	Polyetheretherketon
PES	–	Polyester
PET	–	Polyethylenterephthalat
PP	–	Polypropylene
Prepreg	–	Preimpregnated fibers

Symbol	Dimension	Designation
r	–	Number of columns
R	–	Reed
RTM	–	Resin transfer molding
S	–	Stiffener fabric
$S_i$	m/min	Input speed of feeding
SP	–	Number of possible structures
$S_o$	m/min	Output speed of take-up
SW	–	Number of woven structures
T	–	Regular take-up motion
TD	cm	Travel distance of warp yarn in one machine revolution
tw	Twist per meter	Twist
TW	–	Terry weaving take-up motion
UD	–	Uni-directional
US	–	Ultrasonic
v	mm	Deflection of the central line of a beam
$V_f$	–	Volume fraction of reinforcing material
WD	Yarn/cm	Weft density
x	mm	Coordinate along the length of a beam
X	cm	Distance from fabric to horizontal position of eyelet

---

Symbol	Dimension	Designation
$\alpha_{od}$	degree	Equivalent angle of distortion of over-delivery
$\alpha_{od_i}$	degree	Equivalent angle of distortion of over-delivery, element I
$\alpha_t$	degree	Total twist angle
$\alpha_{tw}$	degree	Twist angle
$\Delta X$	cm	Travelling distance through eyelet
$\eta$	–	Correction factor for transverse modulus
$\eta'$	–	Correction factor for in-plane shear modulus
$\theta$	degree	Angle of distortion
$\nu_{12}$	–	Poisson's ratio
$\nu_{12f}$	–	Poisson's ratio of fibers
$\nu_m$	–	Poisson's ratio of matrix
$\pi$	–	The number Pi

## Chapter 1 - Introduction

From a historical point of view past civilizations were named according to the most advanced materials of their time such as stone, bronze and iron ages. The advancement of the materials was up to a high extent also determining the advancement of the human societies. Intelligent engineering design has evolved to enable the construction of very complex structures with conventional materials. However, the limits of materials are still defining the limits of engineering and feasible technologies [1].

In ancient times metals had little importance whereas natural polymers, composites and ceramics were often used. Afterwards, the skills and construction with metals led the big achievements into the mid of 20<sup>th</sup> century. However in the mid 20<sup>th</sup> century, polymers, composites and ceramics regained their importance as high-end engineering materials [1].

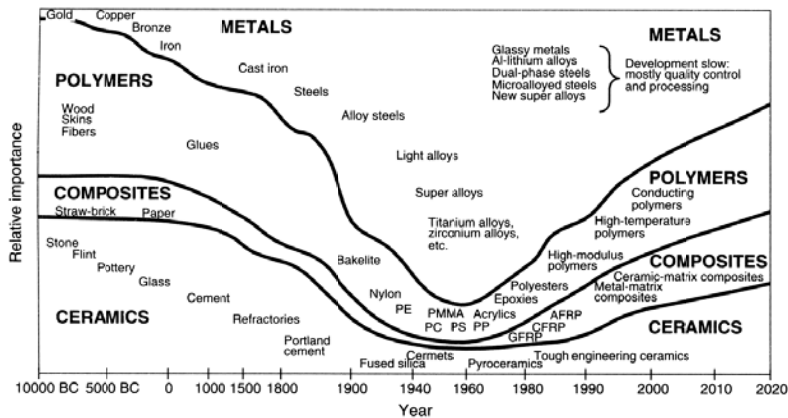


Figure 1: Schematic of the evolution of engineering materials [1]

After 1950s, polymer composites emerged from being exotic niche applications to common engineering materials. Today polymer composites are widely used in aircraft, helicopters, space-craft, satellites, ships, submarines, automobiles, processing equipment, sporting goods and civil engineering applications [2]. There are still many potential applications in such as medicine, micro electronics, nano technology etc.

The expanding application areas of composites naturally require a multi-disciplinary approach in research activities. Composite research had started as a branch of material science and mechanical engineering. Recently it is not uncommon to see collaborative research activities of scientist from mechanical, computer, electronics, textile engineering with mathematicians, physicists, chemists and even medicine doctors [3].

Modelling, mechanical characterization and design of materials are the three dominating research fields in composites. It is crucial to understand and predict the behaviour of composite materials through these studies in order to fully utilize its advantageous properties, spread its use and ensure safety requirements. One pole is the design of constituent materials which deals with the subjects such as interface design, nano-composites or bio-degradability. Another pole is the modelling and characterization of composite structures as well as process modelling. Although textile technologies offer unexhausted potential for near-net-shape and stress-compatible preforms, the intensity of publications in this intermediate field is apparently minor compared with the above mentioned two poles. The general preform structures are explained in textbooks [2] and particular structures are mainly described in patents. There are also some institutions, which develop innovative preforms but avoid both publications and patents as a protection policy.

There may be couple of reasons why intensive research efforts are not invested in the fruitful field of preform development. First of all, still not many textile specialists are working in composite research which leads to the illusion that all the possible textile structures have already been developed. As a result, composite specialists mostly take the textile reinforcement structures available in the market and try to construct best components out of them, instead of actively demanding and designing more suitable textile preforms. High necessary investments would inhibit the research in preforms, for instance a weaving or a knitting machine is much more expensive than a simulation workstation or an RTM device. Another reason would be that the research in textile structures and preforms does not seem scientific enough, although it requires multi-disciplinary thinking, creativity and pattern recognition.

This dissertation is a contribution to the multidisciplinary field of composites. Novel woven preforms and necessary automated technology is developed, concerning the reproducibility and cost-effectiveness.

## Chapter 2 - State of the Art and Aim

Both textile and composites are ancient crafts of mankind. Straw (reinforcement) and mud (matrix) was mixed in order to produce a light but dimensionally stable construction material. Weaving and braiding techniques were known at least 3000 B.C. In the second half of 18<sup>th</sup> century textile technology started the industrial revolution and various types of machines were developed for production with natural fibers mainly cotton and wool. Since 1950s, use of synthetic fibers such as polyester, polyamide, polypropylene, viscose etc. is significantly increasing. The existing textile machinery is also compatible with the mentioned synthetic fiber types. However, high-performance fibers of carbon, glass, aramide etc. necessitates proper modifications on textile machinery. During production with high-performance fibers, material waste should be minimized as well as the damage on the fibers.

This section demonstrates the state of the art structures and technologies in composite and textile fields to set the stage. From state of the art and industrial requirements, the importance of research direction in thermoplastic matrix composites as well as 3D complex preforms will be clearly derived.

### 2.1 Composite Structures

In a broad sense, composite materials can be defined as a combination of at least two materials to generate desirable properties. The final combination of materials results in better properties than the input materials used alone. This definition does not include for instance alloys or polymer blends which are material combinations in atomic level. Also as opposed to alloys, each constituent material in a composite retains its characteristic properties. In most of the cases, composites comprise a bulky and a fibrous part, which are called matrix (e.g. unsaturated polyester) and reinforcement (e.g. glass fiber) respectively. Matrices can be polymers, metals or ceramics whereas polymer based matrices clearly dominates the applications. The objective of matrix is to integrally bind the reinforcement together in order to effectively transfer external loads on to the reinforcement as well as protect it from environmental effects. The matrix gives a composite its shape, appearance, overall durability, on the other hand reinforcement carries most of the loads. Reinforcements



can be in various forms such as chopped fibers, unidirectional filaments and textile structures [4, 5]. Figure 2 and 3 demonstrate the high specific tensile strength and modulus of composite materials in comparison with conventional materials such as metals and wood. High specific strength and modulus can be regarded as the main advantage of composite materials.

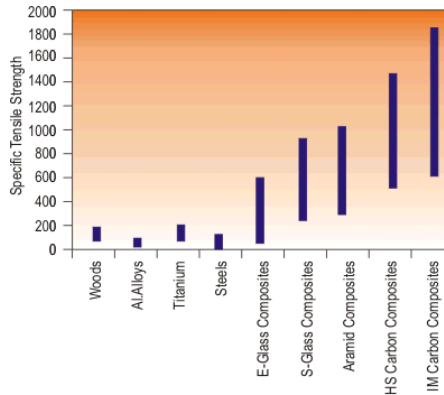


Figure 2: Specific tensile strength of common structural materials [6]

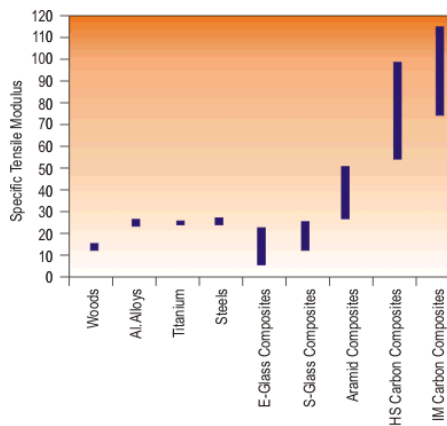


Figure 3: Specific tensile modulus of common structural materials [6]

Like in many fields, the development of advanced polymer composites has primarily been driven by aerospace and military applications, where performance is the main concern. With the time passing, most types of polymer composites became commodity materials in daily life. This transition put more emphasis on the design

and cost aspects in order to gain acceptance in the market where they compete with traditional materials such as wood, steel, concrete etc.

Figure 4 gives an overview of the composite use in aviation, in particular Airbus airplanes. The tendency can clearly be seen that every new airplane has more composite materials. There are still some technical tasks and challenges. For instance it is difficult to join metallic parts with carbon reinforced composites and the behavior of carbon (highly inductive) reinforced composite is still not known if a thunder meets the airplane.

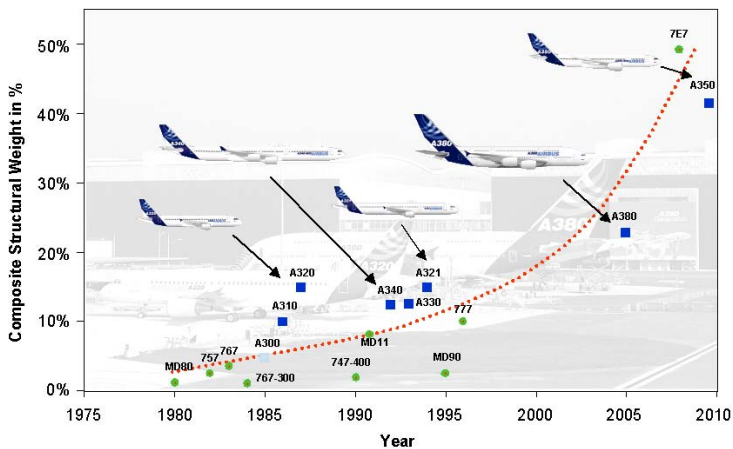


Figure 4: Tendency of composite use in aviation [7]

The practical attainment of the high strength and modulus of composites in the reinforcement direction is complicated by less favorable factors, mainly low transverse properties. To provide improved transverse properties, composites are produced as laminates with varying angles of reinforcements. By this way, final composite part gains some additional performance in transverse direction at the expense of reduced properties in the unidirectional material [8].

### 2.1.1 Manufacturing Aspects

Continuous filament reinforcements, which offer the greatest potential for performance, are used in filament winding and unidirectional composites. Chopped

fibers are usually used in molding compounds because of the ease in the formation of complex shapes. Continuous strand rovings or multiple filament bundles are used for economy of manufacturing thick sections. Mats (random or semi-oriented fibers of varying lengths) are economical reinforcements in bulk and easy to form complex shapes when performance is less important. Woven fabrics of various configurations can be seen as a compromise between maximum performance of unidirectional composites and ease of handling and formability of chopped fibers and mats [8].

Whether the fibers are discontinuous or continuous affects both the processability and mechanical performance of the final composite structure. The reinforcements can be very short fibers of 1-2 mm as used in injection molding. In this case the ease of processability is high whereas the contribution of short fibers to the mechanical performance is low.

### 2.1.2 Advantages of Fiber Reinforcements

Theoretical modulus and strength values for materials can be calculated according to the bond strength between their atoms. However, materials have actual strengths which are several magnitudes lower than the theoretical ones. The reason for this phenomenon is the impurities and flaws within the atomic structure. There are dislocations, missing atoms as well as grain boundaries which reduce the strength and modulus. Removal of these flaws increases the mechanical properties. Small diameter of fibers reduces the chance of inherent flaw in the materials. Generally, decreasing fiber diameter increases the fiber strength [4, 9].

Another important aspect is the transfer of loads onto the reinforcements through matrix. This load transfer is realized with fiber-matrix interface regions. For the same volume fraction of fibers in a composite, the fiber-matrix interface area is inversely proportional to the fiber diameter. For a composite containing  $N$  fibers with diameter  $D$  and fiber length  $L$ , the interface area is:

$$A_1 = N\pi LD \quad (1)$$

If the fiber diameter  $D$  is replaced with a smaller one  $d$ , the new number of fibers  $n_{new}$  in the composite is calculated according to the following formula to keep the volume fraction same.

$$n_{new} = N \left( \frac{D}{d} \right)^2 \quad (2)$$

This formula can be interpreted as; if the fiber diameter is halved, then the number of fibers with reduced diameter should be 4 times as many to keep the volume fraction same. The interface area for the new fiber diameter is:

$$A_2 = n_{new} \pi L d \quad (3)$$

By putting the expression of  $n_{new}$  into the formula of new area results in:

$$A_2 = N \left( \frac{D}{d} \right)^2 \pi L d \quad (4)$$

Then the ratio of fiber matrix interface areas according to the fiber diameters is determined as:

$$\frac{A_2}{A_1} = \frac{D}{d} \quad (5)$$

According to this expression, interface area is inversely proportional to the fiber diameter, which means if the fiber diameter is halved the interface region is doubled.

Fibers can be bent without breaking, which is an important requirement for manufacturing. Bending stiffness decreases with a decrease in fiber diameter.

Bending stiffness is the resistance to bending moments and if a beam is bent by a moment:

$$\frac{d^2v}{dx^2} = \frac{M}{EI} \quad (6)$$

$v$ : deflection of the central line

$E$ : Tensile modulus of the beam material

$M$ : Bending moment

$I$ : second moment of area

$x$ : coordinate along the length of the beam

In the formula above  $EI$  term is the bending stiffness. Second moment of area of a cylindrical beam is:

$$I = \frac{\pi d^4}{64} \quad (7)$$

Thus, the flexibility (inverse of bending stiffness) of a particular material is inversely proportional to the fourth power of its diameter.

Four properties of fibers in a composite effect the final component properties directly which are; length, orientation in the matrix, cross-sectional shape and material.

Use of fibers as load bearing structures is limited, with exception of ropes and cables. Therefore fibers are used as reinforcements in matrices.

### **2.1.3 Matrices**

Matrices are binding fibers together, protecting fibers from the environment and distribute the load. Matrices usually have low mechanical properties compared to fibers, however, they still significantly affect mechanical properties such as transverse modulus and strength, shear modulus and strength, interlaminar shear strength, thermal expansion coefficient and resistance as well as fatigue strength. Polymer matrix composites are mostly used and they are classified into two main groups.

#### **2.1.3.1 Thermosetting matrices**

Epoxy, unsaturated polyester and vinyl ester are the most common thermosetting resins. These resins cover a broad range of properties. Thermosetting resins are delivered in liquid form and after impregnation into the reinforcement, crosslinking of the polymers occurs which leads to a three dimensional network of solid polymers. Curing (crosslinking of polymers) can occur at room temperature, but higher temperatures can be used to achieve optimum crosslinking as well as higher production rates. Relatively high post-cure temperatures are applied in order to minimize further curing and change of material properties during use. Thermosets are brittle materials caused by the crosslinking of polymers. Type of thermoset resin affects the properties significantly, e.g. epoxy resins are generally tougher than unsaturated polyesters and mainly used for high performance composites [5].

#### **2.1.3.2 Thermoplastic matrices**

Unlike thermosetting resins, thermoplastics are not crosslinked. Therefore mechanical properties are derived from structure of the long molecular chains. Amorphous thermoplastics, which have no oriented crystalline blocks of polymers, have high amount of molecular entanglements acting like a crosslink. Semi-crystalline thermoplastics have a high degree of molecular order and alignment. Molecular alignment of semi-crystalline thermoplastics contributes to the mechanical properties. However, after consolidation, semi-crystalline matrices tend to shrink after consolidation which can cause deformations and residual stresses on the final

composite component. Thermoplastics are ductile materials with high failure strains and have good resistance to chemicals. PEEK (poly- ether- ether- ketone) is mostly used in high performance composites. Another feature of thermoplastic resins is creep; which means under constant load the strain tends to increase. From processing point of view, thermoplastic melts have high viscosity because they are already polymeric. High viscosity roughly means high resistance to flow, that makes impregnation of thermoplastic resin into the reinforcement quite difficult. In order to overcome this difficulty, flow distances of the polymers should be kept as short as possible [5].

## 2.2 Textile Preforms

Textile structures are widely used in advanced applications such as aerospace, automobile, machinery, marine and medical areas. Textile structures possess outstanding physical thermal and favorable mechanical properties, in particular light weight, high stiffness and strength, good fatigue resistance, excellent corrosion resistance and dimensional stability [10]. Textile preforms, mainly woven fabrics, are used as reinforcement materials in composites due to their low cost production and easy handling. The design of yarn orientation in textile preforms becomes more and more important in load-bearing complex shape composites

The type of constituent materials in the composite and their interface mainly influences the properties of the final component, however, the fiber architecture also plays a major role. Manufacturing technologies each with characteristic behavior for textile preforms are:

- Weaving
- Warp knitting
- Weft knitting
- Braiding
- Stitching

Weaving is the most widely used manufacturing technique and accounts for the majority of the 2D fabrics produced [11]. Conventional woven fabrics consist of two yarn systems interlaced with each other with an angle of 90°. Horizontally integrated

yarns, along the width, are called weft or pick and the yarns running along the fabric length vertically are called warp. Warp and weft yarns can be interlaced with each other with almost unlimited ways. The way of warp and weft yarn interlacing is called weave. The most basic woven structure is alternating warp and weft interlacing which is known as plain weave.

There is actually no such 2D structure in reality, every structure exist in three dimensions. The notation of textile preforms considers a structure 3D if the reinforcement yarns have significant effect in all three dimensions. Due to the crimp on the yarns, even plain woven fabrics may have varying properties in the third dimension. A slack warp (low tension) woven with a high weft tension leads to the structure in figure 5A, whereas a tight warp (high tension) woven with a low weft tension looks like figure 5B. The rate of warp and weft crimps is adjusted through their tensions. A decrease in tension increases the crimp which decreases the in-plane contribution of yarn and increases the out-of-plane mechanical properties in z-direction.

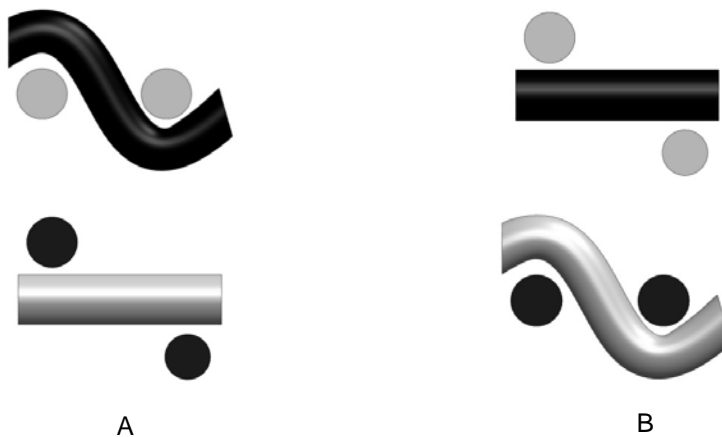


Figure 5: Structural change of plain woven fabrics due to warp (black) and weft (grey) tensions; slack warp (A) and tight warp (B)

A triaxial woven structure consists of three yarn systems; two warp yarn systems and one weft yarn system which are interlacing with each other at  $60^\circ$  (see figure 6). Triaxial woven fabrics have an open structure with higher shear resistance than conventional 2D woven fabrics and almost isotropic in-plane behavior.



Despite the use of 2D structure over a long period of time as reinforcements, there are some drawbacks which limit the industrial use in composites. Laying-up of 2D structures increase the manufacturing costs as well as reduce the precision of the final components. Inferior mechanical properties are also caused by the lack of reinforcement in the direction normal to the plane, mainly higher tendency of delamination.

In a multilayer woven fabric structure, if the warp yarn (sometimes also called binding yarn) moves along a column of weft yarns, its contribution in the z-direction becomes more significant (figure 6). These kind of multilayer woven fabrics are often called as 3D woven fabrics and they offer higher resistance to delamination due to the reinforcement in z-direction.

If the preforms do not have reinforcement fibers in the direction of thickness, damage tolerance and impact resistance are significantly reduced. The trend to delamination is drastically diminished in the case of reinforcement existence in the thickness direction. However undulations, crimp and process damage may reduce mechanical properties [12].

In a composite lamina, reinforcement fibers are oriented in an optimum fashion which fully utilizes the stiffness of fibers. The stack of these structures creates laminates. In this concept, very low transverse stiffness and strength may causes premature matrix cracking. The use of 2D fabrics or  $[0^\circ/90^\circ]$  laminates reduces the problem in in-plane transverse direction, however, the lack of reinforcement in the thickness direction still exhibits low mechanical properties. In particular lack of perpendicular reinforcement causes the slippage of layers and delamination under certain loading conditions.

3D textile structures assemble yarn system in such a way that both in-plane and transverse yarns are integrated into the same structure. Although in the literature, fabric structures with unit cells containing yarns in all three orthogonal directions are considered mainly as 3D, profile weaving should also be considered as 3D.

In order to clarify the notation of 3D textiles, it is convenient to distinguish between 3D geometry of preform and 3D reinforcement structure.

- 3D geometry of preform is the global formation of the textile, independent of the yarn structure in the unit cell. Spiral weaving or profile weaving are 3D structures with possibly 2D or 3D yarn courses in unit cell.
- 3D reinforcement structure has at least three yarn system within the preform structure which are orthogonal to each other, in other words there are yarns oriented in x- y- and z-axis of the coordinate system

Figure 6 demonstrates the overview of existing textile reinforcements. The structures in 1D and 2D are already developed. Research for roving yarns and 2D structures are mainly based on the application of new materials and process optimization. 3D linear element structures are also industrially produced, however, structural and process developments are still necessary up to some extent. 3D plane elements are the most complex types of reinforcements and there is a high level of research necessity in this field, both in structure and process development.



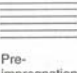

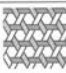










Axis Dimension	0 Non-axial	1 Monoaxial	2 Biaxial	3 Triaxial	4- Multiaxial
1-D		 Roving yarn			
2-D	 Chopped strand mat	 Pre-impregnation sheet	 Plain weave	 Triaxial weave	 Multiaxial weave, knit
3-D	Linear element 	 3-D braiding	 Multi-ply weave	 Triaxial 3-D weave	 Multiaxial 3-D weave
	Plane element 	 Laminate type	 H or I Beam	 Honeycomb type	

Figure 6: Classification of reinforcements [10]

Spacer fabrics are mainly used as preforms for sandwich light weight composites. Next section explains the state of the art spacer fabrics. There are significant chances and challenges concerning the new spacer fabric structures and their applications.

## 2.3 Spacer Fabrics

### 2.3.1 Conventional Spacer Fabrics

Spacer fabrics are special types of 3D fabrics which are characterized by two outer fabric surfaces connected with pile yarns. Warp knitting, weft knitting and weaving technologies are suitable for producing this kind of 3D structures.

#### 2.3.1.1 Woven Spacer Fabrics

Woven spacer fabrics are produced with the so called face-to-face weaving technique. Face-to-face weaving is mainly applied for producing velvet and carpets with high productivity. Two surfaces of carrier woven layers are connected with pile yarns and a cutting mechanism separates these two layers in the middle of pile yarns. Two separate woven layers with cut piles are wound onto rollers through two take-up systems. If the cutting system is omitted, woven spacer fabrics are produced with connecting piles. Along the width of the spacer fabric, pile yarns have a right angle, however, along the length pile yarns are binding the two layers with angle. After consolidation, pile connections have an angle distortion and they have limited capacity to withstand high pressure and shear stresses. Woven spacer fabrics (figure 7) are mainly used as reinforcements for tanks and car parts [13].

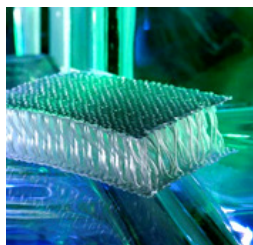


Figure 7: Woven spacer fabric [13]

#### 2.3.1.2 Warp Knitted Spacer Fabrics

Double bed Raschel warp knitting machines are used for the production of warp knitted spacer fabrics. Two layers of fabric layers are produced simultaneously and between them pile yarns are inserted. Warp knitting technology has higher productivity than weaving and weft knitting which is an important advantage for the

production of spacer fabrics. On the other hand there are limitations concerning the pile height between two fabric layers. Unlike woven spacer fabrics, warp knitted spacer fabrics have perpendicular pile connections along the length but inclined pile connections along the width. Warp knitted spacer fabrics with biaxial reinforcement of outer layers also exist with an open grid structure as concrete reinforcement. Warp knitted spacer fabrics (figure 8) are mainly used as comfort and insulation materials in car seats, running shoes, mattresses etc [14, 15].



Figure 8: Warp knitted spacer fabric [14]

### **2.3.1.3 Weft Knitted Spacer Fabrics**

#### **2.3.1.3.1 Circular Weft Knitted Spacer Fabrics**

Circular weft knitted spacer fabrics are produced on a circular knitting machine with a dial and a cylinder. At least three different yarn systems are necessary, two systems for the outer fabric layers and one system of mostly monofilament yarn for the pile connections [16]. Circular weft knitted spacer fabrics (figure 9) have limited chance to insert reinforcement material and they are not used as preforms.

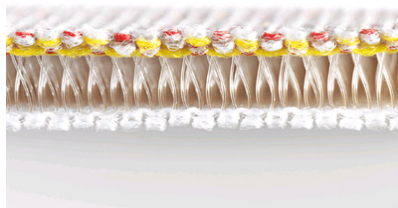


Figure 9: Circular weft knitted spacer fabric [17]

### 2.3.1.3.2 *Flat Weft Knitted Spacer Fabrics*

Spacer fabrics can also be produced with a V-bed flat knitting machine. A tubular knitted fabric is connected with mainly monofilament pile connections. Pile yarns are inserted with a zigzag movement between two fabric layers. Angle of connections can be varied, which enables a construction with a localized adjustment of compression stiffness. The distance between two needle beds is the cause of limited dimensions [18].

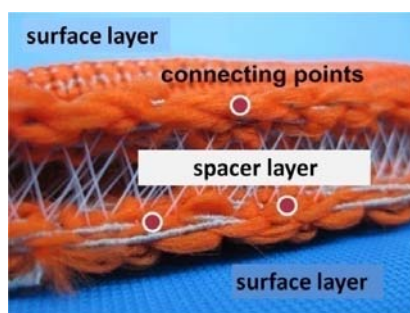


Figure 10: Flat weft knitted spacer fabrics [19]

## 2.3.2 **Spacer Fabrics with Fabric Cross-links**

As shown in the preceding section, conventional spacer fabrics are produced with two layers and connecting pile yarns. For flexural stiff thermoplastic composites, spacer fabrics with fabric cross-links are necessary. The conventional pile connection is not suitable for hot pressing of thermoplastic composites. Spacer fabrics with fabric cross-links have been developed at the Institute of Textile Machinery and High Performance Material Technology of Technische Universität Dresden. Flat knitting and weaving technologies are suitable for the development of this kind of spacer fabrics. These kinds of structures have the advantages of continuous reinforcement along the connecting points of base fabrics and cross-links.

### 2.3.2.1 ***Weft Knitted Spacer Fabrics with Knitted Connections***

Weft knitted spacer fabrics with knitted cross-links are produced with a V-bed flat knitting machine. Loop transfer is used in order to knit 3 layers of knitted fabrics on two needle beds [20-24]. Figure 11 depicts the production steps for V-shaped weft knitted spacer fabrics.

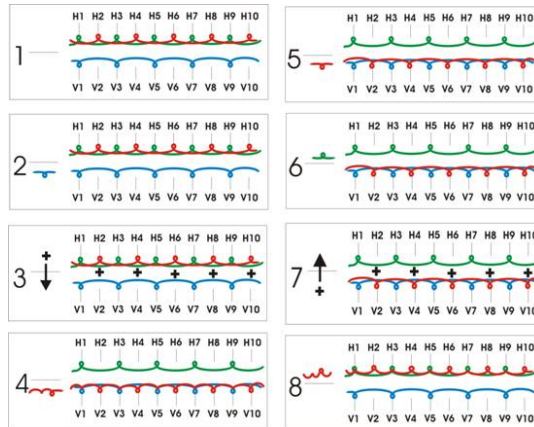


Figure 11: Production steps of V-shaped weft knitted spacer fabrics [20, 21]

Figure 12 demonstrates the V-shaped weft knitted spacer fabric structure from glass yarns. This fundamental technique is further developed to produce spacer fabric structures with various geometries such as curved spacer fabrics and weft reinforcements [25-28].



Figure 12: Weft knitted spacer fabrics with knitted cross-links [20, 21]

### 2.3.2.2 Woven Spacer Fabrics with Woven Connections

Woven spacer fabrics are produced with a modified terry weaving mechanism. Narrow weaving machine was modified and used as a prototype for the further development of the technology in industrial size [21-24, 29, 30]. Figure 13 demonstrates the modified narrow weaving machine with terry weaving mechanism and linear take-up system. With this equipment, U-shaped spacer fabrics from PES yarns were manufactured.



Figure 13: Modified narrow weaving machine [21]

Figure 14 depicts the narrow woven U-shaped spacer fabrics prototypes from PES yarns. The floating warp yarns on the left picture are pulled-back by using terry weaving mechanism. The picture on the right is the final spacer fabric structure with U-shaped cross-links.

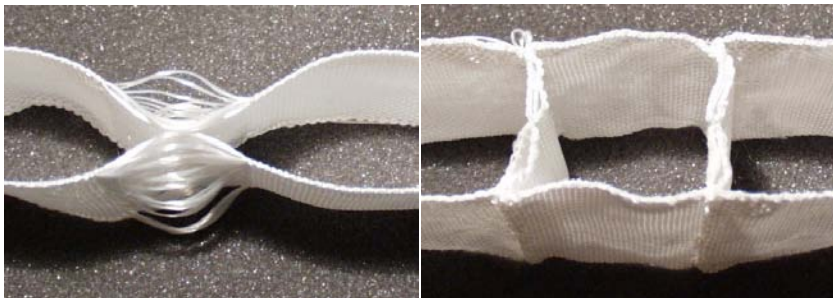


Figure 14: U-shaped narrow woven spacer fabrics from PES yarns. Flat structure without pulling-back of floating yarns (left), final spacer fabric after pulling-back of floating yarns (right) [21]

Needle narrow weaving machine has side needles to bind the inserted weft yarns. During the activation of terry weaving mechanism, the side needles continue holding the weft yarns as loops. When the fabric is moved back and forward, the weft yarn loops must suddenly increase their size enormously. This applies very high stresses on the side needles, and deforms the structure of the woven fabric. After finishing the terry weaving movement, the needles are not able to continue their function because of the very high loop dimensions and fabric deformation. Another point of concern is the negative feeding of warp yarns from warp beams. As the warp beams of the

prototype narrow weaving machine are only driven by the warp tension and the friction mechanism, the pull-back mechanism takes yarn length both from the weaving side and from the warp beam side. This phenomenon avoids removal of the required length of floating warp yarns and the crosslinks are not fully formed. Therefore, further research is necessary for the following points:

- Development of a flexible technology and production methods for the industrial size manufacturing of complex shaped preforms (such as V-, X-shaped, variable crosslink etc.)
- Reproducible continuous preform production
- Application of technical yarns in complex preform weaving
- Increasing the mechanical performance and thickness of composite by non-crimp 3D orthogonal structures

## **2.4 Composite Stiffener Structures**

Large composite panels of naval and aerospace application are an important area where out-of-plane reinforcement is necessitated. Low bending modulus of these structures is a major constraint to overcome in the design of large composite parts, therefore, various types of stiffeners are integrated. Stiffeners are either a stack of laminates perpendicular to the panel or a chamber of laminates with or without foam inside. The connection between the panel and stiffeners is mostly resin, in some cases sewing yarns and resin connection is also applied. Many experimental studies are conducted in order to determine the effects of connection type between stiffeners and panels as well as resin type, fillet radii etc. The lack of reinforcement between stiffeners and panels are recognized and explicitly mentioned as the main cause of failure in the early studies [31]. Matrix connection clearly increases the risk of delamination. Other connection techniques such as sewing increase the cost of production as well as generate inhomogeneity and damage the preform. Figures 15 and 16 demonstrate the state of the art production technique of stiffener structures for aerospace applications. Both the panel and the stiffener parts consist of multiple prepreg layers and the critical connection area between these two parts are manufactured by only matrix connection.



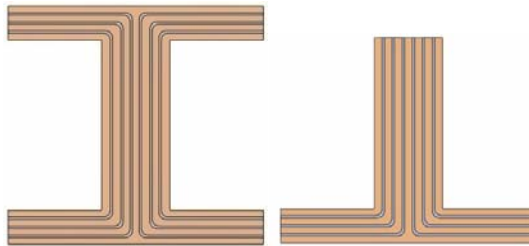
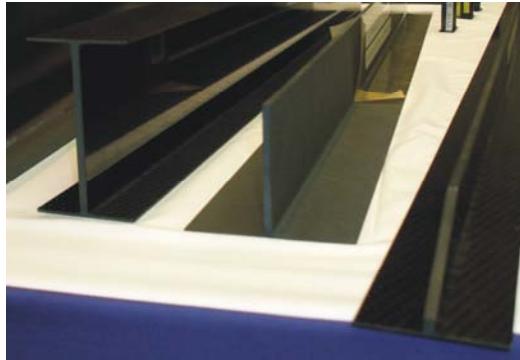


Figure 15: Examples of I-beam and T-beam stiffener structures used in aerospace applications (above) and their internal structure of fabric plies (below) where different color means separate layers [32]



Figure 16: Stiffener structures for aerospace applications (above) and schematic of stacked fabric layers (below) where different color means separate layers [32]

## 2.5 Hybrid Yarns

Fracture toughness and recycling are important advantages to use thermoplastic matrices in composite manufacturing. However, high viscosity of thermoplastics

requires mixing of the reinforcement material and the matrix in the solid state. This mixing process is realized through hybrid yarn production which reduces the flow path of the resin during impregnation and consolidation. One application field of hybrid yarns is car tires in which the two components are mixed in such a way to create a required bimodular behavior [33]. Main application of hybrid yarns is to mix the reinforcement component and the thermoplastic matrix component. Figure 17 demonstrates the possible ways of producing hybrid yarns.

Online hybrid yarn spinning delivers good mixture of matrix and reinforcement components without significant process damage [34-36]. However, online spinning of hybrid yarns is currently available in the market only for the GF/PP and GF/PET material combinations [37]. Commingled yarns are produced with modified air jet texturizing machines [38, 39]. Commingling is a flexible production process which provides good mixture of components in the cross-section. Any material combination can be processed, however, air nozzle damages the reinforcement material [40]. Also, it is not possible to produce thick rovings with commingling process. In friction spinning, reinforcement yarns are in the core of the yarn and the matrix is in short fibre form and wound around the reinforcement [41, 42]. Reinforcement material is covered and protected by the matrix. On the other hand, due to the poor mixture in the cross-section, impregnation is not easily realized. Similar cross-sectional structure is created by micro-braiding [43]. Like friction spinning, micro braiding also protects the reinforcement during further processing. Impregnation does not always reach until the core of the reinforcement if suitable process parameters are not selected [44]. Twisting and covering are not preferred for hybrid yarn production to mix thermoplastic matrix and reinforcement because of the poor mixture in the cross-section.

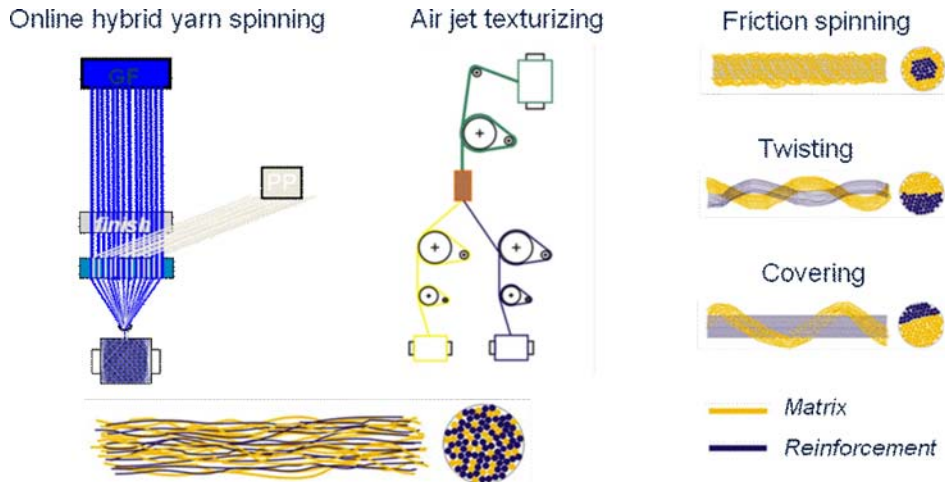


Figure 17: Production techniques of hybrid yarn [24]

## 2.6 Aim of the Thesis

Weaving technology is dominating the market of textile reinforcements for high performance composite materials both with existing and potential applications. 3D profiled woven preforms are necessary to provide reproducibility by reducing the manual works. By considering recycling and cost issues, development of an automated technology for reproducible production of complex woven preforms fulfils the demands of the current composite market. Thermoplastic composites have high ultimate strain, increased fracture toughness, higher impact tolerance, short molding cycles, as well as the great opportunity they offer for rapid and low-cost mass production of high-performance structural components. Therefore, thermoplastic matrix composites are mainly aimed by using commingled yarns, however, profiled woven fabrics can be used as reinforcement for thermoset matrices as well.

The aim of the dissertation is as following:

- Development of a novel notation to analyze and classify 3D woven structures
- Analysis and solutions concerning the weaveability of GF/PP commingled hybrid yarns
- Determination of the effects of weaving and structural parameters on the reinforcement and composites

- 
- Development of industrial size production principles for basic spacer fabric structures with woven cross-links
  - Development of industrial size production techniques for complex spacer fabrics and stiffeners
  - Development of technology, application of mechanical modifications and industrial size manufacturing of preforms

## Chapter 3 - Mathematical Treatment of 3D Woven Structures

Creating surfaces with fibrous materials has been known by mankind since ancient times and weaving is the oldest of these techniques. In conventional weaving, the interlacing of warp and weft yarns creates the textile surface. There are almost unlimited ways of interlacing these two yarn systems, which generates different appearance, touch and mechanical properties. Three basic weave structures, that are called plain weave, twill weave and satin weave, are utilized by weave designers and engineers to derive further weaves. Thickness of conventional weaving is not significant in comparison with its width and length, therefore they can be regarded as 2D weaving. A weave repeat (unit cell) of a 2D woven structure is represented by black and white coloring of a rectangular block of squares. This general notation is demonstrated in figure 18. Square blocks represent the crossing points of warp (vertical black lines) and weft (horizontal white lines). A square is filled with black color if warp yarn is on the top of weft yarn. A square is left white if weft yarn is on the top of warp yarn, in that particular crossing point. The weave repeat is 2x2 which means the smallest repeating weave unit consists of 2 warp and weft yarns. This notation is sufficient for the conventional 2D woven structures.



Figure 18: Weave representation of a plain woven fabric (left) and actual positioning of warp (black color) and weft (white color) yarns (right)

In the literature, some research efforts have been reported to determine the possible number and types of weaves for a given repeat size as well as what kind of patterns of the notation in figure 18 brings a real woven structure. Gu and Greenwood have shown that there is a large discrepancy between the number of weaves that can be woven and the number that are theoretically exist [45]. They claimed that computational analysis with algorithms is necessary to find the exact number of

weaves for a given repeat size. However theoretical analysis would give good approximation to the minimum number of weaves. There are also algorithms developed to check whether the weave represents a single fabric layer or two or more separate fabric layers laying over one another [46, 47]. Dawson introduced an algorithm to identify all families of weaves for a given repeat size. In this study, weave representations are transformed into binary digits. “0” is used for a white square and “1” is used for a black square within the notation of figure 18. Binary numbers represents the weaves and an algorithm is used to subtract the number, which do not generate a woven structure. It is claimed that the number of weave families increases almost exponentially with repeat size, therefore any algorithm would be practicable only over a range of small repeat size [48].

### 3.1 Representation of Multi-layer Woven Fabrics

Multi-layer woven fabrics have significant thickness compared with their length and width, as well as yarn paths going in the z-direction (normal to the fabric plane). Therefore multilayer woven fabrics are also regarded as 3D woven structures. Chen and Potiyaraj have reported about parametric construction of two types of 3D woven fabrics, namely orthogonal and angle-interlock, by using a CAD/CAM system [49]. The general notation for multilayer woven fabrics is the same as the notation for conventional 2D woven structures. There are multiple plies within a multilayer fabric which consists of weft yarns positioned onto each other and these weft yarn layers are connected through warp yarns. Since the general notation includes only two positions which are black and white areas, the weft yarn layers are drawn as if they are positioned next to each other. Figure 19 demonstrates the weave of two separate layers of plain woven fabrics. In the figure, columns represent the warp yarns and horizontal lines represent the weft yarns. U1 and U2 are the first and second yarns of the upper layer plain weave. L1 and L2 are the first and second yarns of the lower layer plain weave.

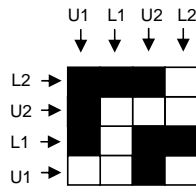


Figure 19: Weave for double layers of separate plain woven fabrics

At the first look, the patterns of plain weave (as in figure 18) for the upper and lower fabrics are not easily seen, although they are already included within the unit cell in figure 19. The reason for this confusion is caused by the additional areas which have to be included into the pattern. These additional areas are created by definition of upper and lower layer fabrics, namely; warp yarns of upper layer should always be on top of the weft yarns of lower layer, and warp yarns of lower layer should always be under the weft yarns of upper layer. According to this definition, areas of all black and all white should be included into the pattern respectively. Figure 20 depicts the 4 building blocks of the pattern shown in figure 19, which are two plain weave structures for upper (figure 20A) and lower fabric (figure 20B), as well as the 2 areas by definition of upper (figure 20C) and lower (figure 20D) layers. The pattern of figure 19 is constructed by the assembly of 4 patterns shown in figure 20. If demanded, there are two ways to connect these two separate fabric layers. First one is adding white squares into the area of figure 20C which means the warp yarns of the upper layer will connect with the weft yarns of the lower layer. Second one is adding black squares into the area of figure 20D. In this case warp yarns of lower layer will connect with the weft yarns of upper layer.

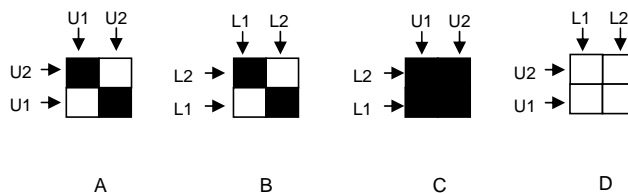


Figure 20: Elements of weave for double layers of separate plain woven fabrics

If 3D weaves are needed to be analyzed, above described notation is insufficient because the information about the yarn course in the z-direction cannot be seen easily. Flat demonstration of a 3D structure with black and white squares which can be translated into binary code does not give enough insight to see the real 3D structure. Therefore two new notations are suggested in the following.

### 3.2 Alternative Ways of Weave Representation

As mentioned before, the areas of black or white regions created by the definition such as in figure 20C and 20D, makes it difficult to analyze a multilayer woven structure. One alternative is to use matrix notation with numbers of suitable mode. Since single layer fabric can be demonstrated by a binary data, such as black and white squares or 1 and 0, for an n-layer fabric, the mode of numbers should be  $n+1$ . In this case, the structure in figure 19 can be reformulated with a matrix of mode 3. It is assumed that weft yarns of upper layer are already positioned over the weft yarns of lower layer. In order to include the important z-direction, side-view of the structure is necessary instead of top view. Figure 21 depicts side-view of two separate plain fabric layers constructed according to the weave shown in figure 19.

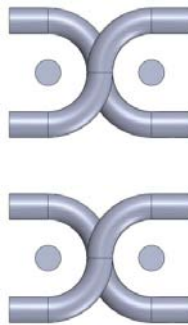


Figure 21: Side-view of double layers of separate plain woven fabrics

The weave of figure 19 with black and white squares can be transferred into binary data [48]. According to the cross-section in figure 21, two layer fabrics can be defined with a matrix of mod 3. The formulation of binary data of weave into mod 3 matrix is shown in the expression 8. In this mod 3 formulation, the number 2 means the upper



position for a warp yarn, the number 1 means the position between upper weft yarn and lower weft yarn, and the number 0 means the lower position under all of the weft yarns. This notation can be applied in the same way to woven fabrics consisting of more than two layers.

$$\begin{pmatrix} 1110 \\ 1000 \\ 1011 \\ 0010 \end{pmatrix}_{\text{mod } 2} \rightarrow \begin{pmatrix} 2110 \\ 1021 \end{pmatrix}_{\text{mod } 3} \quad (8)$$

Changing the mode of the matrix notation creates a more compact representation of what is happening within the structure. However the top-view perspective is still not suitable to gain the necessary insight. The side-view of a multilayer woven fabric gives better idea about how the normal to the plane direction of the fabric is constructed.

The simplest weave, so called plain woven fabric in figure 18, has a unit cell representation with 2x2 squares. The available four squares can be either white or black. Therefore the overall possibilities of pattern OPP within this size of squares can be calculated as in the equation 9 where c is the number of lines (weft yarns) and r is the number of columns (warp yarns). For the unit cell of 2x2, 16 possible configurations exist. Within these 16 configurations, only two patterns define a real woven structure, which are actually the same plain woven fabric (figure 22).

$$\text{OPP}(c, r) = 2^{c \cdot r} \quad (9)$$

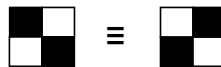


Figure 22: Two equivalent representations of plain woven fabrics

The selection of two possible plain weave structures is a simple matter when the side-view is used instead of top-view. Figure 23 depicts the two possible structures

for a 2x2 unit cell, one of which does not provide a woven structure because of floating (figure 23 left) and the other is the plain woven fabric (figure 23 right). The two equivalent representations of figure 22 exist in the cross-sectional view (figure 23 right). Here the sequence of the two warp yarns creates two equivalent patterns from conventional top-view, however the sequence of warp yarns can be ignored especially when the mechanical characteristics of the structure is mainly concerned.



Figure 23: Side-view of patterns with two warp yarns and two weft yarns. Floating of warp yarns without forming a woven structure (left), plain woven structure (right)

Underlying assumptions to utilize the cross-sectional views of figure 23 as a weaving notation are:

- Weft yarns lay straight between warp yarns as solid cylinders. Crimp of weft yarns in real woven structures is ignored in order to provide simplicity.
- For  $n-1$  numbers of weft yarns lying onto each other,  $n$  warp yarns are available. In figure 23, one layer of weft yarn is drawn and two warp yarns are available.
- Weft yarns are fixed through crossing of warp yarns. Inside of one area created by the crossing of warp yarns, only one weft yarn can exist. The thickness of weft yarns and the possibility of more than one weft yarn within the crossing of warp yarns are irrelevant for the analysis.
- Only two columns of weft yarns are considered.
- No warp yarn follows the same route.
- According to the 3rd assumption, all warp yarns start in successive positions, in order to avoid double weft yarns within the same crossing area of warp yarns.

Figure 24 demonstrates the six possible structures which are constructed according to above mentioned assumptions; in particular two weft yarn layers, two weft yarn columns and three warp yarns with three available positions. If  $n$  is the number of warp yarns, the number of possible structures  $SP$  can be calculated by factorial of number of warp yarns (equation 10).

$$SP = n! \quad (10)$$

According to this expression, figure 23 demonstrates the  $2!$  possibilities and figure 24 demonstrates the  $3!$  possibilities. Out of the six possible structures in figure 24, the first three 1-3 do not create a woven structure. Only the last three structures 4-6 can be regarded as woven structures. The reason is the floating warp yarns in the first three structure which fails to integrate all the weft yarns. Structure number 6 also includes a floating warp yarn between weft layers, however, the remaining warp yarns close the structure and create a woven structure. Figure 24 also includes algebraic definitions with three digits shown under the structures. In the cross-sectional notation of woven structures, the number and positions of weft yarns are fixed, and the courses of warp yarns determine the structure. Only two weft yarn columns are used to keep simplicity, therefore two numbers are sufficient to determine the course of one warp yarn, namely, the starting position of a warp yarn and the finishing position. Positions of the warp yarns are numbered from top to bottom. For instance, the structure number 3 in figure 24 is described as 213, which means the warp yarn in second position (between two weft yarns) goes to the first position (upper position on both weft yarns). Therefore the first digit has the number "2". With the same logic, the warp yarn in position 1 (upper position) goes to the warp yarn position 2. Therefore the second digit is 1. The warp yarn in the third position (lower position) stays in the same position, that is, the number 3 is in digit 3.

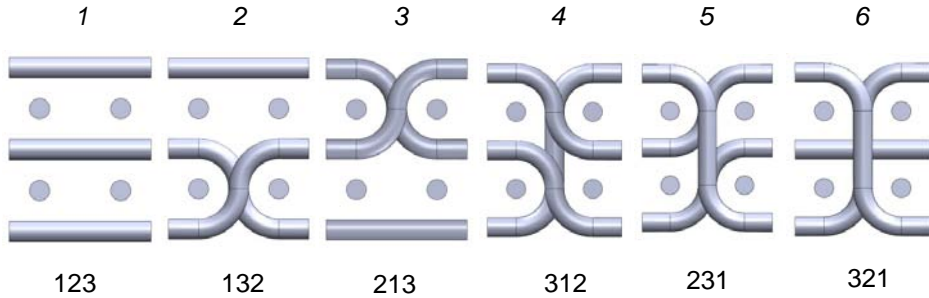


Figure 24: Possible structures with 2 weft yarn layers, 2 weft yarn columns and 3 warp yarns

The number of woven structures SW with number of warp yarns  $n$ , within the possible structures of  $n!$  can be calculated as in the equation 11.

$$SW_1 = 1$$

$$SW_n = n! - \sum_{i=1}^{n-1} (SW_{n-i} * i!) \quad \text{for } n = 2,3,4 \dots \quad (11)$$

The logic of the equation 11 is based on the subtraction of structures with floating warp yarns (in figure 24, structures 1 and 2) and the structures which create a smaller number of weft layers (in figure 24, structure 3). The algebraic notation shown in figure 24 is helpful to construct and appreciate the meaning of the equation 11. Let the woven structures with  $n=4$  be the subject of the analysis. According to the equation 11, the number of woven structures is calculated as shown in the expression 12.

$$SW_4 = 4! - (SW_3 * 1! + SW_2 * 2! + SW_1 * 3!) \quad (12)$$

The total number of structures are given as  $4!$ . Figure 25 depicts the individual blocks of structures which do not represent a woven structure, thus they should be

subtracted from the total 4!. SW1 is defined as 1 in the equation 4, which means that the uppermost warp yarn is floating. This structure is symbolized as the algebraic expression with a 1 in the first digit. There are 3! structures which have a 1 in the first digit. SW2 is the number of woven structures with two warp yarns. As shown in figure 23, SW2 is 1, and the algebraic notation starts with a "21" in the first two digits. The remaining two digits are in total 2!. SW3 is the number of total woven structures with 3 warp yarns. Figure 24 shows that there are three possible woven structures with structure numbers 4-6. These three structures have the algebraic notations "312", "231" and "321". In all these three cases the last digit can only be "4", which is 1!. All the above mentioned possibilities, which generate a local woven structure and therefore do not create a whole woven structure, are subtracted from n! as in the equation 11.

$$\begin{array}{l}
 SW_1 \left\{ \begin{array}{l} 1 \_ \_ \_ \Rightarrow 3! \end{array} \right. \\
 SW_2 \left\{ \begin{array}{l} 21 \_ \_ \Rightarrow 2! \end{array} \right. \\
 SW_3 \left\{ \begin{array}{l} 312 \_ \Rightarrow 1! \\ 231 \_ \Rightarrow 1! \\ 321 \_ \Rightarrow 1! \end{array} \right.
 \end{array}$$

Figure 25: Subtraction blocks to determine the woven structures with 4 warp yarns SW4

Table 1 depicts the development of possible structures SP and the woven structures SW according to the number of weft yarn layers from one to six.

warp yarns (n)	weft yarn layers (n-1)	weft yarn columns	possible structures (SP=n!)	woven structures (SW)
2	1	2	2	1
3	2	2	6	3
4	3	2	24	13
5	4	2	120	71
6	5	2	720	461
7	6	2	5040	3447

Table 1: Development of possible structures SP and the woven structures SW according to the number of warp and weft yarns

After looking closely at the structures in figure 24, it can be figured out that not all the 3 woven structures are independent. In fact, structure number 5 can be regarded as the symmetry of the structure number 4 both according to x-axis (horizontal) and y-axis (vertical). The determined woven structures SW are further distributed into 5 groups due to the symmetry. The schematics as well as the definitions are given in table 2. The starting woven structure is positioned on the upper left and called "main". Symmetries of x-, y-, and diagonal-directions are positioned accordingly.

Definition of symmetry group	Schematic of symmetry group
<p>1. x, y and diagonal symmetries are same as the main weave</p>	
<p>2. Diagonal symmetry is same as the main weave; x and y symmetries are same</p>	
<p>3. x, y and diagonal symmetries are all different from the main weave</p>	
<p>4. x symmetry is same as the main weave; y symmetry is same as diagonal symmetry</p>	
<p>5. y symmetry is same as the main weave; x symmetry is same as diagonal symmetry</p>	

Table 2: Symmetry groups of woven structures

Figure 26 demonstrates the symmetries of the woven structure 51243 as an example. This woven structure belongs to the symmetry group 3 which is explained in table 2. It can be seen that all x-, y- and diagonal symmetries are different from the main woven structure 51243.

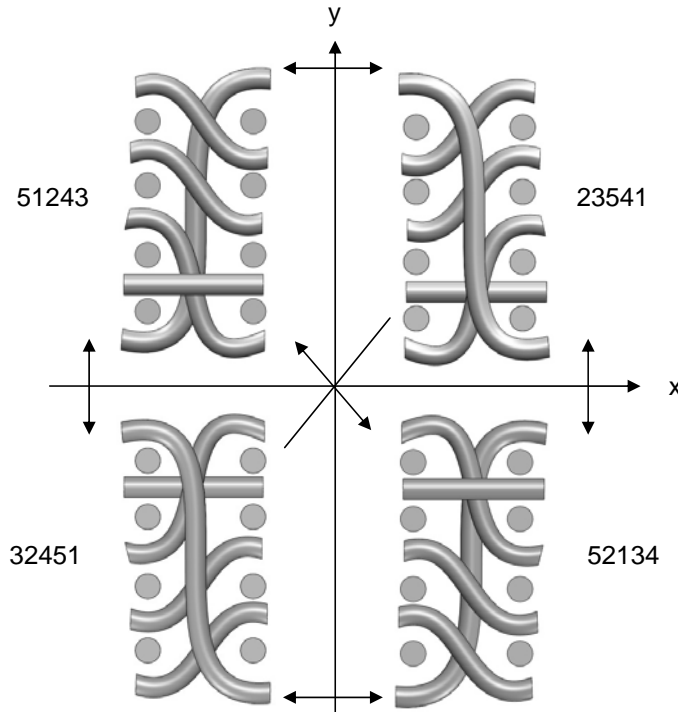


Figure 26: Symmetries of the woven structure 51243

The symmetry groups can be identified with algebraic notation as well. Figure 27 shows the operations to determine the x and y symmetries of a given woven structure. Operations I and II are applied to a given algebraic expression to find the x symmetry. Operation I turns the sequence of the algebraic expression, which means 51243 is rewritten from back to forward to get 34215. Operation II changes the numbers with their symmetries according to the middle point of the number set. In figure 27, the operation II changes 34215 to 32451, where the number set is  $\{1, 2, 3, 4, 5\}$  and the middle point of the number set is the number "3". Therefore, the first digit is 3 and it remains. The second digit is 4 and it is changed to 2, because the symmetry of 4 according to the middle point 3 is 2. The operations III and IV change a given



algebraic expression to its y symmetry. First, the main algebraic expression 51243 is written in open form, i.e.  $5 \rightarrow 1$  means that the warp yarn goes from the position 5 in the first weft yarn column to the position 1 in the second weft yarn column. After writing the routes of all the warp yarns, the sequence is changed, namely  $5 \rightarrow 1$  becomes  $1 \rightarrow 5$ . After operation III, the left hand side of the number columns is in order from 1 to 5. Operation IV merely makes the right hand side of the number columns in ascending order. The left hand side of the number columns read from top to bottom gives the y symmetry as 23541.

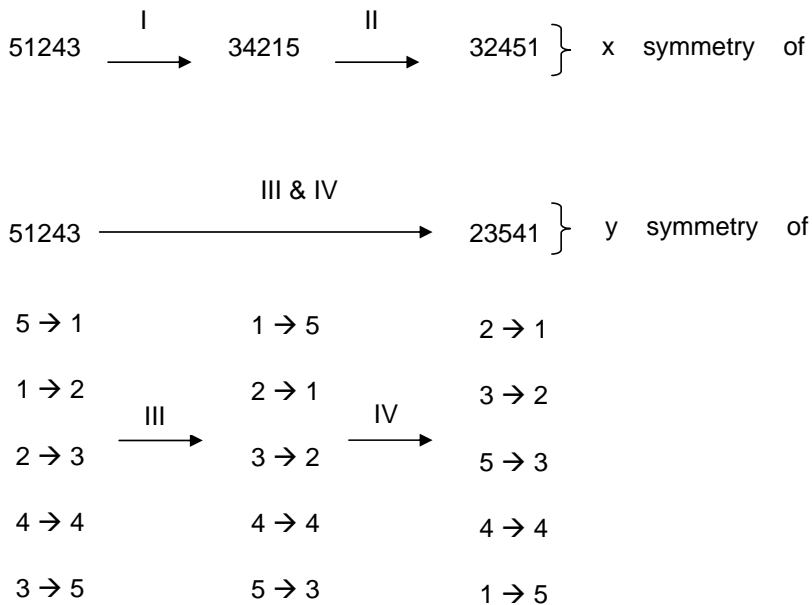


Figure 27: Algebraic operations to determine the x symmetry (I & II) and y symmetry (III & IV) of a given woven structure

According to the operations shown in figure 27, distribution of woven structures to the five symmetry groups are executed. The results up to  $n=5$  is shown in table 3. Symmetry groups 1, 2, 3, 4, and 5 define one, two, four, two and two woven structures respectively. Thus, in table 3 under symmetry groups, the numbers of woven structures are expanded as the multiplication of independent woven structures

in brackets. For example, if the number of warp yarns ( $n$ ) is taken as five, symmetry group 2 has 20 woven structures which consist of 10 independent woven structures.

$n$	(SW)	Independent woven structures	symmetry group 1	symmetry group 2	symmetry group 3	symmetry group 4	symmetry group 5
2	1	1	1 (1*1)	0	0	0	0
3	3	2	1 (1*1)	2 (1*2)	0	0	0
4	13	7	3 (3*1)	4 (2*2)	4 (1*4)	2 (1*2)	0
5	71	26	3 (3*1)	20 (10*2)	44 (11*4)	2 (1*2)	2 (1*2)

Table 3: Distribution of woven structure according to the symmetry groups

Although a 2-tuple data can be described by an algebraic expression as utilized above, there are still limitations to gain insight. One dimension of the data is the digit number which is not easily visible. Therefore, it is advantageous to draw the number pairs in a Cartesian coordinate plane, which represent the starting and ending positions of warp yarns. This transformation shows the equivalent representation of woven fabric symmetry in analytical geometry. If the number of weft yarn columns is increased from two to  $n$ , the data can still be presented in  $n$ -tuple space.

Figure 28 demonstrates the  $x$ -,  $y$ - and diagonal symmetries of the woven structure 51243 on coordinate axis, which was already shown in figure 26 with cross sectional and algebraic notation. In this figure, the starting positions of warp yarns within the first weft yarn column are given in the  $x$ -axis and the ending positions are given in the  $y$ -axis. For instance, the point (1,2) means that the warp yarn is moving from the first position in the first weft yarn column to the second position in the second yarn column. From the representations in figure 28, it is obvious that;

- $x$ -symmetry of the woven structure (32451) can be found by finding the symmetries of all the points according to the middle point, which is (3,3) in the given example
- $y$ -symmetry of the woven structure (23541) is the symmetry of all the points according to  $y=x$  line, and

- diagonal symmetry of the woven structure (52134) is the symmetry of all the points according to the line with a gradient of -1 and includes the middle point. Here the middle point is (3,3) and the line is  $y=6-x$ .

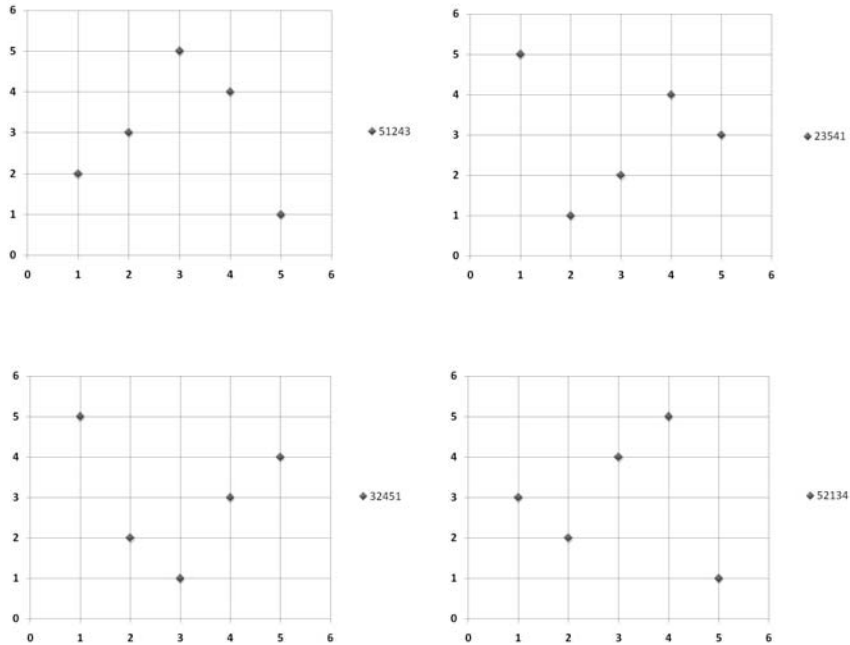


Figure 28: Representations of the symmetries of 51243 on Cartesian coordinate plane

### 3.3 Conclusion

Normal to the plane direction defines the multilayer woven structures, thus it is the most important dimension. Therefore, this section starts analyzing multilayer woven structures from their cross sectional views. An equation is derived to determine the real woven structures for two weft yarn columns and any number of warp yarns. Furthermore, symmetry groups within the real woven structures are identified. Algebraic expressions and Cartesian coordinates are utilized to find the symmetries of given woven structures. Independent woven structures, which are not symmetries of each other, are important to determine the realizable mechanical properties. As future work, the equations which describe the development of each of five symmetry groups as well as the independent woven structures are necessary. Moreover, the

cases where the number of weft yarn columns is three or more should be analyzed with multidimensional data. If the warp yarn lengths in the woven structure are different, then also different feeding systems are necessary. It would be useful from production point of view to group the woven structures according to the number of different warp yarn lengths.

## Chapter 4 - Weaveability of Commingled Hybrid Yarns

The viscosities of fully polymerized thermoplastics are around two to three orders of magnitude higher than their thermoset counterparts [50]. In order to overcome the difficulties of impregnation caused by high viscosity of thermoplastics, reinforcement materials (e.g. carbon, glass) and thermoplastic polymer (e.g. PP, PEEK) are already mixed in solid state. The aim of solid state mixing is to reduce the flow path of polymers during impregnation. This mixture is processed into preforms mostly with textile machinery. Thermoplastic polymers in the preform are melted under the application of pressure and temperature (e.g. pultrusion, compression molding), and consolidated [51-53].

Commingled yarns can be produced with a modified air-jet texturizing machine (figure 29). The most important modification is the type of air nozzle used. Commercial air nozzles are available, which claim to reduce the damage on the reinforcement yarns during processing and offer a better mixture in the cross-section. Especially for commingled yarns, a good mixture in the cross-section is crucial, because the main idea of commingling process is to reduce the flow paths of the viscous thermoplastic resin. Another important modification for commingling process is the bobbin winding device. Commingled yarns should be wound up with a constant yarn tension with higher bending radii of machine elements to minimize the damage on the yarn. Besides material mixing and high production rates, commingled yarns embody structural elongation which enables a smoother processing with textile machinery. During commingling process, reinforcement yarns are damaged by the applied air pressure in the nozzle, which can be seen as a drawback. Another disadvantage of commingled yarns was identified from processing point of view while executing trials on high packing densities of 3D near-net shape woven preforms [21-24]. Harnesses apply forces on the warp yarns in both normal and longitudinal direction during weaving. These forces should be minimized by reducing the warp yarn tension especially for the brittle reinforcement yarns. However, reduced warp yarn tension with high packing density increases the probability of stuck yarns in the shed and causes unclear shed opening. After commingling, yarns become more voluminous and open. Depending on the structure, high packing density commingled yarns

showed higher production stops than conventional materials, which necessitates improvement for the industrial production.

Over-delivery of input yarns is necessary for the formation of the commingled structure [39]. This indicates the possibility of slightly twisting the commingled yarn to create a more compact yarn structure without causing significant effect on the composite properties. In the literature, contributions about the effects of twisting on high performance yarns were reported however no study is available about the effect of twisting on the commingled yarns and their composites. Within the scope of this study, main aim is to determine whether twisting can be applied on commingled yarns in order to improve the processing behavior on textile machinery. The effect of twisting level both on the yarn and composite properties were analyzed to see how the physical and mechanical properties were changed. A yarn model with serially connected linear bar elements was introduced to consider the varying contribution of bulky and knot areas in the commingled yarn structure. Over-delivery of the constituent materials during commingled yarn production was modeled as an equivalent angle distortion of a lamina. Both yarn-yarn and metal-yarn friction areas occur during weaving. As the surface of the commingled yarn is altered through twisting, its effects on the friction coefficients between yarn-yarn and yarn-metal were analyzed.



Figure 29: Air-jet texturizing machine utilized for commingled yarn production (left) and detail view of the air nozzle (right)

## 4.1 Experimental

### 4.1.1 Materials

The GF/PP commingled yarns were produced with the commercial input materials of 300 tex glass (E 35, P-D Glasseiden GmbH, Germany) and 3 x 32 tex polypropylene (Prolen H, CHEMOSVIT FIBROCHEM a.s., Slovakia) which resulted in a fiber volume fraction of 52% in UD composites. Commingled yarns were produced with 4 bar air pressure in the nozzle and a winding speed of 100 m/min. In order to generate the commingled structure, input cylinders deliver the glass and polypropylene yarns with a higher speed than the output cylinder which is removing the final commingled yarn out of the air-nozzle. This setting is called over-delivery and defined as the percentage ratio of the speed difference to the output cylinder speed. Equation 13 shows the calculation of over-delivery  $OD$ , where  $S_i$  is the input speed of feeding cylinders and  $S_o$  is the output speed of take-up cylinders.

$$OD = \frac{S_i - S_o}{S_o} * 100 \quad (13)$$

Over-delivery of glass yarns was kept at a value of 2% to avoid damage and extensive loss of orientation. Over-delivery of polypropylene yarns was 8%, therefore polypropylene filaments had higher entanglement than glass filaments and were tending to be at the outer part in the cross-section.

Produced commingled yarns were twisted (DirecTwist, Agteks) with 0, 5, 10, 15, 20, 40 and 60 tpm (twist per meter) and compared with the reference yarn which was commingled without any further process. 0 twist per meter in the trials actually means winding to another bobbin by using the same twisting machine. Winding without twist was done to isolate the effect of extra processing on the yarn properties. 5 to 20 tpm were the main experiments of concern whereas 40 and 60 tpm experiments demonstrated extreme values. Uni-directional (UD) composites were produced with compression molding. Processing conditions for compression molding is shown in figure 30.

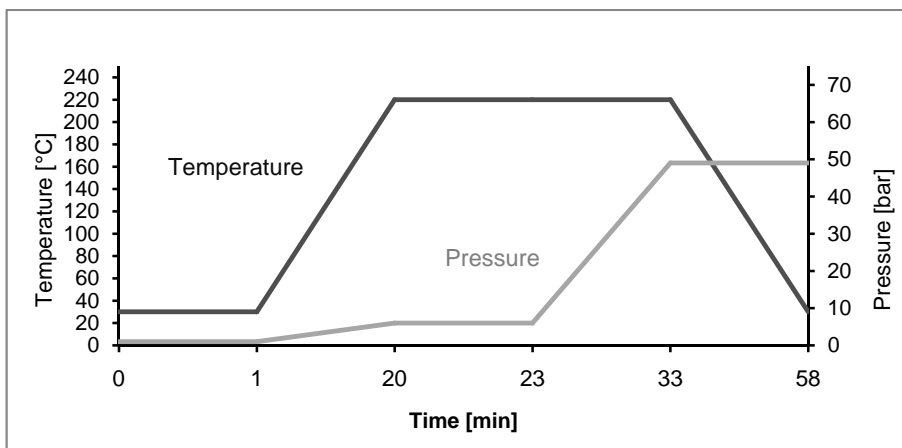


Figure 30: Processing parameters for compression molding of UD-composite plates

#### 4.1.2 Testing Procedure

Yarn profiles as well as yarn-yarn and yarn-metal friction coefficients were determined by using dynamic tensile tester (LH-402 CTT-DTT Attachment, Lawson Hemphill Inc. USA). A CCD camera was used to measure the yarn diameter values with 3.25 micron precision when the yarn was moving at a speed of 100 m/min. Yarn-metal and yarn-yarn friction coefficients were determined dynamically according to



ASTM D-3108, and ASTM D-3412. Tensile tests for yarns were executed with 20 specimens according to the norm DIN EN ISO 2062, with a clamping length of 500 mm and testing speed of 25 mm/min (Z100, Zwick GmbH & Co. KG). Tensile tests of UD-composites were executed according to DIN EN ISO 527-4. Upper and lower clamping areas were 50 mm each, and the testing lengths of the specimens were 150 mm. 0° specimens had a width of 15 mm and 90° specimens had a width of 25mm. 12 specimens for 0° and 8 specimens for 90° were tested for each twisting level and the reference. Testing speeds for both 0° and 90° were 2mm/min. Confidence intervals with 95% were determined according to Student's t-distribution.

## **4.2 Results and Discussion**

### **4.2.1 Commingled Yarn Structure**

Commingling process is based on the mixing of materials through an air nozzle. As in the air jet texturizing process, commingling process creates a special yarn structure with two different areas which are called as bulky and knot areas (figure 31). Continuous air pressure through the nozzle creates distinctive areas; in bulky region the materials are voluminous and open whereas in knot areas they are intermingled together. Various process parameters such as nozzle type, air pressure, take-up speed etc. affect the frequency and intermingling intensity of knot areas, however a fully control on this phenomenon is not possible. In the case of commingled yarns, a better mixture of reinforcement and matrix materials occurred in the knot area. Figure 31 demonstrates the cross-sectional observations from bulky and knot areas, dark points are polypropylene and the light points are glass filaments.

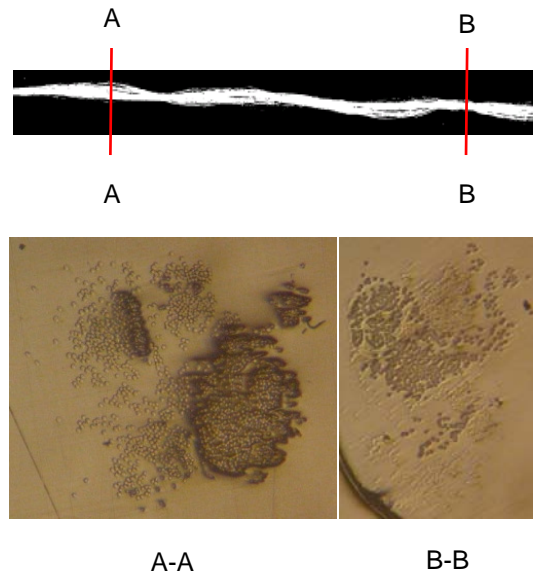


Figure 31: Cross-sectional observations of bulky (A-A) and knot (B-B) areas of GF/PP commingled yarns

Profile scanning results demonstrated a progressive improvement of commingled yarn evenness with increasing twist (figure 32). Bulky and sticky regions on commingled yarns were the main cause of production stops during weaving. The number of events, which is defined as  $\pm 50\%$  variations in yarn diameter, was decreased from 42 events/m to the interval of 30-35 events/m for all twisting ratios.

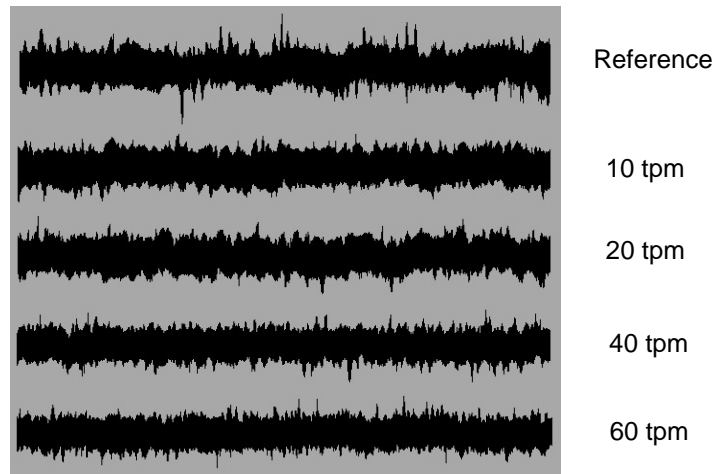


Figure 32: Comparison of GF/PP commingled yarn profile, from top to bottom; reference commingled yarn, 10tpm, 20tpm, 40tpm, 60tpm

Mean values of yarn diameter (figure 33) were increased for 0 tpm and 5 tpm samples, which was caused by the effect of the additional process step. After 10 tpm, yarn diameter decreased gradually. The standard deviation of every sample was less than the reference commingled yarn, thus more regular yarn structure was generated. Small yarn diameters enable denser packing of material during weaving. 3rd degree regression polynomial in figure 33 has a local minimum around 55 tpm. After 60 tpm the diameter would not change significantly, however, the regression polynomial increases. Therefore the regression polynomial can be used for interpolation between the twisting values of 0 tpm and 60 tpm, but twisting values more than 60 tpm cannot be estimated with extrapolation.

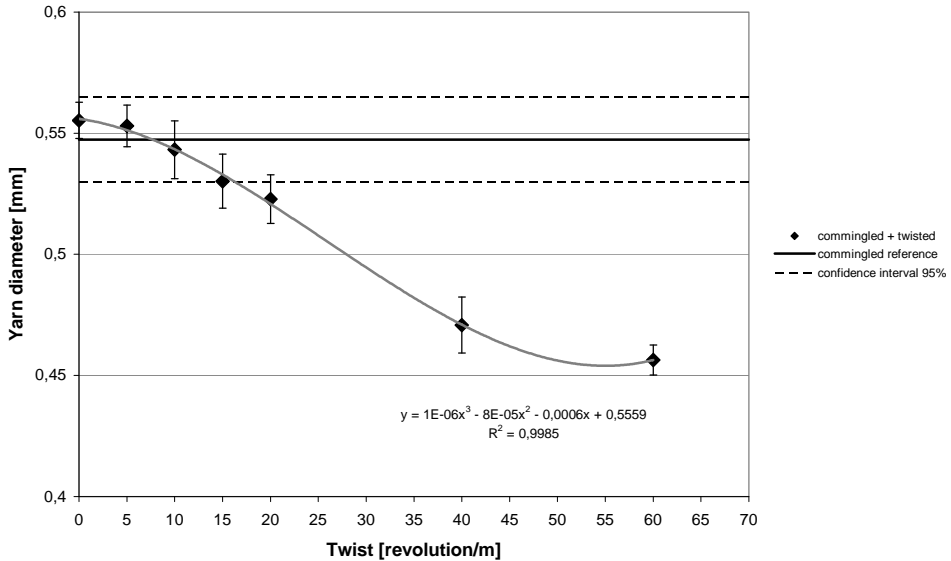


Figure 33: Effect of twisting on the diameter of GF/PP commingled yarns

#### 4.2.2 Commingled Yarn Friction Properties

In the literature the increase of friction coefficient for both yarn-to-yarn and yarn-to-metal with increasing twist values of multifilament yarns was reported [54]. Increasing twisting levels decreases the cross-sectional area and increases the hardness. The overall structure as well as the surface of commingled yarns are different than multifilament yarns. Twisting increases the surface roughness of a conventional multifilament yarn. On the other hand, commingled yarns already have a high surface unevenness caused by the air-nozzle during production. Twisting increases the surface evenness of a commingled yarn which generates a tendency of decrease in coefficient of friction. Friction coefficient depends on the interaction of both touching surfaces. In the case of yarn-metal experiments, polished surface of the metal part suppressed the reduction tendency for the coefficient of friction. On the other hand, yarn-yarn friction had a linear decrease with increasing twist levels (figure 34). Yarn-metal friction coefficient increases with the increase of testing speed, so during weaving weft yarns yield around 20 % higher friction coefficients than warp yarns.

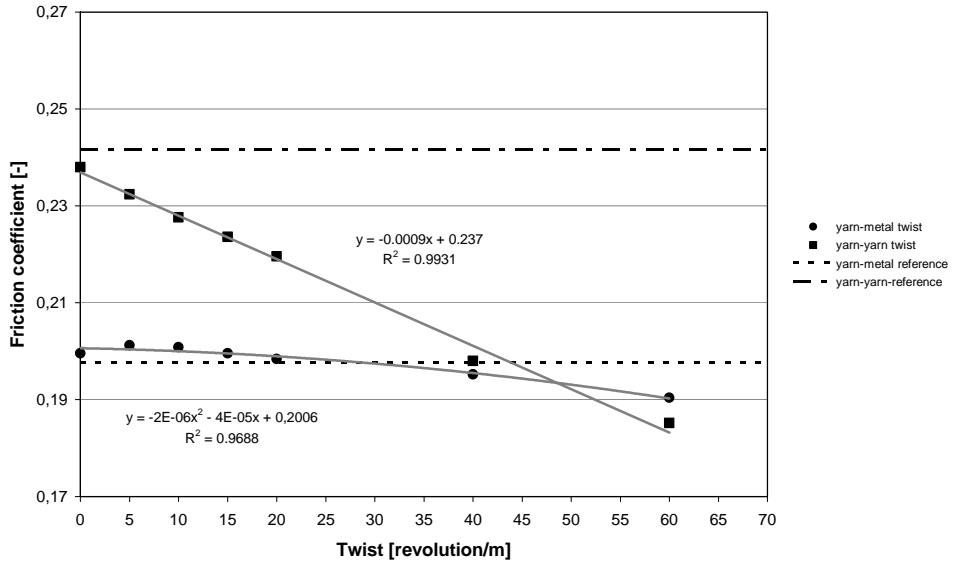


Figure 34: Effect of twisting on yarn-yarn and yarn-metal friction of GF/PP commingled yarns

### 4.2.3 Yarn Mechanical Properties

Figure 35 demonstrates the two different regions of commingled structure, therefore, the modulus of elasticity was modeled with two linear bar elements. This model aims to represent the varying contribution of the bulky and knot regions of commingled yarns on the tensile modulus. In the bulky region, voluminous structure is mainly created by the matrix material (PP), while reinforcing material (GF) remains straight. In the knot region, over-delivery of reinforcing material is consumed by the intensive intermingling. The two elements in figure 35 represent the bulky area with straight reinforcement and the knot area with intermingled reinforcement yarns. The boundary of bulky and knot region cannot be always clearly defined. In addition, the intensity of intermingling in knot regions varies too. Under tensile loading, actual commingled yarns change their internal structure and yield a bi-modular behavior. In the following model, bi-modular behavior and the transition regions are omitted to simplify the analysis.

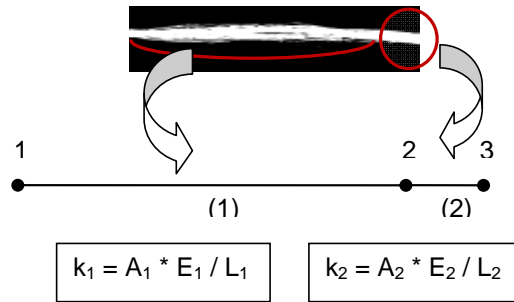


Figure 35: Yarn structure and model for determining the E-modulus of commingled yarns

The overall E-modulus was determined by the stiffness equation of serial springs (Equation 14)

$$\frac{1}{k} = \frac{1}{k_1} + \frac{1}{k_2} \quad (14)$$

After putting the stiffness values of  $k_1$  and  $k_2$  into Equation 2, with the same cross-sectional areas  $A$ ;

$$\frac{L_1 + L_2}{E * A} = \frac{L_1}{E_1 * A} + \frac{L_2}{E_2 * A} \quad (15)$$

The assumption of same cross-sectional area is valid because the total area of the constituent fibers in the cross-section is same everywhere.

Rewriting equation 15;

$$E = \frac{E_1 * E_2 * (L_1 + L_2)}{L_1 * E_2 + L_2 * E_1} \quad (16)$$

In the literature a model was derived from laminate theory to determine the effect of twist on the E-modulus of some technical yarns such as Kevlar<sup>®</sup>, Vectran<sup>®</sup> etc. [55]. The model is in very good agreement with experimental data. Twisted yarn samples in those experiments should yield reduction of modulus which is caused by both the structural change by twisting and the yarn damage throughout processing. However, the damage on the yarns caused by twisting was not considered. Another previous study predicted the relation between twisting angle and E-modulus of Nylon yarns with Equation 17 [56]. This equation progressively overestimated the E-modulus of technical yarns [55]. This slight overestimation compared with the experimental results is more reasonable to isolate only the effect of twisting without considering the yarn damage. Therefore, in this study Equation 17 was utilized to determine the reduction in modulus of elasticity caused by twisting.

$$E_{re}(\alpha) = E_z * \cos^2(\alpha) \quad (17)$$

Over-delivery of input materials in commingling process is necessary in order to create the knot areas, and most of the additional material length is integrated in these areas because the bulky region can easily be stretched during further processing. The twist angle equivalent of over-delivery ratio was calculated according to Equation 18, where  $\alpha_{od}$  is the twist angle equivalent caused by over-delivery and  $OD$  (%) is the over-delivery of input material.

Over-delivery of the reinforcement material within commingled hybrid yarn can be approximated as an angle distortion of a lamina. The input length of the reinforcement material is the hypotenuse of a right triangle and the output length is the adjacent side. Figure 36 demonstrates this approximation where  $OD$  is the over-delivery as percentage and  $\theta$  is the angle of distortion.

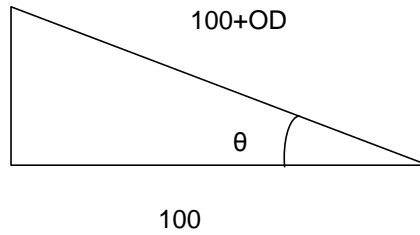


Figure 36: Equivalent angle distortion caused by over-delivery of reinforcing material

The inverse trigonometric function of cosine gives the equivalent of the distortion angle as shown in the equation 18.

$$\alpha_{od} = \cos^{-1}\left(\frac{100}{100 + OD}\right) \quad (18)$$

According to the assumption that the over-delivered material is mainly consumed in the knot areas, where the length is a ratio of overall yarn length, Equation 18 can be rewritten as;

$$\alpha_{od,i} = \cos^{-1}\left(\frac{100 * \frac{L_i}{\sum_{j=1}^n L_j}}{100 * \frac{L_i}{\sum_{j=1}^n L_j} + OD_i}\right) \quad (19)$$

Equation 19 is the general expression of how to distribute the angle distortion between n linear bar elements. The subscript i was used to distribute the overall over-delivery on the commingled yarn to the identified number of different regions.  $\alpha_{od,i}$  stands for the angular distortion of the particular region and  $L_i$  is the representative length of that region. The summation symbol with  $L_j$  stands for the total representative length of the yarn. According to the model in figure 35 there are two regions which represent the bulky and knot areas.



Twist angle  $\alpha_{tw}$  (degree) can be calculated according to the Equation 20, where  $d_{av}$  (mm) is the average yarn diameter and  $tw$  (tpm) is the twist value per meter.

$$\alpha_{tw} = \tan^{-1}\left(\frac{\pi * d_{av} * tw}{1000}\right) \quad (20)$$

The total twist angle  $\alpha_t$  is determined through superposition of the nominal twisting angle  $\alpha_{tw}$  and the twist angle equivalent of over-delivery  $\alpha_{od}$  as in Equation 21. After putting Equation 21 into Equation 17, Equation 22 can be generated, which was used to calculate the modulus of elasticity of one element in figure 35.

$$\alpha_t = \cos^{-1}\left(\frac{100 * \frac{L_i}{\sum_{j=1}^n L_j}}{100 * \frac{L_i}{\sum_{j=1}^n L_j} + OD_i}\right) + \tan^{-1}\left(\frac{\pi * d * tw}{1000}\right) \quad (21)$$

$$E_{re\_i}(\alpha) = E_i * \cos^2\left\{\cos^{-1}\left(\frac{100 * \frac{L_i}{\sum_{j=1}^n L_j}}{100 * \frac{L_i}{\sum_{j=1}^n L_j} + OD_i}\right) + \tan^{-1}\left(\frac{\pi * d * tw}{1000}\right)\right\} \quad (22)$$

With the introduction of damage factor to the Equation 16 and the rule of mixtures the final equation for the determination of E-modulus becomes;

$$E_{re}(\alpha) = D_r(\alpha_{tw}) * \frac{E_{r1} * E_{r2} * (L_1 + L_2)}{L_1 * E_{r2} + L_2 * E_{r1}} * Vf + \frac{E_{m1} * E_{m2} * (L_1 + L_2)}{L_1 * E_{m2} + L_2 * E_{m1}} * (1 - Vf) \quad (23)$$

Where  $E_{r1}$  is E-modulus of reinforcement element 1 (bulky region),  $E_{r2}$  is E-modulus of reinforcement element 2 (knot region),  $E_{m1}$  is E-modulus of matrix element 1 (bulky region),  $E_{m2}$  is E-modulus of reinforcement element 2 (knot region). All E-moduli are calculated with Equation 22.  $D_r$  is the damage factor which is a function of twist angle

$\alpha_{tw}$  and multiplies only the reinforcement elements.  $V_f$  is the volume fraction of the reinforcing material.

Some simplifications and assumptions were done for the calculations. Based on the visual information, the length of the bulky region was approximately 9 times the length of knot region which was reflected in the model with the length of elements. The reduction of E-modulus through twisting was mainly caused by the damage on the material because the orientation of the reinforcement material was not significantly affected within the trials. Over-delivery of glass yarns were 2%, in the calculations it is assumed that all this extra length is integrated into the knot area. Over-delivery of polypropylene was 8%, in the calculations it was assumed that the additional length was equally consumed in both bulky region and knot areas. An interesting phenomenon was the increase of both breaking force and E-modulus of commingled yarns after further processing. After twisting with  $0^\circ$  (only winding), yarn samples had higher E-modulus and breaking force than the reference yarn (figure 37). This is caused by the restructuring of the knot areas under tension, the yarn was stretched and the orientation of the reinforcement material in knot areas was increased. Figure 37 demonstrates the E-modulus and breaking force comparison of twisted and reference GF/PP commingled yarns. 40 tpm sample had almost same E-modulus and breaking force values as the reference sample. Reduction of E-modulus started with 60 tpm sample however the breaking force was still same as the reference yarn. These results indicate that the higher intermingling of filaments through twisting increases the mechanical properties of commingled yarns. Damage on glass fibers cannot be easily detected with yarn testing.

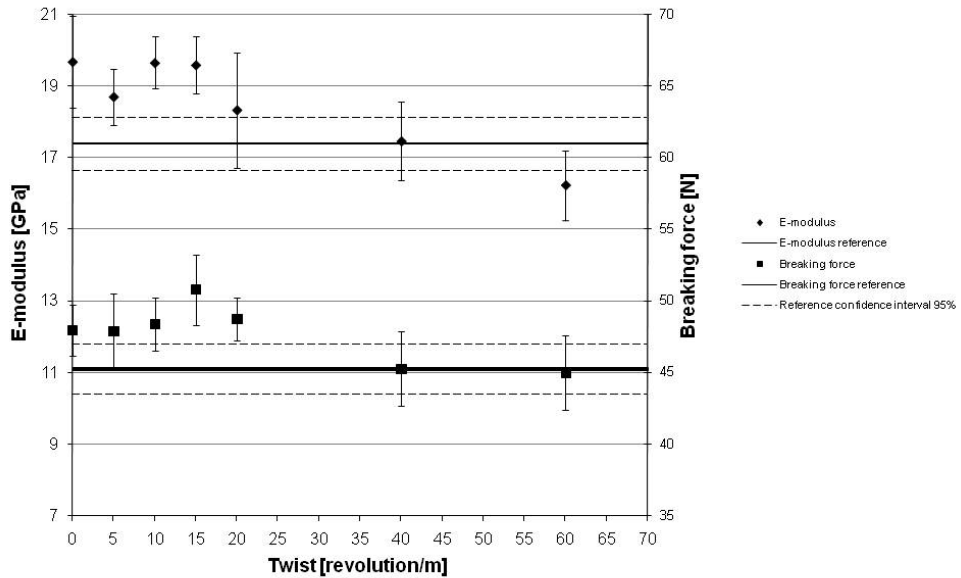


Figure 37: Effect of twisting on E-modulus and breaking force of GF/PP commingled yarns

By using Equations 22 and 23, theoretical E-modulus values were calculated for all the samples. Calculated theoretical E-modulus values were divided into 4 regions (figure 38) which were; measured E-modulus values during experiments as in figure 37, loss of E-modulus caused by over-delivery during commingling (Equation 19), loss of E-modulus caused by twisting (Equation 20) and loss of E-modulus caused by the commingled process damage (difference between the theoretical E-modulus and the sum of the mentioned 3 regions). Although the y-axis presents the percentage of the regions within theoretical E-modulus values, the nominal E-modulus values (GPa) can be seen on the histograms. These results indicate that the commingling process reduces the yarn stiffness almost 50%. The damage factor  $D_r$  of equation 23 was taken as 1.0 in order to show the deviation from the theoretical modulus values.  $D_r$  (around 0.5) can be used as an adjustment parameter to fit the experimental data. It is an important question whether the E-modulus reduction of commingled yarns affects the E-modulus of UD-composites in the same fashion.

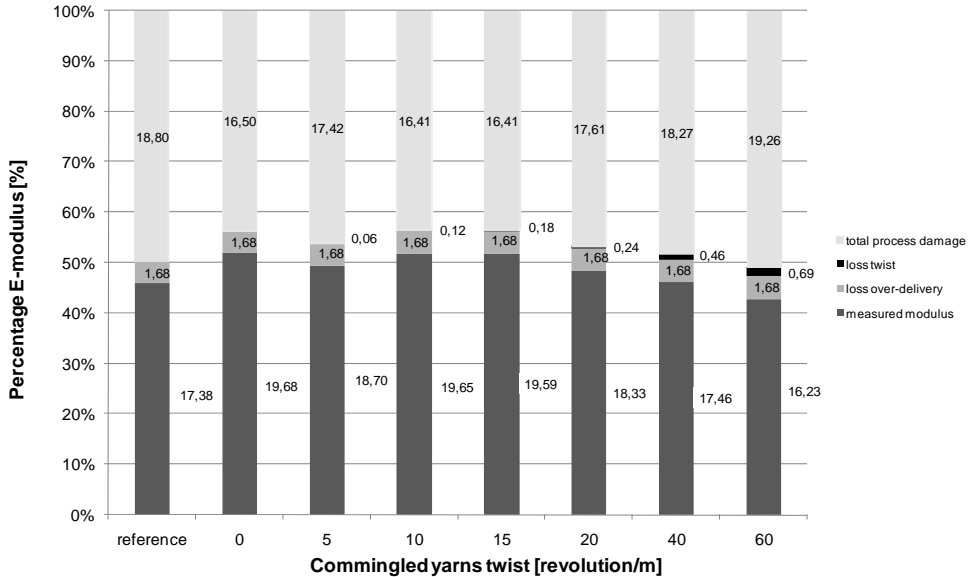


Figure 38: Distribution of E-modulus parts; difference between theoretical and measured modulus values

#### 4.2.4 UD-Composite Properties

The  $0^\circ$  and  $90^\circ$  E-modulus calculations were executed according to laminate theory [4, 5]. Unlike the calculations for yarn E-modulus, UD-composite calculations were based on the homogeneous distribution of the glass filament in the PP matrix. Off-axis angle equivalent of over-delivery value for glass yarn was integrated to the equation, thus the UD composites structures were assumed to have a slight angle distortion.

Slab models deliver sufficient approximation to the elastic constants of a lamina. Within this model, aligned long fiber composites were treated as if the two constituents of matrix and reinforcement are bonded together. Relative thicknesses of slabs were determined according to the volume fractions of fiber and matrix. Interface regions as well as local stress concentrations were ignored.  $E_L$  (E-modulus fiber direction) is calculated according to equal strain assumption for both matrix and fiber in longitudinal direction. The equation 24 is also called as “the rule of mixtures” and delivers a very good approximation. Discrepancies may result from the different

poisson's ratios of matrix and reinforcement, however, it can be theoretically proved by the Eshelby model that the deviation is small under all conditions [57, 58].

$$E_L = E_{Lf} * Vf + E_m * (1 - Vf) \quad (24)$$

Transverse modulus of a composite with unidirectional fibers can also be approximated by a slab model which assumes an equal stress condition for matrix and fibers. The stress field is complex under transverse loading and in the literature, especially for thermoplastic matrices, underestimation of transverse modulus was reported. The modified equation for the transverse modulus contains a correction factor  $\eta$  [5, 59, 60]. If  $\eta$  is taken as 1, the equation becomes the usual expression derived from an equal stress assumption for matrix and reinforcement. In order to fit the experimental data,  $\eta$  was taken as 0.6 which compensates the above mentioned underestimation of transverse modulus.

$$E_T = \frac{Vf + \eta * (1 - Vf)}{\frac{Vf}{E_{Tf}} + \frac{\eta * (1 - Vf)}{E_m}} \quad (25)$$

The expression for the in-plane shear modulus is analogous to the expression of transverse modulus because it assumes equal shear stress on the matrix and fibers. In order to avoid the underestimation,  $\eta'$  parameter with 0.6 is applied in the calculations.

$$G_{12} = \frac{Vf + \eta' * (1 - Vf)}{\frac{Vf}{G_{12f}} + \frac{\eta' * (1 - Vf)}{G_m}} \quad (26)$$

Since the equal strain assumption is applicable to a UD lamina, the poisson's ratio can be determined by "the rule of mixtures".

$$\nu_{12} = \nu_{12f} * Vf + \nu_m * (1 - Vf) \quad (27)$$

According to the above expression, 2% over-delivery of glass filaments was equivalent to 11.36° off-axis angle distortion. The off-axis longitudinal and transverse stiffness were calculated according to laminate theory. The relation between stress and strain tensors in the principal material direction is given in Equations 28.

$$\{\sigma\} = [Q]\{\epsilon\}$$

$$[Q] = \begin{bmatrix} Q_{11} & Q_{12} & 0 \\ Q_{12} & Q_{22} & 0 \\ 0 & 0 & Q_{66} \end{bmatrix}$$

$$Q_{11} = \frac{E_1}{1 - \frac{\nu_{12}^2 E_2}{E_1}}$$

$$Q_{12} = \frac{\nu_{12} E_2}{1 - \frac{\nu_{12}^2 E_2}{E_1}}$$

$$Q_{22} = \frac{E_2}{1 - \frac{\nu_{12}^2 E_2}{E_1}}$$

$$Q_{66} = G_{12} \quad (28)$$

The transformation of the stresses from principal material direction to an arbitrary coordinate system can be done with a modified reduced-stiffness matrix [Q] as in Equations 29, where  $m = \cos \theta$  and  $n = \sin \theta$ .

$$[Q'] = \begin{bmatrix} Q'_{11} & Q'_{12} & Q'_{16} \\ Q'_{12} & Q'_{22} & Q'_{26} \\ Q'_{16} & Q'_{26} & Q'_{66} \end{bmatrix}$$

$$Q'_{11} = Q_{11}m^4 + Q_{22}n^4 + 2m^2n^2(Q_{12} + 2Q_{66})$$

$$Q'_{12} = m^2n^2(Q_{11} + Q_{22} - 4Q_{66}) + (m^4 + n^4)Q_{12}$$

$$Q'_{16} = [Q_{11}m^2 - Q_{22}n^2 - (Q_{12} + 2Q_{66})(m^2 - n^2)]mn$$

$$Q'_{22} = Q_{11}n^4 + Q_{22}m^4 + 2m^2n^2(Q_{12} + 2Q_{66})$$

$$Q'_{26} = [Q_{11}n^2 - Q_{22}m^2 + (Q_{12} + 2Q_{66})(m^2 - n^2)]mn$$

$$Q'_{66} = (Q_{11} + Q_{22} - 2Q_{12})m^2n^2 + Q_{66}(m^2 - n^2)^2 \quad (29)$$

The modulus in the arbitrary x and y directions are defined as in Equations 30.

$$E_x = Q'_{11} - \frac{Q'^2_{12}}{Q'_{22}}$$

$$E_y = Q'_{22} - \frac{Q'^2_{12}}{Q'_{11}} \quad (30)$$

Stiffness value in longitudinal direction is found as 34.13 GPa which is underestimating the experimental results. Experimental results of longitudinal E-modulus in figure 39 show agreement with the nominal stiffness values according to the rule of mixtures. This indicates that the angle distortion caused by the over-delivery is disappeared during compression molding under tension. Modulus of elasticity in 0° direction is not much affected from twisting. Statistically, only the modulus of elasticity of the 60 tpm sample can be regarded as a reduction. On the other hand, the effect of further processing can be easily seen from the tensile

strength reduction starting immediately with 0 tpm sample. All the samples had an overall tendency of strength reduction, however, between 0 tpm and 60 tpm samples, it cannot be concluded that higher twist reduces the strength more than lower twist.

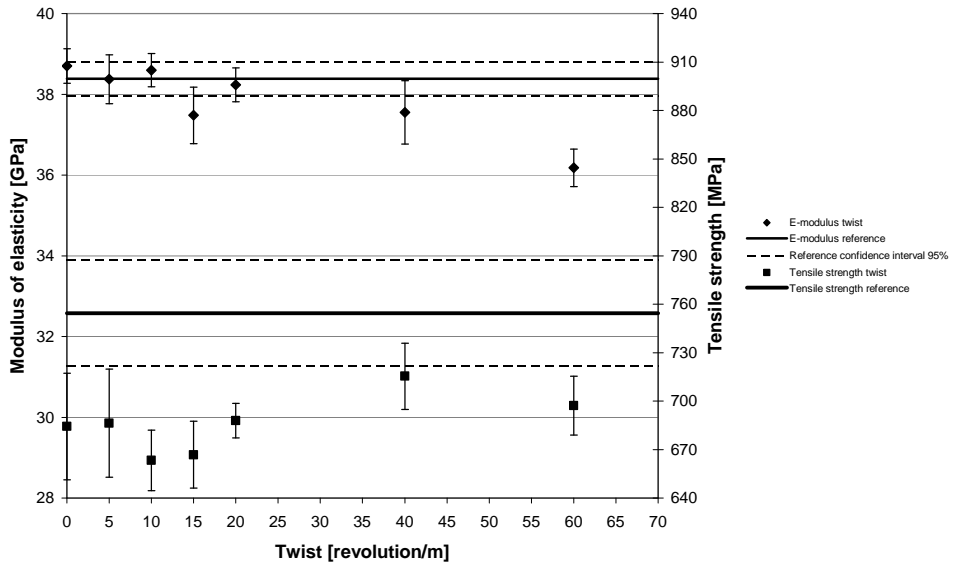


Figure 39: Modulus of elasticity and tensile strength of UD composites from GF/PP commingled yarns in 0°

Lamina stiffness calculation in transverse direction, 3.98 GPa, is in good agreement with overall experimental results (figure 40). It can be seen in figure 33 that the yarn diameter is decreasing after 10 tpm. As the UD performs were prepared with the same amount of material, increasing compactness of the reinforcement material leads to greater resin rich areas. This reduces the E-modulus in transverse direction. Transverse tensile strength shows a slight reduction tendency with increasing twist level.



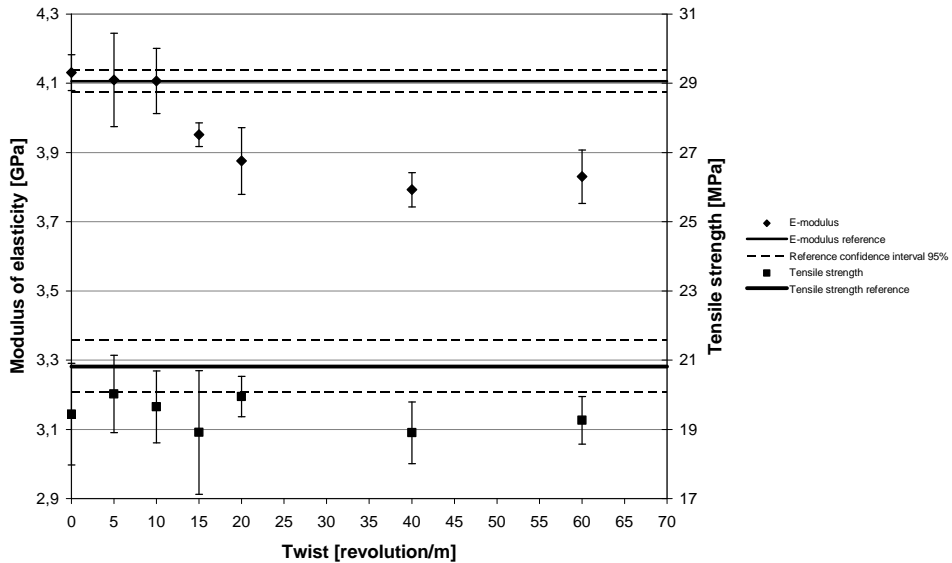


Figure 40: Modulus of elasticity and tensile strength of UD composites from GF/PP commingled yarns in 90°

### 4.3 Conclusion

Effects of twisting on the mechanical properties of GF/PP commingled yarns are analyzed. This study is initiated through the production stops caused by the open and sticky commingled yarn structure during weaving of dense 3D woven preforms. A decreasing tendency of the yarn friction coefficient is observed unlike the results of other studies in the literature. The decrease is almost linear for yarn-yarn friction. Twisting decreases the average yarn diameter and creates a more compact and even structure. In commingled yarns, two distinctive areas can be recognized. These areas have varying mixing quality and yarn consumption. Increase of both E-modulus and tensile strength of commingled yarns are observed until 40tpm. A model is presented to calculate the yarn distortion effects on the E-modulus for over-delivery and twisting. Most of the E-modulus reduction can be explained with the damage on the material and structure change. The differences between the theoretical and calculated values were not observed in the UD-experiments. Longitudinal UD E-modulus values lay close to the theoretical values. A statistically confident reduction was observed after 40 tpm. However UD tensile strength values of twisted samples

were around 10% less than the reference commingled yarn. E-module in transverse direction starts decreasing with 20 tpm which correlates with the reduction in yarn diameter. A slight decrease in transverse tensile strength was observed. Twist application on commingled yarns creates more compact yarn structure which can increase productivity in dense woven preform manufacturing. Up to 20 tpm twist levels can be applied where a longitudinal strength reduction of about 10% can be tolerated without any E-modulus reduction.

## **Chapter 5 - Mechanical Characterization of 2D Woven**

### **Preforms and Composite Panels from GF/PP**

#### **Hybrid Yarn**

Before starting with the target woven spacer fabrics, it is important to execute experiments concerning the mechanical characteristics of 2D woven fabrics and their composites. The aim of this section is to determine the process damage on the reinforcement material as well as the effect of structural parameter in particular weft density and number of plies.

Compression molding causes significant change of thickness during consolidation of thermoplastic matrix preforms. If a constant weave is selected, increasing the weft density results in higher weight per unit area as well as a higher thickness of the final composite. On the other hand higher weft density changes the inner structure of the woven fabric and processing conditions. A weaving machine with a dobby shed opening mechanism has a limited number of heddle frames (mostly up to 24). The weaving machine, which was used for the development of spacer fabrics, had 16 heddle frames. Spacer fabrics with woven cross-links have four different areas, two for upper and lower layers and two for the cross-links. The production principle will be explained in the following sections. These four areas have four heddle frames each for the construction of weave. Figure 41 demonstrates the selected double layer X-twill weave for the woven areas of spacer fabrics. Double layer woven fabric provides sufficient thickness after compression molding, and the X-twill weave is homogenous due to its both diagonal directions. Usual twill weaves have only one diagonal direction which results in anisotropic in-plane mechanical properties.



Figure 41: X-twill weave (left) L: lower weft yarn, U: upper weft yarn, and woven fabric (right)

## 5.1 Experimental

### 5.1.1 Materials

Woven fabrics with the above defined weave were produced with weft densities of 7, 8, 9 and 10 yarn/cm. Warp density was 20 yarn/cm for every sample. Commingled hybrid yarns, which were defined in section 4, were used both as warp and weft yarns. Compression molding technique was used with the same settings of section 4. In order to increase the wall thickness of spacer fabrics, it is possible to lay flat woven fabrics above and under the spacer fabrics, and they can be pressed together. Therefore, within the design of experiments, 1, 2 and 3 layers of flat woven fabrics were consolidated and tested.

### 5.1.2 Testing procedure

Tensile tests were executed according to DIN EN ISO 527-5. Upper and lower clamping areas were 50 mm each, and the testing lengths of the specimens were 150 mm. Both weft and warp direction samples had the width of 25 mm. Testing speed were 2 mm/min. 4 point bending tests were executed according to DIN EN ISO 14125. Sample length was 60 mm and sample width was 15 mm. Testing speed of bending was 2 mm/min. Charpy impact test was executed according to ISO 179-2. Confidence intervals with 95% were determined according to Student's t-distribution.

## 5.2 Results and Discussions

Fabric mass per unit area increases with the increase of weft density. Table 4 demonstrates the variation of mass per unit area for the woven fabric samples with 7-10 yarn/cm. This increase directly affects the final composite thickness which is shown in table 5.

Weft density [yarn/cm]	7	8	9	10
Mass per unit area [g/dm <sup>2</sup> ]	11.307	11.960	12.389	13.065

Table 4: Relation between weft density and mass per unit area

		Weft density [number of yarns/cm]			
		7	8	9	10
Number of Layers	1	0,68mm	0,71mm	0,73mm	0,77mm
	2	1,36mm	1,4mm	1,46mm	1,53mm
	3	2,03mm	2,1mm	2,19mm	2,28mm

Table 5: Thicknesses of consolidated woven fabrics

Changing of process parameters on the weaving machine also changes the amount of damage on the materials. Process damage on the materials during weaving is mainly caused by friction through feeding, shear and bending caused by the heddle frames, shear stresses caused by beat-up and the friction and buckling caused by the take-up motion. Conventional materials such as cotton compensate these stresses with their internal elongation. Reinforcement materials such as glass fibers are mostly brittle and they are prone to damage particularly under bending along a small radius. In this sense, heddle frames are the most critical machine elements where process damage occurs. Changing of weft density also changes the flow rate of material, thus higher weft density results in higher number of cycles of warp yarns through the heddle frames. Figure 42 depicts the schematic of shed opening.

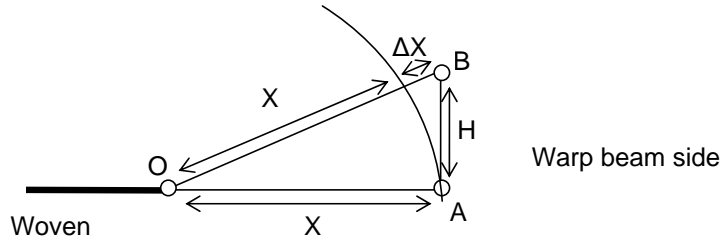


Figure 42: Schematic of shed opening

The elongation of technical yarns is negligible, so the position change of eyelet from point A to point B is compensated from the warp beam side. Any point on the warp yarn must travel the distance  $\Delta X$  through the eyelet of heddle frame. Weft density determines the number of cycles, in which the warp yarn can pass through this distance under buckling and shear stresses.  $\Delta X$  can be calculated according to the equation 31 where  $X$  is the distance between the woven fabric line and the horizontal position of eyelet, and  $H$  is the distance between the horizontal position and the maximum height of eyelet.

$$\Delta X = \sqrt{X^2 + H^2} - X \quad (31)$$

In every cycle of the weaving machine, warp yarns travel the distance  $TD$  which is the inverse of weft density  $WD$  (equation 32).

$$TD = WD^{-1} \quad (32)$$

In order to find the number of cycles  $NC$  for warp yarns to pass through the heddle frames, the expression of  $\Delta X$  is divided by the travel distance in one cycle  $TD$  which gives:

$$NC = \left[ \sqrt{X^2 + H^2} - X \right] * WD \quad (33)$$

From equation 33, it can be seen that the number of cycles to pass through the heddle frame is directly proportional to the weft density. Therefore it is expected to have higher damage on the warp yarns processed with higher weft densities.

Figure 43 compares the breaking force of unprocessed reference GF/PP commingled yarns and the processes steps after warp beam preparation and the woven fabric manufacturing with different weft densities. As expected, the tendency of reduction in breaking force can clearly be seen both on the weft and the warp yarns.

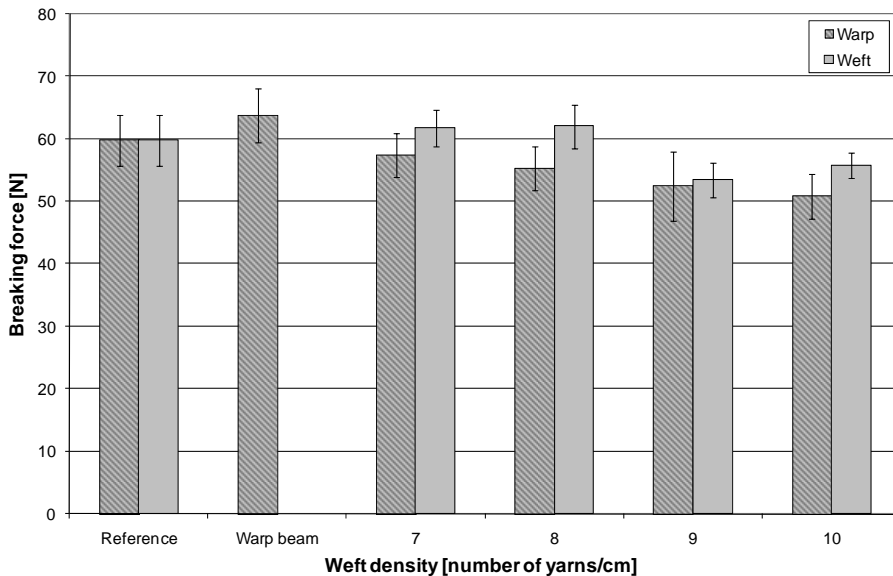


Figure 43: Change of yarn tensile strength after beaming and weaving

Woven fabric tensile test results are depicted in figure 44. The tendency of breaking force reduction of fabrics in warp direction with increasing weft density is higher in comparison with the tendency of individual yarns. The reason for this phenomenon is that both warp yarn crimp and damage on the yarn increases with higher weft density. In weft direction, breaking force increases with higher weft density simply due to the increased number of yarns. Therefore the process damage cannot be seen directly from the breaking force of the fabric.

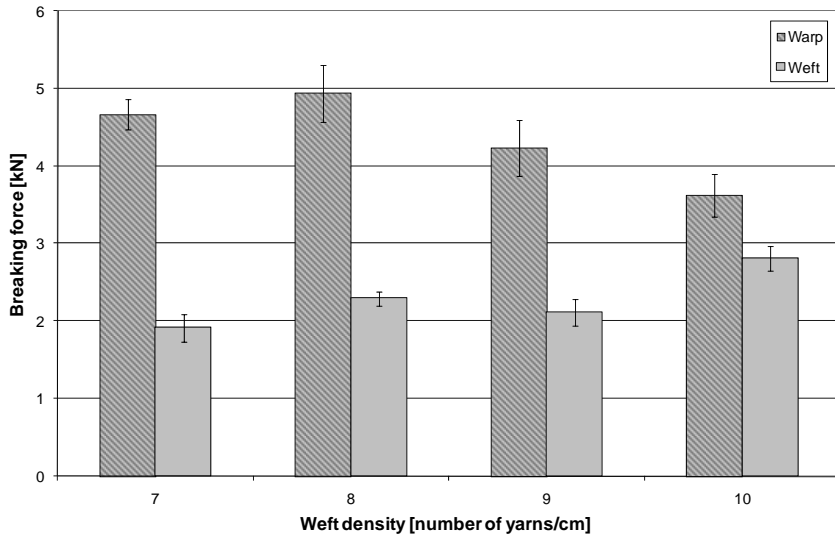


Figure 44: Tensile strength of woven fabrics with different weft densities

Compression molding causes extensive deformation of woven fabrics in the normal direction. Depending on the process conditions and the fabric structure, the thickness of the final composite is around 20% of the thickness of woven fabric. This deformation in the normal direction results in the sinus form of warp yarns, which can be seen in figure 45 for different weft densities. It can be clearly seen from the figure that the increasing weft density also increases the lateral deformation. Thus the period of sinus form in the sample with the weft density of 10 yarn/cm is shorter than that of the sample with the weft density of 7 yarn/cm.



Figure 45: Composite surfaces with weft densities of 7 to 10 from left to right



Figure 46 – 48 demonstrate the results of tensile tests in warp and weft directions with weft densities 7-10 and 1-3 plies. Increasing weft density slightly increases both modulus of elasticity and tensile strength in weft direction. Higher weft density changes the structure of the reinforcement particularly the curvature of warp yarns along the weft yarns increases. Higher curvature of warp yarns results in smaller resin rich areas which has a positive effect on tensile behavior. On the other hand higher weft density reduces the modulus of elasticity and tensile strength drastically. Process damage on the warp yarns are higher with higher weft density (figure 43), but the reduction of properties is mainly caused by the distortion of the reinforcement material.

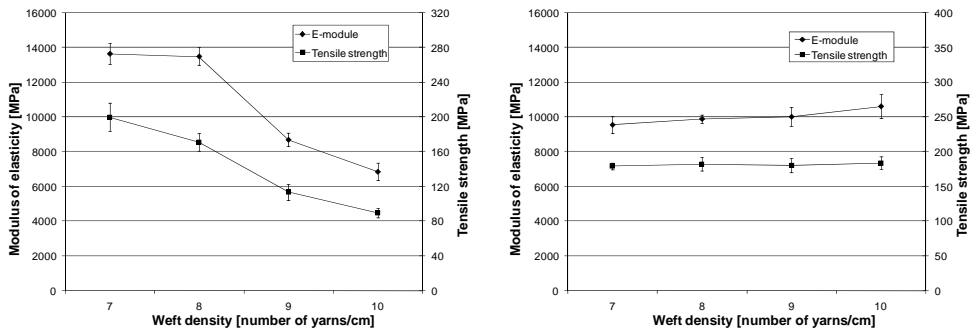


Figure 46: Modulus and tensile strength of 1 layer consolidated fabrics in warp direction (left) and weft direction (right)

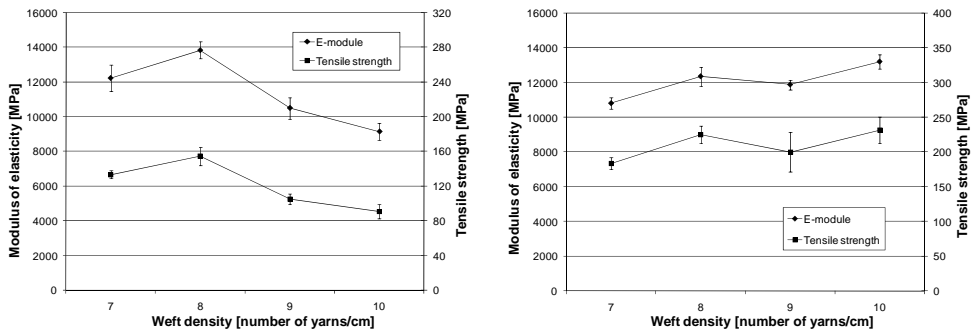


Figure 47: Modulus and tensile strength of 2 layer consolidated fabrics in warp direction (left) and weft direction (right)

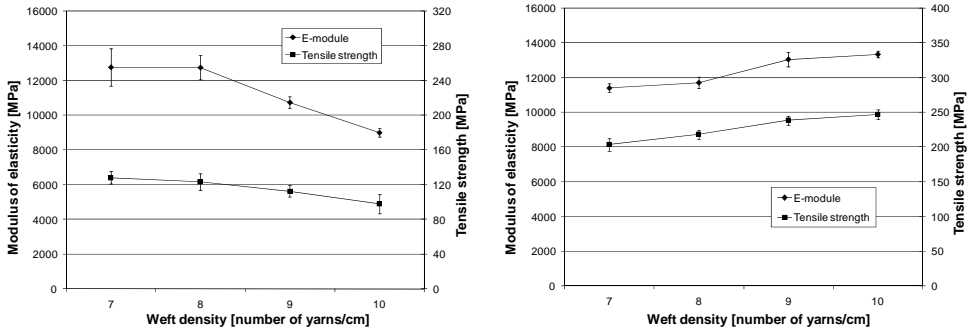


Figure 48: Modulus and tensile strength of 3 layer consolidated fabrics in warp direction (left) and weft direction (right)

Bending and impact tests were conducted with two and three layers consolidated woven fabrics. One layer fabrics did not have the sufficient thickness. Flexural strength increases with increasing weft density in the weft direction. However, flexural strength reduces with increasing weft density in the warp direction (figure 49). Impact strength is mostly affected by the thickness of the samples, therefore, increasing of weft density and the number of plies increases the total impact energy (figure 50).

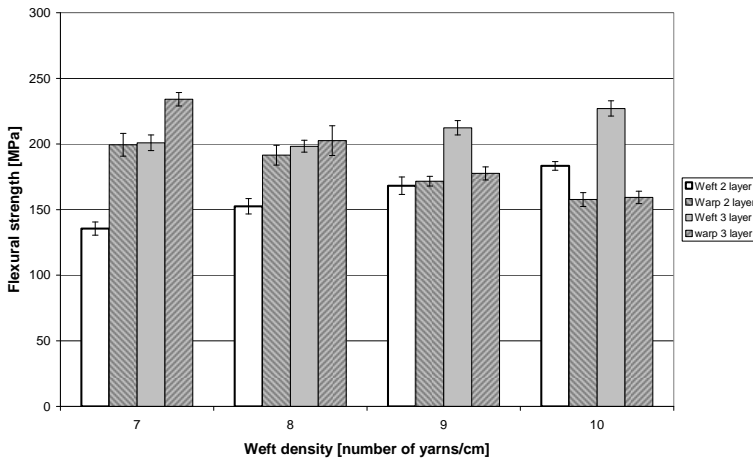


Figure 49: Flexural strength of 2 and 3 layer consolidated fabrics in warp and weft direction

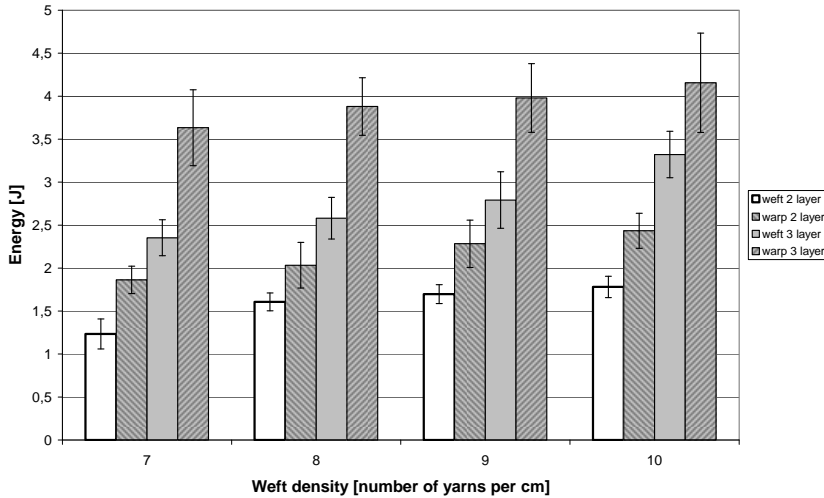


Figure 50: Impact strength of 2 and 3 layer consolidated fabrics in warp and weft direction

### 5.3 Conclusion

Woven fabrics with commingled yarns are subject to extensive deformation in the out-of plane direction when manufactured by hot press molding. Higher weft density increases the final composite thickness, however, it also increases the crimp of warp yarns, thus reduces the in-plane mechanical properties. Increasing weft density increased the damage both on weft and warp yarns. Single, double and triple layers of separate woven fabrics were pressed and consolidated with four different weft densities. In warp direction, significant decrease of modulus and strength was observed mainly due to the increasing crimp of internal structure. In weft direction, a slight increase of modulus and strength with increasing weft density was observed which was caused by the compact reinforcement structure and the reduced resin rich areas

According to these results, higher crimp which was caused by higher weft density reduces the tensile properties significantly. Therefore, the yarn crimp should be avoided inside the woven structure. It is advantageous for tensile properties to adjust the component thickness by multiple layers of woven fabrics with lower weft density instead of using fewer layers of woven fabrics with higher weft density.

## Chapter 6 - Principals of Spacer Fabric Production

According to the mentioned frame under state of the art, development of woven sandwich perform structures are necessary to extend the use of thermoplastic matrix composites in demanding structural applications. As for every technology aiming a wide spread application, cost is an important aspect which should be considered from the very beginning of the development. Proper use of automation can both increase the product quality as well as decrease the production costs significantly.

### 6.1 Terry Weaving Technology

Novel woven sandwich preforms should have two outer woven layers which are connected also with woven layers. This is necessitated in order to use commingled yarns in the structure and consolidate the thermoplastic matrix easily. Main difficulty in producing such woven sandwich preforms is how to create woven structures of crosslinks which lay normal to the fabric plane. The terry weaving technology, which is used for terry towel production, proves suitable as the basis.

Figure 51 demonstrates the production principle of the terry weaving in four steps:

- Step I: Weaving starts with a regular base fabric "B" of any kind. In the figure take-up direction "T" is shown with a solid arrow from right to the left near the base fabric. Additional temporary take-up of terry weaving mechanism "TW" is also shown with a dotted solid arrow. This mechanism is explained under step III. Care should be taken that the "TW" and "T" act together and simultaneously. Beat-up motion of the reed "R" is shown with a solid and a transparent reed element.
- Step II: When the required position of the stiffener fabric "S" is reached, the warp yarns of the base fabric "B" is divided into two groups. One of the warp yarn groups continue to weave with the inserted weft yarns and create the stiffener fabric "S". The other warp yarn group however does not connect with the weft yarns and create a yarn floating "F" under the stiffener fabric. An

important aspect is that the stiffener layer is not necessarily always on the top. The positions of stiffener "S" and floating "F" structures are interchangeable.

- Step III: After the double length of the required stiffener height is woven, the floating yarns and the stiffener fabric are woven together as one layer over a couple of connecting weft yarns "C". In this moment the fabric is still flat and the weaving machine necessitates two additional mechanisms to remove the floating yarns out of the structure back to the warp beam direction. First mechanism moves the fabric back to the shed, which is called terry weaving mechanism. Terry weaving mechanism is an additional take-up device which stores exactly the same length of the floating warp yarns "F" step by step. After completing the stiffener "S" and the connection section "C", the additionally stored length is suddenly moved back to the shed. This sudden motion is demonstrated with a longer dotted arrow "TW" from left to the right. Second mechanism pulls back the now loose floating yarns and give them again tension. Beat-up moves the connection section "C" to the base fabric "B". Stiffener fabric "S" pleats into itself and creates a double layer woven structure normal to the base fabric plane. During this movement, heddle frames cross each other and increase the tension of warp yarns as well as the friction between the warp and weft yarns in the fabric, which keeps the closed stiffener in its position. There is a critical level of friction between the warp yarns and weft yarns of the connection section "C". If the friction is too low, the stiffener will be created however it will open up after the reed goes back to its dwelling position. On the other hand if the friction is too high, the beat-up motion of the reed will not be able to move the connection section "C" to the base fabric "B". This will also lead to an uncompleted closure of the stiffener, which is characterized by a triangular stiffener and remaining floating yarns.
- Step IV: Base fabric production continues as in Step I. As the warp yarn consumption of the stiffener part and the floating part are not the same, at least two warp beams are necessary to feed the yarns of the stiffener and floating parts.

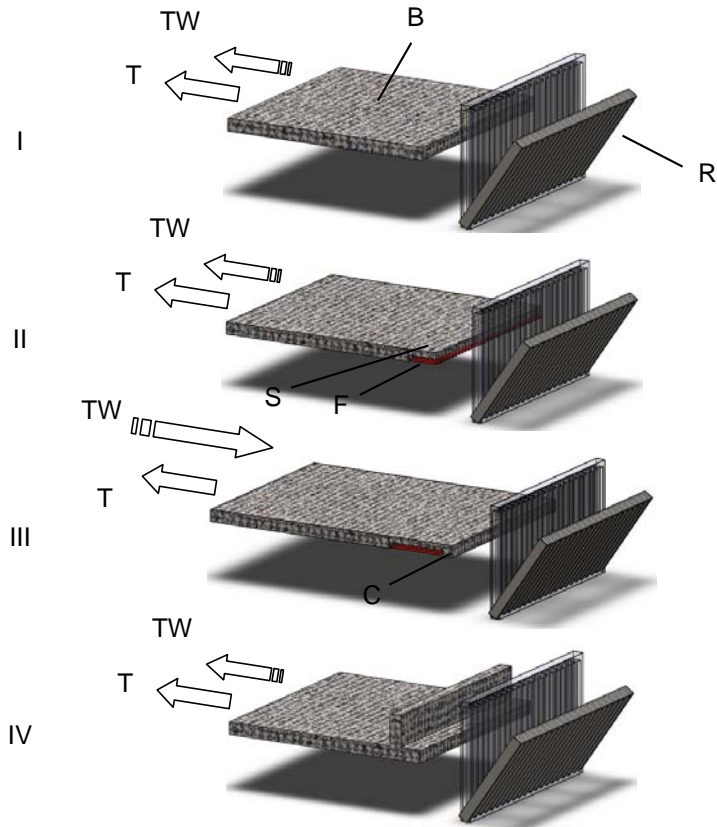


Figure 51: Production principle of terry weaving from side view, B: base fabric, R: reed, S: stiffener fabric, F: floating warp yarns, C: connection between stiffener and floating yarns

The question arises what would be the limitations of structures which can be created by this method. The height of the stiffener is first of all determined by the stroke of the terry weaving mechanism and pull-back mechanisms. For the continuous production, also the length between the fabric creation line and the dwelling position of reed should be considered. This means after moving the still flat stiffener and the floating into the shed as in the step III of figure 51, there should not be a jam and the fabric should in maximum barely touch the reed. If a short production stop can be tolerated, the defined structures can be produced on any weaving machine by turning the take-up and warp beam backwards manually. In this case the fabric can be gradually

delivered into the shed and there is not much limitation for the height of the stiffener. However the reproducibility would be an issue of concern.

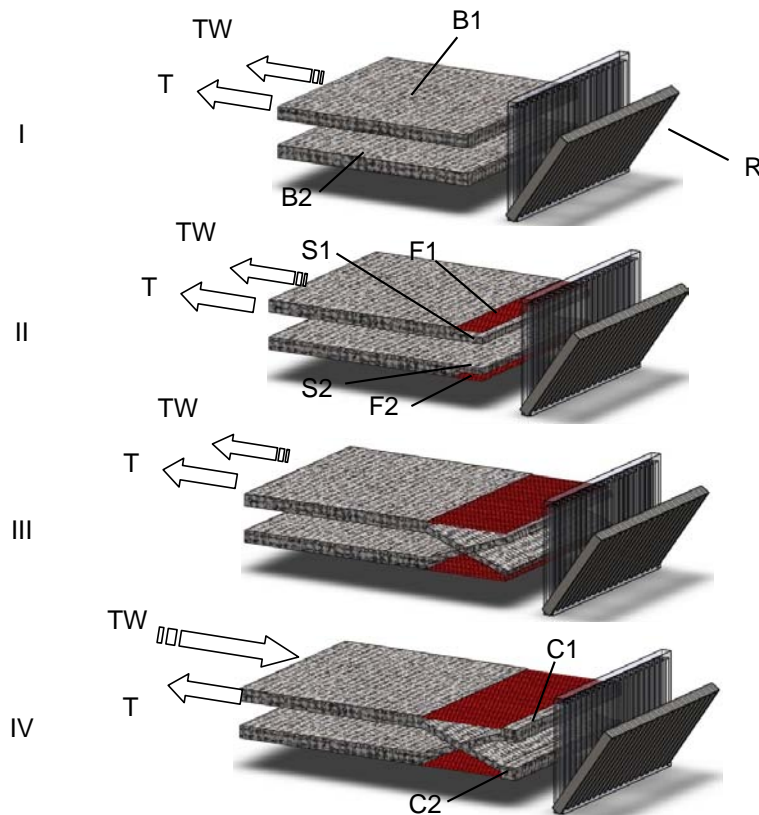
## 6.2 U-shaped Spacer Fabrics

Above defined terry weaving technology can be utilized to produce woven spacer fabrics with woven crosslinks. The connection of the two outer woven fabric layers with crosslinks can be constructed in various ways [21-24, 29, 30]. The following crosslink construction provides higher structural homogeneity and more continuity of reinforcement yarns along the whole structure. Figure 52 demonstrates the production principle of spacer fabrics with woven crosslinks in 5 steps which are:

- Step I: Weaving starts with base fabrics “B1” and “B2” of any kind. These two layers of base fabrics are not connected with each other. In the figure take-up direction “T” is shown with a solid arrow from right to the left near the base fabric. Additional temporary take-up of terry weaving mechanism “TW” is also shown with a dotted solid arrow. Care should be taken that the “TW” and “T” act together and simultaneously both on the “B1” and “B2” layers. Beat-up motion of the reed “R” is shown with a solid and a transparent reed element.
- Step II: When the required position of the stiffener fabrics “S1” and “S2” is reached, the warp yarns of the each base fabrics “B1” and “B2” are divided into two groups. One of the warp yarn groups of each base fabric continues to weave with the inserted weft yarns and creates the stiffener fabrics “S1” and “S2”. The other warp yarn groups do not connect with the weft yarns and create yarn floatings “F1” and “F2” above and under the stiffener fabrics.
- Step III: in order to have continuous reinforcement yarns between the base fabrics, the stiffener fabrics “S1” and “S2” cross each other in the middle of the final crosslink length. After this crossing point, stiffener fabric “S2” continues weaving on top of the stiffener fabric “S1”.
- Step IV: After the required height of crosslink is woven, the floating yarns and the stiffener fabrics are connected again as one layer over a couple of connecting weft yarns “C1” and “C2”. “C1” is the connection of “F1” and “S2”. “C2” is the connection of “F2” and “S1”. In this moment the fabric is still flat. Terry weaving mechanism is activated to move the flat fabric back to the shed.

This sudden motion is demonstrated with a longer dotted arrow "TW" from left to the right. The pull-back mechanism removes the floating yarns "F1" and "F2". Beat-up moves the connection sections "C1" and "C2" to the base fabrics "B1" and "B2". Stiffener fabrics "S1" and "S2" are closed during beat-up and a double layer woven crosslink is created between two woven base fabric layers "B1" and "B2". During this movement, heddle frames cross each other and increase the tension of warp yarns as well as the friction between the warp and weft yarns in the fabric, which keeps the closed stiffener in its position.

- Step V: Weaving continues as defined in the step I. Stiffness of the crosslink between two base fabric layers is not enough to keep its vertical structure, so it will be bent between two base fabric layers.





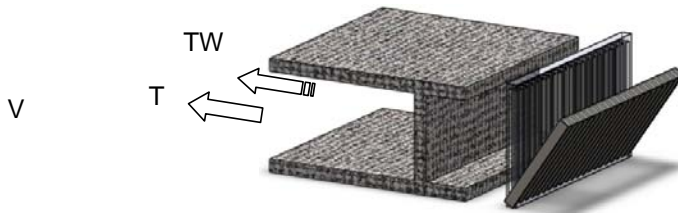


Figure 52: Production principle of U-shaped spacer fabrics, B: base fabric, R: reed, S: stiffener fabric, F: floating warp yarns, C: connection between stiffener and floating yarns

Figure 53 demonstrates the detailed view of the crossing point of crosslinks. There are no connections between the warp yarns coming from the top fabric and the warp yarns coming from the bottom fabric. This kind of weave is advantageous to reduce the joint effect at the crossing point.

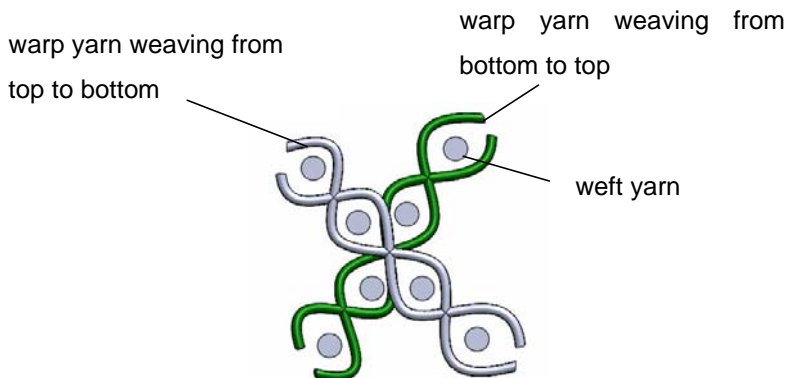


Figure 53: Crosssectional view of the crosslink side change

Figure 54 depicts a weave model of U-shaped spacer fabrics with plain weave along the base and stiffener parts. Different colors represent different yarn systems and it can be obviously seen that the reinforcement is continuous along the structure.

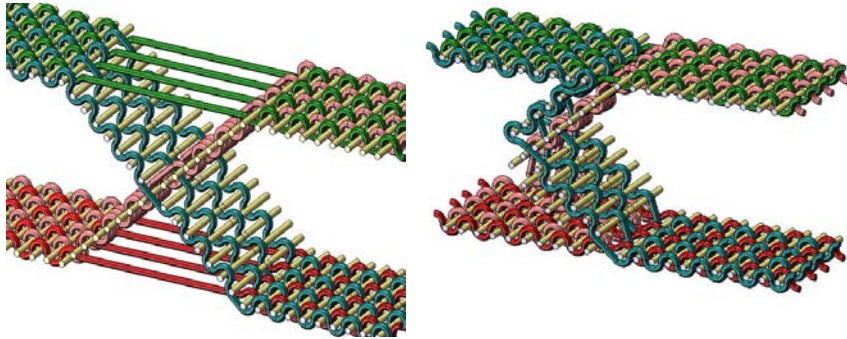


Figure 54: CAD model of a U-shaped spacer fabric

Connections of the crosslink and the base fabrics are critical points concerning the local stresses. In order to round the edges in these connection areas, the weaving structure should be further improved. According to the weaving principle defined in figure 52, woven crosslinks can be produced however they would have sharp edges. To avoid this potential problem, a “rounding weft yarn” is integrated into the very beginning of the floating parts. This means that the floating parts “F1” and “F2” do not begin directly floating after the separation point, but they start with a woven part containing only one weft yarn. The effect of the rounding weft yarn is depicted in figure 55.

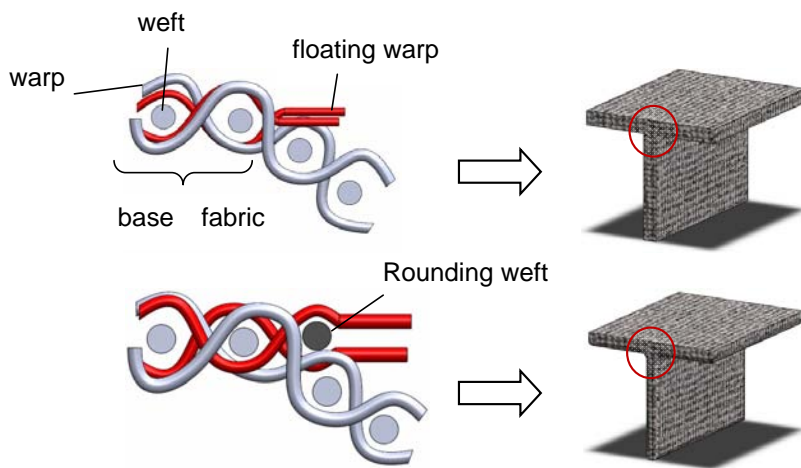


Figure 55: Effect of rounding weft yarn

### 6.3 X-shaped Spacer Fabrics

Above defined production principle for the U-shaped spacer fabric structures are suitable for pure bending. These structures can be extended to further cross-sectional geometries. One of the possibilities is X-shaped spacer fabrics. This cross-section can provide better resistance to shear loading and impact. However, there are some challenges for molding of thermoplastic composites, which are caused by the sharp edges of the profile. The structure would deform during thermo-pressing with sharp edges. Production principle of X-shaped spacer fabrics is similar to that of U-shaped fabrics. There are two differences which are;

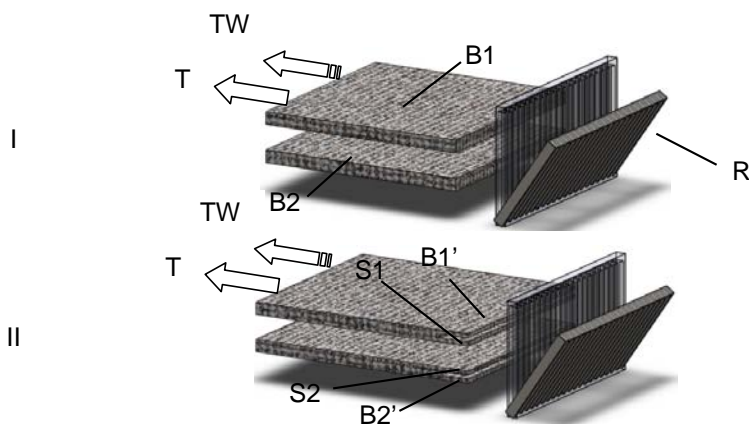
- Beginning parts of the floating yarns are further woven and they create the base parts of upper and lower triangular section of the X-shape.
- The backwards movement of terry weaving mechanism should fit the length of the floating section.

Production steps for X-shaped spacer fabrics are explained below according to the steps in figure 56:

- Step I: Weaving starts with base fabrics "B1" and "B2" of any kind. These two layers of base fabrics are not connected with each other. In the figure take-up direction "T" is shown with a solid arrow from right to the left near the base fabric. Additional temporary take-up of terry weaving mechanism "TW" is also shown with a dotted solid arrow. Care should be taken that the "TW" and "T" act together and simultaneously both on the "B1" and "B2" layers. Beat-up motion of the reed "R" is shown with a transparent and solid reed element.
- Step II: When the required position of the stiffener fabrics "S1" and "S2" is reached, which will be the upper left and lower left edge of the final X shape, the warp yarns of the each base fabrics "B1" and "B2" are divided into two groups. One of the warp yarn groups of each base fabric continues to weave with the inserted weft yarns and creates the stiffener fabrics S1 and S2. The other warp yarn groups also continue weaving and create the B1' and B2' parts.
- Step III: In order to have continuous reinforcement yarns between the base fabrics, the stiffener fabrics "S1" and "S2" cross each other in the middle of the final crosslink length. After this crossing point, stiffener fabric "S2" continues

weaving on top of the stiffener fabric “S1”. After weaving of B1’ and B2’, their warp yarns start floating without any connection with weft yarns as shown in the figure with “F1” and “F2”. Depending on the required dimensions of B1’, B2’ and “S1”, “S2”, crossing of the “S1” and “S2” can take place before or after the B1’ and B2’ parts start floating.

- Step IV: After the required dimension of crosslink is woven, the floating yarns and the stiffener fabrics are connected again as one layer over a couple of connecting weft yarns “C1” and “C2”. In this moment the fabric is still flat. “C1” is the connection of “F1” and “S2”. “C2” is the connection of “F2” and “S1”. Terry weaving mechanism is activated to move the flat fabric back to the shed. This sudden motion is demonstrated with a longer dotted arrow “TW” from left to the right. The pull-back mechanism removes the floating yarns “F1” and “F2”. Beat-up moves the connection sections “C1” and “C2” to the base fabrics B1’ and B2’. Stiffener fabrics “S1” and “S2” are closed during beat-up and an X-shape woven crosslink is created between two woven base fabric layers “B1” and “B2”. During this movement, heddle frames cross each other and increase the tension of warp yarns as well as the friction between the warp and weft yarns in the fabric, which keeps the closed stiffener in its position.
- Step V: Weaving continues as defined in the step I. Stiffness of the crosslink between two base fabric layers is not enough to keep its vertical structure, so it will be bent between two base fabric layers.



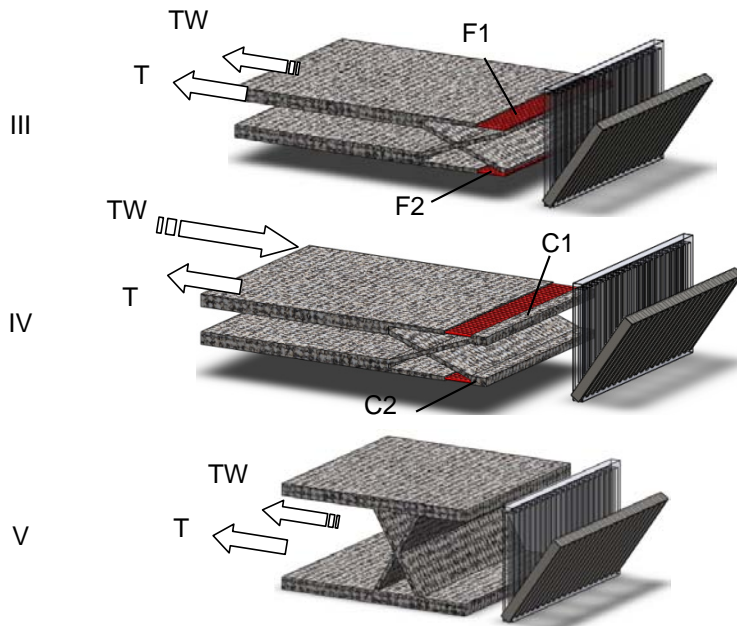


Figure 56: Production principle of X-shaped spacer fabrics, B: base fabric, R: reed, S: stiffener fabric, F: floating warp yarns, C: connection between stiffener and floating yarns

## 6.4 V-shaped Spacer Fabrics

Another basic possibility of cross-sectional profile is the V-shape. In this type, two base layers are connected with upwards and downwards moving diagonal crosslinks [29, 30]. This creates triangular crosslinks, which would be more stable under shear loading compared with U-shaped profiles. However, V-shaped molding for thermoplastic composites has same difficulties as X-shape, which are caused by the sharp edges.

Production steps for V-shaped spacer fabrics are explained below, based on the steps in figure 57:

- Step I: Weaving starts with base fabrics “B1”, “B2” and the stiffener fabric “S” of any kind between base fabrics. These two layers of base fabrics are not connected with each other. In the figure take-up direction “T” is shown with a solid arrow from right to the left near the base fabric. Additional temporary take-up of terry weaving mechanism “TW” is also shown with a dotted solid arrow. Care should be taken that the “TW” and “T” act together and

simultaneously both on the “B1” and “B2” layers. Beat-up motion of the reed “R” is shown with a transparent and solid reed element.

- Step II: When the required position of the connection point between “B1” and “S” is reached, the warp yarns of the base fabrics “B1” and “B2” start floating without any weft insertion. After this point, only stiffener part continues weaving with weft insertion.
- Step III: After the required dimension of crosslink is woven, the floating yarns of “F1” are connected with the stiffener fabric “S” over couple of weft yarns. In this moment the fabric is still flat. “C” is the connection of “F1” and “S”. To keep the same length between upper and lower parts of the preform, lower base fabric “B2” also weaves the same length of “C” before activation of terry weaving. Afterwards terry weaving mechanism is activated to move the flat fabric back to the shed. This sudden motion is demonstrated with a longer dotted arrow “TW” from left to the right. The pull-back mechanism removes the floating yarns “F1” and “F2”. Beat-up moves the connection section “C” and the small part of “B2”. Stiffener fabric “S” is closed during beat-up and one side of the final triangular profile is created between two woven base fabric layers “B1” and “B2”. During this movement, heddle frames cross each other and increase the tension of warp yarns as well as the friction between the warp and weft yarns in the fabric, which keeps the closed stiffener in its position.
- Step IV: Weaving continues as defined in the step I. Stiffness of the crosslink between two base fabric layers is not enough to keep its vertical structure, so it will be bent between two base fabric layers. This time step II and III are necessary to connect the stiffener layer “S” with the lower base fabric “B2”.

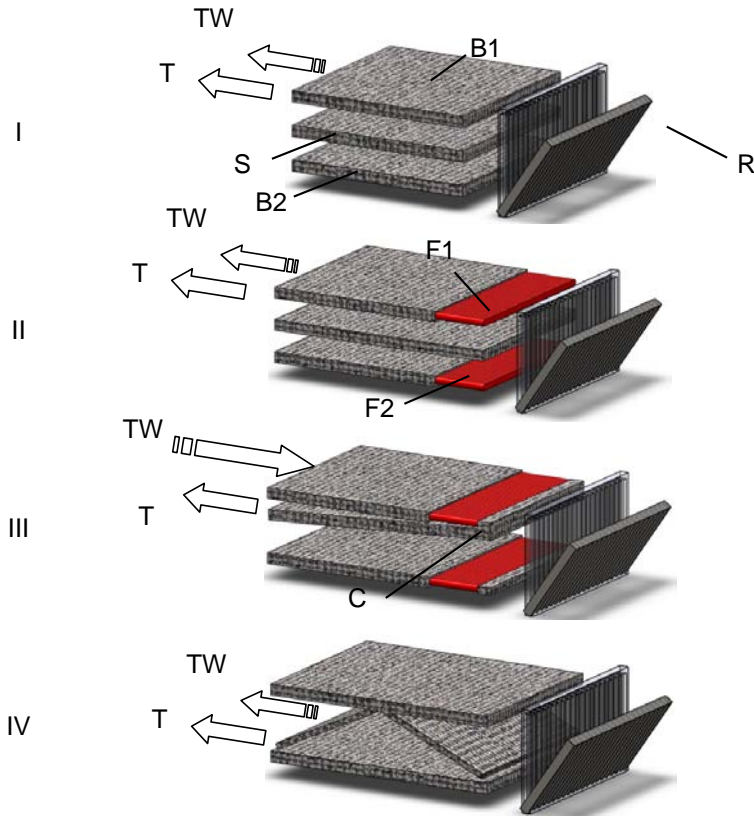


Figure 57: Production principle of V-shaped spacer fabrics, B: base fabric, R: reed, S: stiffener fabric, F: floating warp yarns, C: connection between stiffener and floating yarns

Sandwich composite materials with continuous reinforcement along the structure can be produced with the above described principles. Three basic connection types of crosslinks are called U-, V- and X-shape spacer fabrics. Schematic components with these kinds of crosslinks are demonstrated in figure 58.

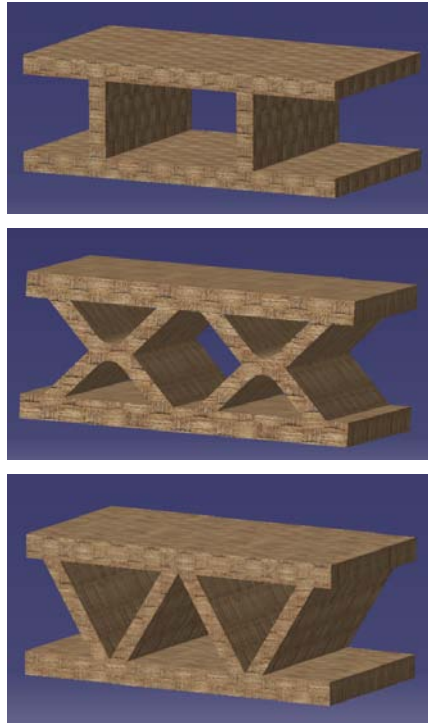


Figure 58: Schematic of sandwich composite components with U-, X- and V-shape spacer fabrics used as preforms

Yarn crimp usually causes reduction of tensile mechanical properties of the final composite component. According to the mechanical characterization of section 5, woven structures without crimp are necessary. 3D orthogonal woven structures yield straight warp yarn weft yarn connected with binding yarns [10]. It is possible to produce these structures with a conventional weaving machine. By using 3D orthogonal weave on the base fabrics, the final thickness of the component is increased and straight integration of reinforcement yarns without crimp is realized. Figure 59 demonstrates the 3D orthogonal weave consisting of 4 warp yarn layers and 5 weft yarn layers connected with binding yarns as well as the U-shaped spacer fabric with this kind of base fabric. It is also possible to create crosslinks with 3D orthogonal weave.



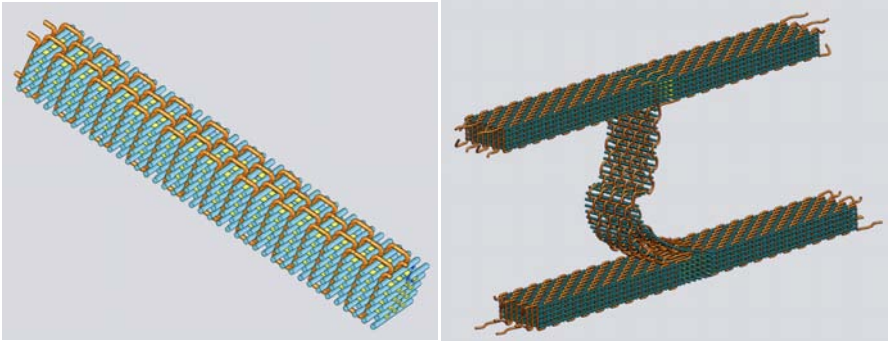


Figure 59: CAD model of orthogonal 3D spacer fabrics (left) and the layer structure of orthogonal 3D woven fabric (right)

## Chapter 7 - Production Principals of Complex Spacer Structures and Stiffeners

In the preceding section, production principles of three fundamental woven connection types (U, X, V) for spacer preforms are described. Another possibility is the use of well-known 3D orthogonal weaves both in the base and stiffener parts. The development of production technology for these basic spacer fabric types with woven crosslinks leads to further implications as well. First of all, heights of the U-, X- and V-shape crosslinks can be varied throughout the structure. Unlike the descriptions above which start with a double or triple layer fabric in Step I, it is possible to start weaving of spacer fabrics from a single layer. Gradually starting single layer can be divided into two separate layers and the whole structure can be woven with increasing and decreasing dimensions of crosslinks. By this method, aerodynamic structures can be produced as shown in figure 60. Lengths of the two base fabrics (upper and lower parts) should be symmetric along the middle axis. Additional take-up devices are necessary to create asymmetric sandwich profiles.

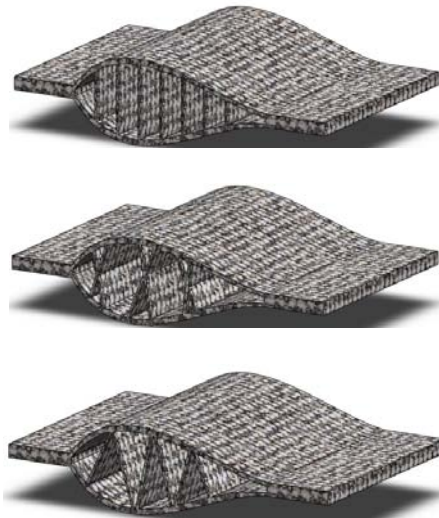


Figure 60: Structures with variable heights of the U-, X- and V-shape crosslinks

## 7.1 Variations of X-shaped Spacer Fabrics

Crossing point of the stiffener parts within the preceding explanations of U- and X-shaped spacer fabrics are exactly in the middle of the final length. Another possibility is to create an asymmetrical crossing point for these structures. Asymmetrical crossing point for U-shaped spacer fabrics would leave either remaining floating yarns or generate a kind of pocket with the longer side of the crosslink. On the other hand, asymmetrical crosslinks for X-shaped spacer fabrics offers the possibility of immediately changing the height of spacer fabrics. Figure 61 demonstrates the change of height by using asymmetric X-shaped crosslinks. According to triangle inequality, the length of part A should be shorter than the sum of the parts B and C. In the limiting condition; length of part A is equal to the sum of part B and C, the triangle disappears and a rectangular chamber with a higher height can be produced, which is also demonstrated in figure 61.

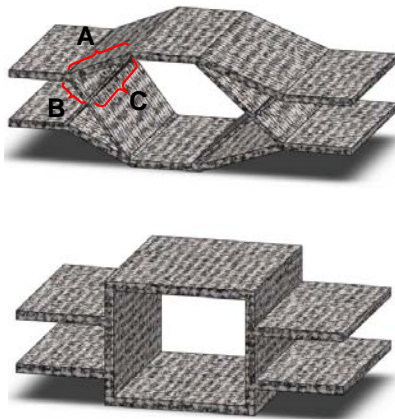


Figure 61: Spacer fabrics with asymmetric X-shaped crosslinks; gradual change of height (top) and immediate change of height (bottom)

Another variation of the X-shape spacer fabrics is shown in figure 62. After the stiffener parts comes together at the crossing point to change their position, two layers of stiffener fabrics can be woven as one layer for a while. This method enables the production of double chamber crosslinks.

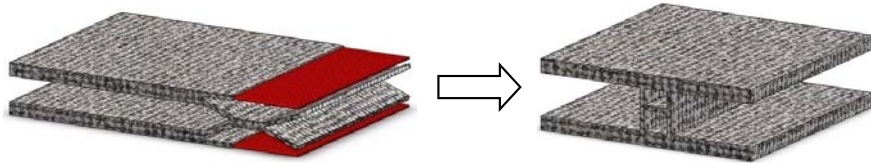


Figure 62: Variation of X-shape spacer fabrics to produce double chamber crosslinks, before pull-back (left) and after pull-back (right)

## 7.2 Preforms for Panels with Integrated Stiffeners

In order to manufacture preforms with integrated stiffeners and structural continuity in one step, terry weaving technique is utilized. Terry weaving is mostly used for weaving of towels with pile yarns standing out-of-plane. Same technique can be used to produce pleats in the normal direction to the main woven surface. Two additional mechanisms are necessary for terry weaving which are temporary storage mechanism and warp yarn pull-back mechanism. At the beginning point of stiffener, warp yarns are divided into two systems, one of them continues weaving while the second system floats without any connection to inserted weft yarns (figure 63 dotted lines). The warp yarns, which are producing the stiffeners and the warp yarns for floating should be fed from separate warp beams. After completing the required stiffener dimensions, two separated warp yarn systems are connected along 2 or 3 weft insertions. Then, temporary storage mechanism moves the fabric immediately backwards in the opposite direction of fabric production while yarn pull-back mechanism removes the floating warp yarns back to the warp beam direction. Beat-up with reed closes the structure and gives its final 3D shape. Increased friction after beat-up and heddle frame crossing avoids the opening of the structure. This technique can be applied continuously with conventional production speed of weaving machines.

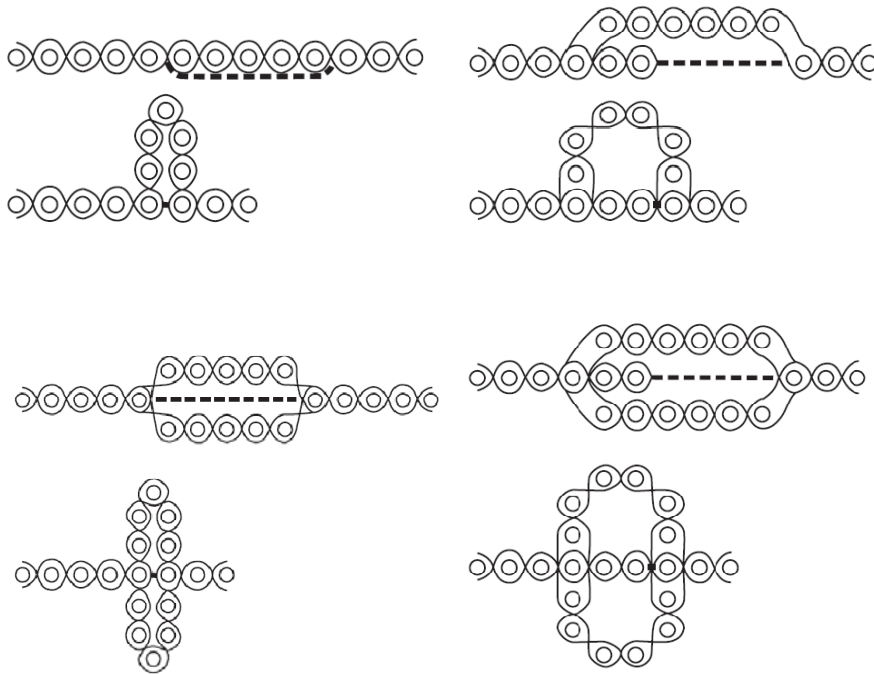


Figure 63: Weaving technique of symmetric and asymmetric stiffener structures; before and after beat-up

The dotted lines in figure 63 represent the floating warp yarns which are pulled back during continuous production. The position of the pulled-back warp yarns are demonstrated with a black dot in the final 3D shape. These dots only show the position of closing, in the actual final structure there is no discontinuity. Figure 64 demonstrates the basic symmetric and asymmetric stiffener structures which can be produced with the same terry weaving system.

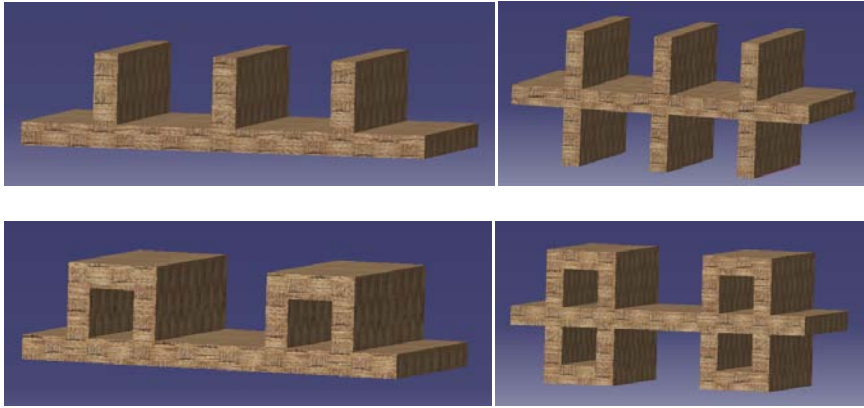


Figure 64: Panel structures with various types of stiffeners

Symmetric stiffener structures of figure 64 can be produced with a double rapier velvet weaving machine VTR-23 of Van de Wiele Belgium. As described above, temporary storage and warp yarn pull-back mechanisms are necessary for terry weaving which are developed and integrated to the conventional weaving machine at ITM (Institute of Textile Machinery and High Performance Material Technology) of Dresden University of Technology. Thick and 3D preforms woven with reinforcement yarns may be damaged and also fluctuations of warp tension may occur if a conventional tangential take-up is used. Therefore, in addition to the mechanisms for terry weaving, a linear take-up system consisting of two roller pairs was developed in cooperation of ITM and IWM (Institute of Machine Tools and Control Engineering) of Dresden University of Technology.

Spacer fabrics with woven cross-links can also have additional out-of-plane stiffeners in one or both direction. Figure 65 demonstrates the production method of such spacer fabrics, which is similar to the method of U-shaped spacer fabrics. The only difference is that the stiffener parts of upper and lower fabrics are again divided into two, one of which stays outer side and generates the out of plane extension of the stiffener.

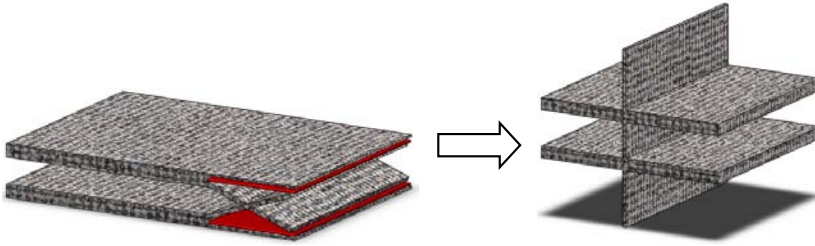


Figure 65: Spacer fabrics with woven cross-links and integrated out of plane stiffeners

If on the weaving machine more than one warp yarn pull-back mechanism is utilized, the stiffener structures can be branched, namely stiffeners can also be freely positioned on other stiffeners as well as base fabric. Figure 66 demonstrates the production steps of multiple stiffeners. Production steps for multiple stiffeners are:

- Step I: Weaving starts with a regular base fabric “B” of any kind. In the figure take-up direction “T” is shown with a solid arrow from right to the left near the base fabric. Additional temporary take-up of terry weaving mechanism “TW” is also shown with a dotted solid arrow. Care should be taken that the “TW” and “T” act together and simultaneously. Beat-up motion of the reed “R” is shown with a transparent and solid reed element.
- Step II: When the required position of the stiffener fabric “S1” is reached, the warp yarns of the base fabric “B” is divided into two groups. One of the warp yarn groups continue to weave with the inserted weft yarns and create the stiffener fabric “S1”. The other warp yarn group however does not connect with the weft yarns and create a yarn floating “F1” under the stiffener fabric. An important aspect is that the stiffener layer is not necessarily always on the top. The positions of stiffener “S” and floating “F” structures are interchangeable.
- Step III: After reaching the position of the secondary stiffener, which will be on top of the primary stiffener, the warp yarns of the primary stiffener layer “S1” are again divided into two groups. One of these groups continues weaving to create the secondary stiffener “S2”, and the other group of warp yarns starts floating as “F2”.

- Step IV: When the required length of the secondary stiffener “S2” is completed, the warp yarns of “S2” and the floating warp yarns of “F2” are connected over a couple of weft yarns. This connecting area for the stiffener is shown as “C2” in the figure. In this moment, the terry weaving mechanism moves the flat fabric back to shed and the pull back mechanism controlling the warp yarns of “F2” removes the remaining length of the yarns. Beat-up of the reed “R” pushes the connecting point “C2” back to the beginning of “S2” and the secondary stiffener “S2” is constructed.
  
- Step V: After completing the secondary stiffener “S2”, weaving process continues in the same way as described in step II. In this step, weaving of the stiffener part “S1” and the floating yarns “F1” still continue.
  
- Step VI: When the final length of stiffener “S1” is reached, the floating yarns “F1” and the stiffener part “S1” are connected over a couple of weft yarns. This connecting area is demonstrated with “C1”. The terry weaving mechanism moves the flat fabric back to shed and the pull back mechanism controlling the warp yarns of “F1” removes the remaining length of the yarns. Care should be taken that only one terry weaving mechanism is sufficient to move the fabric back to the shed. The warp yarn pull-back mechanisms of step IV and VI should be different, because the yarn consumption of “F1” and “F2” are different. Therefore warp yarns of “F1” and “F2” should be fed from different warp beams. Beat-up of the reed “R” pushes the connecting point “C1” back to the beginning of “S1” and the secondary stiffener “S1” is constructed.
  
- Step VII: Now there is one primary stiffener “S1” positioned on the base fabric and one secondary stiffener “S2” positioned on the secondary stiffener “S1”. Weaving continues with any woven structure of base fabric.



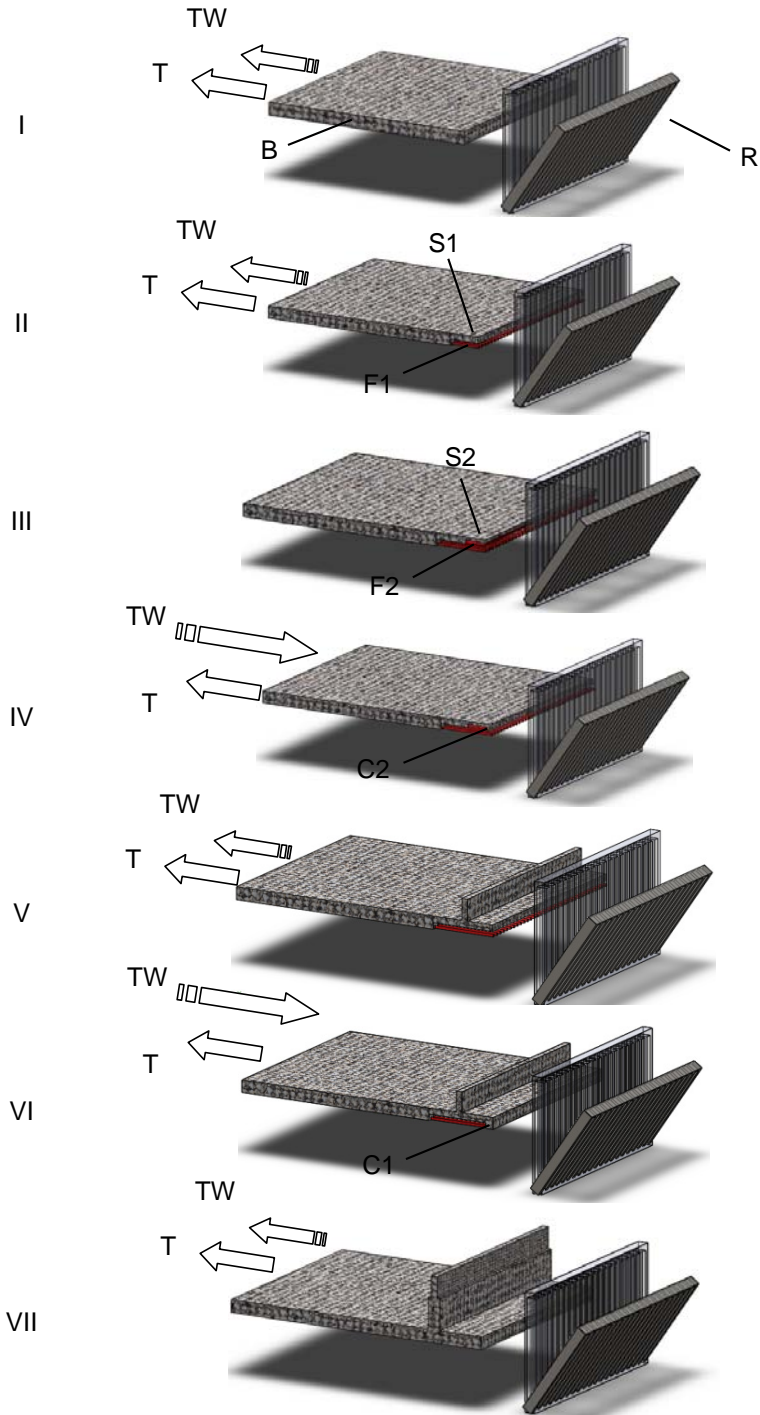


Figure 66: Production method of base fabric containing integrated multiple stiffeners

Figure 66 deals with the simplest type of multiple stiffeners. This technique can be applied to create many different cross-sections. It should be noted that the stiffeners consist of two plied layers, therefore they can be flat as shown in figure 66, but they can also be freely formed into any cross-section with the same circumference. Figure 67 depicts some of the possible multiple stiffener structures. In this figure, I and II are actually the same structures where I uses flat stiffener layers and II demonstrates the free forming of secondary stiffeners "S2" and "S3" into circles. Figure 67-III shows three levels of stiffeners which necessitates three separate warp yarn pull-back mechanism. Figure 67-IV demonstrates the possibility of symmetric structures with two levels of stiffeners.

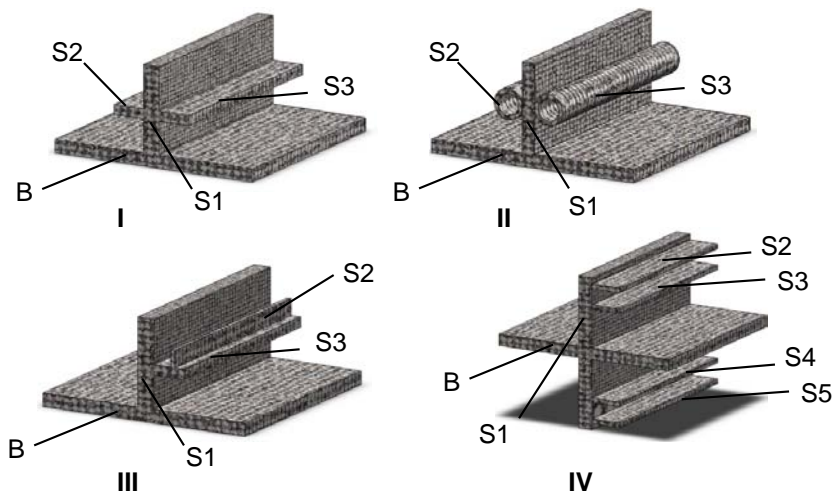


Figure 67: Examples of possible preforms with multiple stiffeners, B: base fabric, S1: primary stiffener, S2-S5: further stiffener layers

## Chapter 8 - Modifications and Realization of Spacer Fabric Weaving Technology

The explained concept of spacer weaving in the preceding section requires the integration of a terry weaving mechanism as well as a warp thread pull back mechanism for the weaving machine. Both additional mechanisms must be synchronized. Figure 68 illustrates the conception of the technology with a modified double rapier face-to-face weaving machine. Terry weaving mechanism works as a temporary storage in the vertical direction. Warp thread pull-back mechanism is responsible for the reverse movement of the floating yarns to close the woven crosslinks between two outer layers. All the other elements defined in the figure are standard elements of a conventional double rapier face-to-face weaving machine.

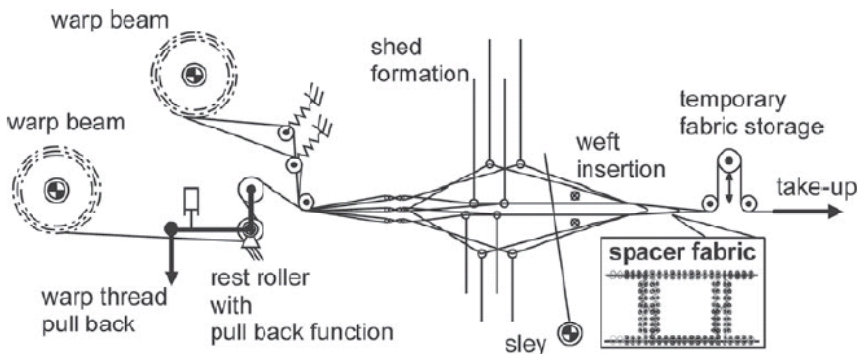


Figure 68: Technological concept of spacer fabric production with terry weaving [61]

### 8.1 Terry Weaving Mechanism

The terry weaving mechanism consists of two subsystems: The warp yarn pull-back system and the fabric storage system. The warp yarn pull-back is carried out from the back rest roller with an additional pneumatic drive (figure 69). There are two functions integrated into the warp yarn pull-back system. One of them is the tensioning of the

warp yarns by pulling the arm in the vertical direction. The second function is to clamp the arm horizontally to keep the warp yarn tension and positions constant. The second function is necessary because during the closing of the cross-links by beat-up, the tension of warp yarns alone is not sufficient. Without clamping of the arm, floating yarns move together with the reed and the cross-link is not fully created.



Figure 69: Warp yarn pull-back mechanism

Temporary fabric storage system is the main part of terry weaving mechanism and acts in synchronization with the pull-back system (figure 70). Fabric storage system has two stationary cylinders which are guiding the fabric out of the shed and one driven cylinder which is temporarily storing a defined fabric length. In every revolution of the machine, a defined length of fabric is stored through the upwards movement of the red colored cylinder in Figure 70 left. After completing the required predetermined length, the warp thread pull-back system puts extra tension on the warp yarns and the fabric storage instantaneously moves the fabric into the shed (counter-take-up direction). This technique closes the yarn floatings and continuously creates a woven crosslink connection normal to the weaving direction without any manual work.

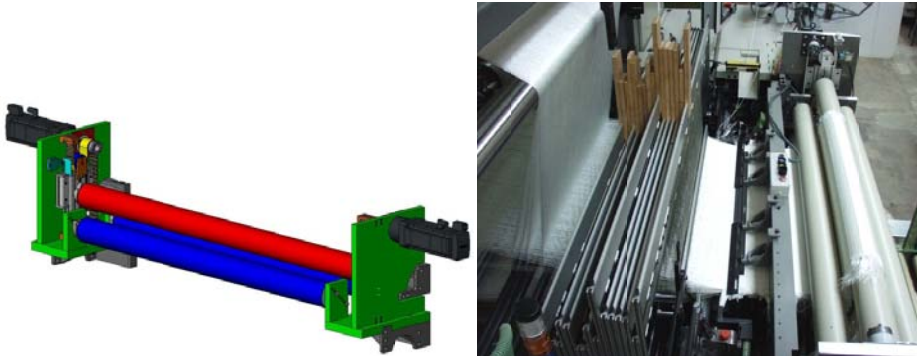


Figure 70: Terry weaving mechanism, CAD concept (left) and application (right) [24]

## 8.2 Linear Take-up System with Cutting and Laying Mechanism

A take-up motion is required for every weaving process which removes the produced fabric with a defined velocity out of the weaving zone. The velocity should be adjustable in order to generate the required weft density. In addition, the take-up force must be in equilibrium with the holdback torque of warp beams and with friction forces in the shed-zone. Usually tangential take-up rolls transmit the velocity and the force to the woven fabrics. The fabrics are wound around the take-up rolls as shown in figure 71. This technology has some disadvantages regarding spacer fabrics with woven crosslinks such as:

- buckling of outer layers and crosslinks in the spacer; hereby exists a risk of glass fiber damage by using conventional tangential take-up system and thus decisively degradation of the mechanical properties of composites
- warp tension variations and reduction of reproducibility caused by the different differential take-up velocity of the inner and the outer layer
- deformation of flexible fabrics; a problem for the handling operations in the next steps of the process chain

Therefore the 3D spacer fabrics should be removed with a linear take-up in the longitudinal direction. A special take-up device with high level of automation is developed in cooperation of ITM and IWM at Dresden University of Technology [61-

63]. This device enables the transmission of take-up forces without buckling and damage of the preform. Slack spacer preforms are quasi solidified with the insertion of supporting bars. The linear take-up motion system is characterized by some straight line arranged roll-pairs. Within every roll-pair one roll can be engaged to the other roll with a defined contact force. In front of the linear take-up motion system a gripper inserts supporting bars in the hollow space of the woven fabrics, a second gripper takes out the bars from the fabrics at the back side of the take-up motion system. Each roller has a servo direct drive. The first roll-pair behind the rapier weaving machine is in closed-loop angle control and with adjustable transmission ratio synchronous to the main shaft of the weaving machine. The transmission ratio is a linear function of the desired weft density in spacer fabric. This results in defined geometry of the woven fabric. The next pair is in closed-loop torque control. The reference values for the torques are precalculated from the average take-up forces. So, the take-up forces are equally partitioned between the roll-pairs.

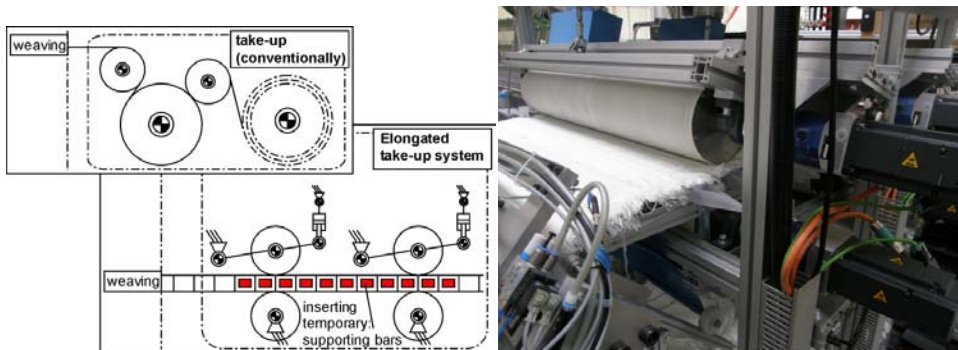


Figure 71: Schematic of conventional and new linear take-up concepts (left) and application of linear take-up [61, 62]

Figure 72 depicts the cutting and laying mechanism integrated at the exit of the take-up system. Necessary numbers of spacer fabric chambers are entered into the controlling unit of the take-up. Numbers of chambers are counted by an inductive counter which determines the final preform length. In the beginning and final chamber of a preform part, supporting bars are not removed. The preform parts are cut between the final chamber of the preceding preform part and the beginning

chamber of the next preform part. Remaining supporting bars inside the preform makes the handling easier.

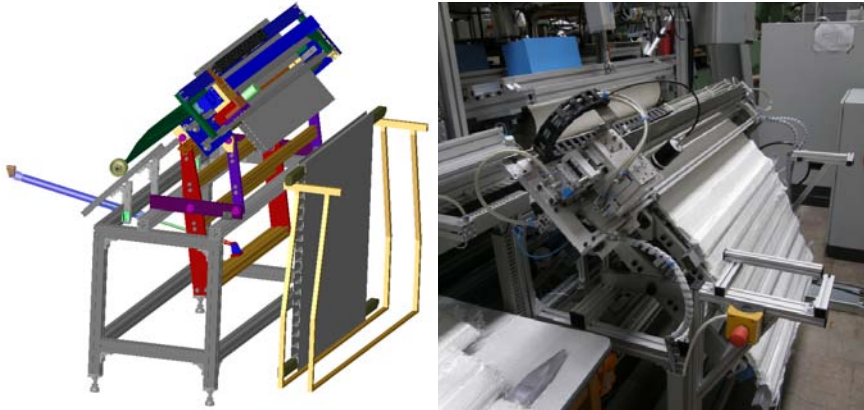


Figure 72: Cutting and laying mechanism, realization (left) and CAD (right) [61, 62]

Integrated ultrasonic cutting device eliminates the manual work and provides automation by cutting the required preform length during weaving. Cutting of preforms with a knife causes loose edges. Ultrasonic cutter consolidates the edges of the preform which is advantageous for further handling (figure 73).

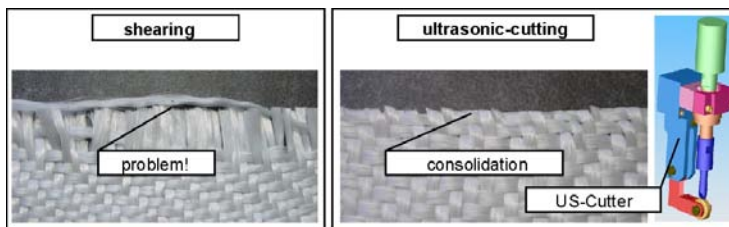


Figure 73: Local consolidation of edges with ultrasonic cutter [61]

### 8.3 Spacer Fabric Production

Reproducible manufacturing of U-shaped woven spacer fabrics is realized with the successful integration and synchronization of face-to-face weaving machine, terry weaving mechanism and linear take-up mechanism. Production width of the weaving

machine is one meter. Figure 74 demonstrates the dimensions and a close view of weaving zone during production of spacer fabrics. Woven cross-links are not stiff enough to keep the distance therefore after the cross-link formation, they are plied between two outer layers.

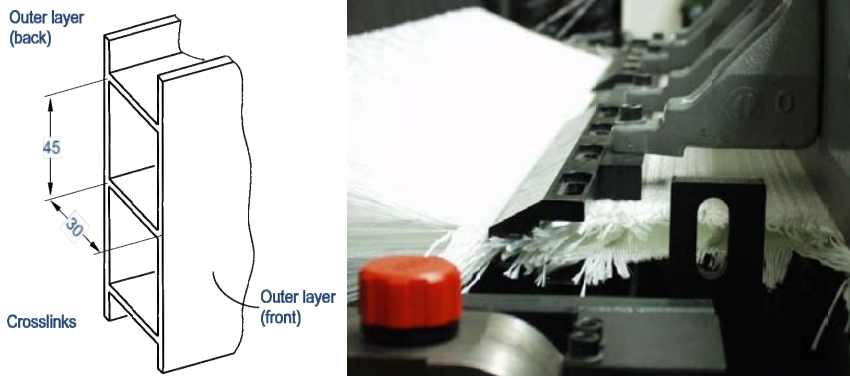


Figure 74: Spacer fabric production: Dimensions (left) and close view of weaving zone (right)

Figure 75 depicts the development steps of spacer fabrics, from CAD model to consolidated thermoplastic matrix sandwich composite. Laboratory size hot-pressing machine (COLLIN P300 PV, Dr. Collin GmbH, Germany) is used for pressing of spacer preforms into sandwich composite parts. Dimensions of the sample are 180 mm x 230 mm with 30 mm height. Special tools are designed by the Institute of Solid Mechanics at Dresden University of Technology [64].



Figure 75: U-shaped spacer fabric from concept to sandwich composite; CAD (left), woven preform (middle), composite (right)



A sandwich composite with higher dimension of 900 mm x 900 mm is pressed at the Institute of Lightweight Engineering and Plastic Technology (ILK) at Dresden University of Technology. Figure 76 demonstrates the produced composite component. With the integration of hot-press station after the weaving process, required dimensions of sandwich composite components can be produced with a high level of automation.



Figure 76: Sandwich composite component from spacer fabrics

## Chapter 9 - Conclusion and Outlook

Achieving energy efficiency and reduction of CO<sub>2</sub> emission belong to the main challenges of governments and research institutions in the 21st century. Increased use of renewable energy sources alone is not sufficient to achieve the ambitious objectives of the governments. Simultaneously, novel production methods should be developed which yield high automation level, minimum number of production steps and high reproducibility.

In composite industries, simple shaped parts have been already produced with automated systems. However, complex shaped composite structures are still being produced with mostly manual work. Extra production steps for tailoring and connecting these parts not only significantly increases the production costs, but also the product quality and the energy efficiency is decreased.

Woven preforms are mainly used as the textile reinforcement for composite structures. Therefore integrated 3D near-net-shape woven preforms are very important to extend the use of composites and to reach energy efficiency both during the production process and end use of the components.

Automated industrial size production of woven spacer fabrics with woven crosslinks are realized within the scope of this dissertation. Analysis of the 3D woven structures brings insights about the possible yarn interlacings and their effects on the mechanical properties of the final component. Concerning the effect of yarn interlacing, the expression which determines the possible woven structures for two weft yarn blocks is derived. Further research is necessary to understand the pattern of symmetry and multiple weft yarn blocks.

Commingled hybrid yarns are necessary to mix the reinforcement and thermoplastic matrix materials in solid state, which enables the significant reduction of process cycle time for consolidation. However, commingled process makes the input materials voluminous which causes production problems with textile machinery. Slightly twisting of commingled yarns enables compacter yarn structures with less variation of diameter and less coefficient of friction. Therefore twisted commingled hybrid yarns can be applied in the case of high density preform production, especially if the open structure of commingled yarns cause production stops.

Increasing of weft density also increases the crimp on the yarn. The tensile and bending properties are significantly affected by the increase of yarn crimp. Impact energy however increases with the increasing sample thickness and no direct relation between yarn crimp and the impact energy is identified. In order to minimize the yarn crimp, 3D orthogonal weave is used on the base fabrics.

Terry weaving mechanism is used to produce woven surfaces normal to the carrier woven fabric. This technique is applied to develop the fundamental connection types of U-, X-, and V-shaped spacer fabrics. Terry weaving technique can be applied to produce complex preforms such as spacer fabrics with variable crosslink heights and panels with integrated stiffeners. If the weaving machine has multiple warp yarn pull-back mechanisms, it is possible to construct multiple layers of stiffeners. Stiffeners are two layer plied fabrics which can be freely formed into required cross-section.

A conventional double rapier face-to-face weaving machine is modified in order to realize the industrial scale production of complex preforms in various shape and geometry of spacer fabrics. Modification of existing machinery is advantageous and flexible for wide spread application of preform production. Terry weaving and warp yarn pull-back mechanisms with their controlling units are developed which enables the closing of floating yarns and creating woven structures normal to the carrier fabric. Linear take-up system is necessary to remove a 3D structure out of the weaving zone without causing deformation and tension differences on the preforms. A tailored linear take-up system with supporting rollers is developed. Exit of the take-up system includes cutting and laying mechanism which provides automated preparation and delivery of required preforms into the molding station.

Within the scope of this dissertation, 9 layer 3D orthogonal fabrics are used in the base fabric. As future work, machine setting should be changed to apply the non-crimp structures also in the stiffener part. Curved spacer fabrics are necessary to fit the contours of a composite component. Additional take-up system should be applied to compensate the length difference of upper and lower base fabrics, which is caused by the curvature. In order to understand and control the complex interactions of the weaving machine and the applied modifications, it is necessary to simulate the yarn tension behavior during the process.

As mentioned in the section V-shaped spacer fabrics, it is a challenge to develop a tool to press the sharp edge of a V-shape connection. On the other hand, the connection part of the V-shape spacer fabric can be extended to create a trapezoid cross-section. This type of spacer fabrics can be consolidated in compression molding and they offer higher shear resistance compared to the U-shaped structured.

An edge component can also be created by omitting one of the base fabrics in a spacer fabric chamber. The spacer fabric structure can be plied around the missing base fabric and a perpendicular edge connection can be produced.

Weft yarn selection and jacquard shed opening system can be combined to realize connections of inductive yarns within the spacer fabric structures. Copper or carbon yarns can be integrated into the preform during weaving process. By this way, sensor networks for structural health monitoring can be created without additional process steps.

## Appendix: Advantage of Sandwich Materials

The cross-sections of many beams and frameworks are in the forms of I-, T- beams or channel bars. These shapes afford better resistance to bending with a minimum amount of material and weight. Lightweight construction has two dimensions, one of which is using light materials in the overall structure, the other one is to have optimized geometries tailored to the application and the stress fields. Figure A1 demonstrates two rectangular plates as reference to compare the advantage of sandwich construction. Figure A1-i has the wall thickness of  $2.552h$  which is selected to compare a U-shaped sandwich material with two walls each of the thickness  $h$  and a crosslink with a width of  $h$  and a height of  $8h$ . Figure A1-ii has the thickness of  $3.104h$  to compare a V-shaped sandwich material with two walls each of the thickness  $h$  and a crosslink with a width of  $h$  and a height of  $8h$ .

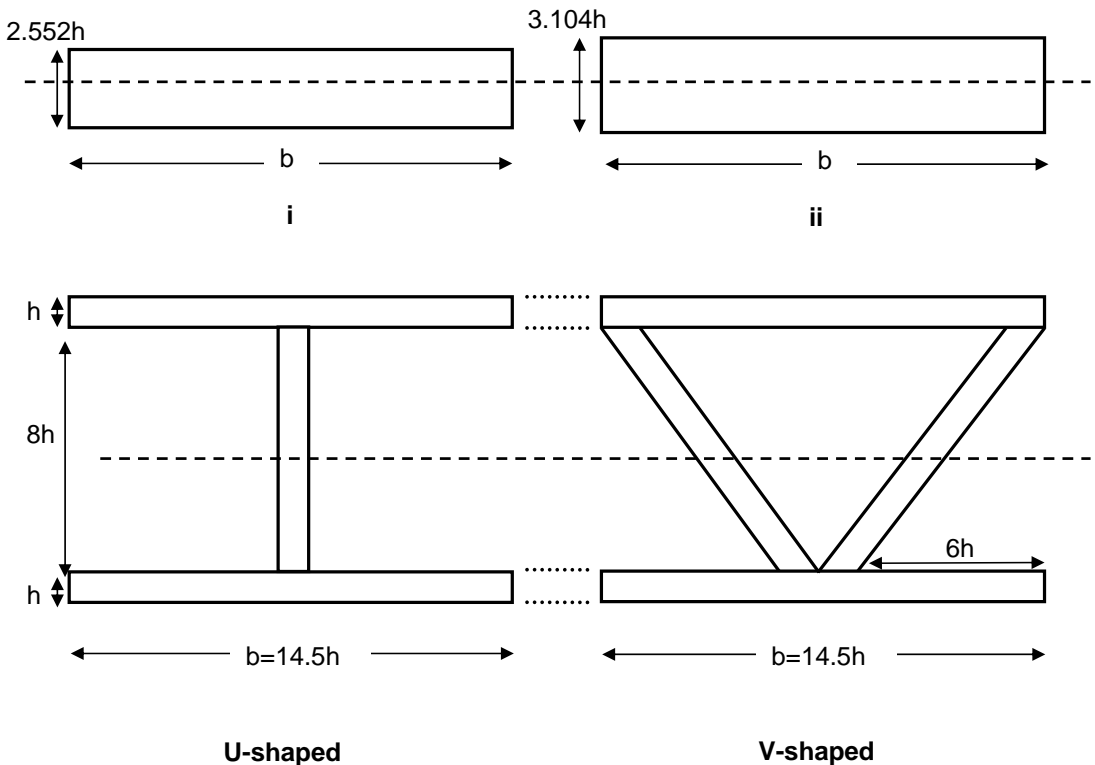


Figure A1: Cross-sections of panels; with  $2.552 h$  thickness (i) and  $3.104 h$  thickness (ii); Cross-sections of unit cells for composites from U-shaped and V-shaped spacer fabrics

The equations 1 and 2 give the amount of the second moment of the area which can be regarded as the resistance to bending.

$$I_i = 1.385bh^3 \quad (1)$$

$$I_{ii} = 2.492bh^3 \quad (2)$$

Cross-section of unit cells for the composites from U-shaped and V-shaped spacer fabrics are demonstrated in figure A1 with corresponding dimensions to compare with the panels. X-shaped spacer fabrics have very similar values to V-shape therefore they are not included into this analysis. I-profile in figure A1 is the unit cell of a sandwich composite from U-shaped spacer fabrics. In order to fully define the geometry of the V-shaped cross-section, the width  $b$  of is arbitrarily selected as  $14.5h$ .

The second moment of area for the U-shape is calculated as:

$$I_U = 632.333h^4 \quad (3)$$

The second moment of area for the V-shape is calculated as:

$$I_V = 696.333h^4 \quad (4)$$

If the expression  $b$  for width is changed to  $14.5h$  in the equations 1-4, it is possible to compare the bending stiffness of U-shaped and V-shaped sandwich structures with the rectangular panels which have the same amount of material respectively.

	2.552h panel	U-shape	3.104h panel	V-shape
second moment of area normalized with the panels separately	1	31.487	1	19.271

Table A1: Comparison of sandwich and panel structures with same amount of material

## List of Figures

Figure 1: Schematic of the evolution of engineering materials [1] .....	1
Figure 2: Specific tensile strength of common structural materials [6].....	4
Figure 3: Specific tensile modulus of common structural materials [6] .....	4
Figure 4: Tendency of composite use in aviation [7].....	5
Figure 5: Structural change of plain woven fabrics due to warp (black) and weft (grey) tensions; slack warp (A) and tight warp (B).....	11
Figure 6: Classification of reinforcements [10].....	13
Figure 7: Woven spacer fabric [13].....	14
Figure 8: Warp knitted spacer fabric [14].....	15
Figure 9: Circular weft knitted spacer fabric [17].....	15
Figure 10: Flat weft knitted spacer fabrics [19] .....	16
Figure 11: Production steps of V-shaped weft knitted spacer fabrics [20, 21] .....	17
Figure 12: Weft knitted spacer fabrics with knitted cross-links [20, 21].....	17
Figure 13: Modified narrow weaving machine [21] .....	18
Figure 14: U-shaped narrow woven spacer fabrics from PES yarns. Flat structure without pulling-back of floating yarns (left), final spacer fabric after pulling-back of floating yarns (right) [21] .....	18
Figure 15: Examples of I-beam and T-beam stiffener structures used in aerospace applications (above) and their internal structure of fabric plies (below) where different color means separate layers [32] .....	20
Figure 16: Stiffener structures for aerospace applications (above) and schematic of stacked fabric layers (below) where different color means separate layers [32] .....	20
Figure 17: Production techniques of hybrid yarn [24] .....	22
Figure 18: Weave representation of a plain woven fabric (left) and actual positioning of warp (black color) and weft (white color) yarns (right) .....	24
Figure 19: Weave for double layers of separate plain woven fabrics.....	26
Figure 20: Elements of weave for double layers of separate plain woven fabrics.....	26
Figure 21: Side-view of double layers of separate plain woven fabrics .....	27
Figure 22: Two equivalent representations of plain woven fabrics .....	28

Figure 23: Side-view of patterns with two warp yarns and two weft yarns. Floating of warp yarns without forming a woven structure (left), plain woven structure (right) .....	29
Figure 24: Possible structures with 2 weft yarn layers, 2 weft yarn columns and 3 warp yarns .....	31
Figure 25: Subtraction blocks to determine the woven structures with 4 warp yarns SW4 .....	32
Figure 26: Symmetries of the woven structure 51243 .....	35
Figure 27: Algebraic operations to determine the x symmetry (I & II) and y symmetry (III & IV) of a given woven structure.....	36
Figure 28: Representations of the symmetries of 51243 on Cartesian coordinate plane .....	38
Figure 29: Air-jet texturizing machine utilized for commingled yarn production (left) and detail view of the air nozzle (right).....	42
Figure 30: Processing parameters for compression molding of UD-composite plates .....	43
Figure 31: Cross-sectional observations of bulky (A-A) and knot (B-B) areas of GF/PP commingled yarns .....	45
Figure 32: Comparison of GF/PP commingled yarn profile, from top to bottom; reference commingled yarn, 10tpm, 20tpm, 40tpm, 60tpm.....	46
Figure 33: Effect of twisting on the diameter of GF/PP commingled yarns .....	47
Figure 34: Effect of twisting on yarn-yarn and yarn-metal friction of GF/PP commingled yarns.....	48
Figure 35: Yarn structure and model for determining the E-modulus of commingled yarns.....	49
Figure 36: Equivalent angle distortion caused by over-delivery of reinforcing material .....	51
Figure 37: Effect of twisting on E-modulus and breaking force of GF/PP commingled yarns.....	54
Figure 38: Distribution of E-modulus parts; difference between theoretical and measured modulus values .....	55
Figure 39: Modulus of elasticity and tensile strength of UD composites from GF/PP commingled yarns in 0° .....	59



Figure 40: Modulus of elasticity and tensile strength of UD composites from GF/PP commingled yarns in 90°.....	60
Figure 41: X-twill weave (left) L: lower weft yarn, U: upper weft yarn, and woven fabric (right) .....	63
Figure 42: Schematic of shed opening .....	65
Figure 43: Change of yarn tensile strength after beaming and weaving.....	66
Figure 44: Tensile strength of woven fabrics with different weft densities .....	67
Figure 45: Composite surfaces with weft densities of 7 to 10 from left to right .....	67
Figure 46: Modulus and tensile strength of 1 layer consolidated fabrics in warp direction (left) and weft direction (right) .....	68
Figure 47: Modulus and tensile strength of 2 layer consolidated fabrics in warp direction (left) and weft direction (right) .....	68
Figure 48: Modulus and tensile strength of 3 layer consolidated fabrics in warp direction (left) and weft direction (right) .....	69
Figure 49: Flexural strength of 2 and 3 layer consolidated fabrics in warp and weft direction.....	69
Figure 50: Impact strength of 2 and 3 layer consolidated fabrics in warp and weft direction.....	70
Figure 51: Production principle of terry weaving from side view, B: base fabric, R: reed, S: stiffener fabric, F: floating warp yarns, C: connection between stiffener and floating yarns .....	73
Figure 52: Production principle of U-shaped spacer fabrics, B: base fabric, R: reed, S: stiffener fabric, F: floating warp yarns, C: connection between stiffener and floating yarns .....	76
Figure 53: Crosssectional view of the crosslink side change.....	76
Figure 54: CAD model of a U-shaped spacer fabric .....	77
Figure 55: Effect of rounding weft yarn.....	77
Figure 56: Production principle of X-shaped spacer fabrics, B: base fabric, R: reed, S: stiffener fabric, F: floating warp yarns, C: connection between stiffener and floating yarns .....	80
Figure 57: Production principle of V-shaped spacer fabrics, B: base fabric, R: reed, S: stiffener fabric, F: floating warp yarns, C: connection between stiffener and floating yarns .....	82

Figure 58: Schematic of sandwich composite components with U-, X- and V-shape spacer fabrics used as preforms .....	83
Figure 59: CAD model of orthogonal 3D spacer fabrics (left) and the layer structure of orthogonal 3D woven fabric (right).....	84
Figure 60: Structures with variable heights of the U-, X- and V-shape crosslinks.....	85
Figure 61: Spacer fabrics with asymmetric X-shaped crosslinks; gradual change of height (top) and immediate change of height (bottom).....	86
Figure 62: Variation of X-shape spacer fabrics to produce double chamber crosslinks, before pull-back (left) and after pull-back (right).....	87
Figure 63: Weaving technique of symmetric and asymmetric stiffener structures; before and after beat-up .....	88
Figure 64: Panel structures with various types of stiffeners.....	89
Figure 65: Spacer fabrics with woven cross-links and integrated out of plane stiffeners .....	90
Figure 66: Production method of base fabric containing integrated multiple stiffeners.....	92
Figure 67: Examples of possible preforms with multiple stiffeners, B: base fabric, S1: primary stiffener, S2-S5: further stiffener layers .....	93
Figure 68: Technological concept of spacer fabric production with terry weaving [61] .....	94
Figure 69: Warp yarn pull-back mechanism .....	95
Figure 70: Terry weaving mechanism, CAD concept (left) and application (right) [24] .....	96
Figure 71: Schematic of conventional and new linear take-up concepts (left) and application of linear take-up [61, 62].....	97
Figure 72: Cutting and laying mechanism, realization (left) and CAD (right) [61, 62].....	98
Figure 73: Local consolidation of edges with ultrasonic cutter [61].....	98
Figure 74: Spacer fabric production: Dimensions (left) and close view of weaving zone (right) .....	99
Figure 75: U-shaped spacer fabric from concept to sandwich composite; CAD (left), woven preform (middle), composite (right).....	99
Figure 76: Sandwich composite component from spacer fabrics.....	100

## List of Tables

Table 1: Development of possible structures S and the woven structures SW according to the number of warp and weft yarns .....	33
Table 2: Symmetry groups of woven structures.....	34
Table 3: Distribution of woven structure according to the symmetry groups.....	37
Table 4: Relation between weft density and mass per unit area.....	64
Table 5: Thicknesses of consolidated woven fabrics .....	64

## Bibliography

- [1] ASTRÖM, B.T.: *Manufacturing of Polymer Composites*. Nelson Thornes Ltd, Cheltenham, 2002
- [2] TONG, L. ; MOURITZ, A.P. ; BANNISTER, M.K.: *3D Fibre Reinforced Polymer Composites*. Elsevier Science Ltd, Oxford, 2002
- [3] DFG: Collaborative Research Centre (SFB) 639: Textile-reinforced composite components for function-integrating multi-material design in complex lightweight applications. In: <http://www.tu-dresden.de/mw/ilk/sfb639/>, 06.11.2010
- [4] KAW, A.K.: *Mechanics of Composite Materials*. Taylor & Francis, Boca Raton, 2006
- [5] HULL, D. ; CLYNE, T. W.: *An Introduction to Composite Materials*. Cambridge University Press, Cambridge, 1996
- [6] <http://www.azom.com/Details.asp?ArticleID=962>, 12.08.2009
- [7] HERMANN, A. ; EBERTH, U.: Textilien für die Flugzeugstruktur - Stand der Technologie und Herausforderungen. In: *44. Internationale Chemiefasertagung, Dornbirn*, 21.-23.9.2005
- [8] DOSTAL, J.A.: *Engineered Materials Handbook Vol. 1 Composites*. ASM International, Metals Park, Ohio, 1987
- [9] ASHBY, M. ; SHERCLIFF, H. ; CEBON, D.: *Materials Engineering, Science, Processing and Design*. Butterworth-Heinemann, Oxford, 2007
- [10] HU, J.: *3-D Fibrous Assemblies*. Woodhead Publishing Ltd., Cambridge, 2008
- [11] STOBBE, D. ; MOHAMED, M.: 3D Woven Composites: Cost and Performance Viability in Commercial Applications. In: *Proceedings of 48th International SAMPE Symposium and Exhibition*, Long Beach, CA, 11-15.05.2003
- [12] MIRAVETE, A.: *3-D Textile Reinforcements in Composite Materials*. Woodhead Publishing Ltd., Cambridge, 1999

- [13] <http://www.parabeam.nl>, 10.12.2010
- [14] [http://www.baltex.co.uk/technical\\_textiles.html](http://www.baltex.co.uk/technical_textiles.html), 10.12.2010
- [15] MACHOVA, K.: *Abstandstextilien als Kaminsystem für Sport- und Outdoor-Bekleidung*, Technische Universität Dresden, Dissertation, 2007
- [16] ANAND, S.: Spacers – At the Technical Frontier. In: *Knitting International*. 110(1305), pp. 38-41, 2003
- [17] [http://www.mayercie.de/docs/586\\_Prospekt\\_e\\_Maerz\\_09.pdf](http://www.mayercie.de/docs/586_Prospekt_e_Maerz_09.pdf), 22.11.2010
- [18] ABOUNAIM, M.: Process development for the manufacturing of flat knitted innovative 3D spacer fabrics for high performance composite applications. Dresden, Technische Universität Dresden, Dissertation, 2011
- [19] CHERIF, CH. ; DIESTEL, O. ; TRÜMPER, W. ; SACHSE, C.: *IGF-Forschungsvorhaben Nr. 15580 BR, Formgerechte 3D-Abstandsflachgestricke für orthopädische Produkte*, Institute of Textile Machinery and High Performance Material Technology TU Dresden, 01.03.2008 – 30.06.2010
- [20] ÜNAL, A. ; HOFFMANN, G. ; CHERIF, CH.: Development of weft knitted spacer fabrics for composite materials. In: *Melliand English Textilberichte 87-4*, pp. E49-E50, 2006
- [21] TORUN, A.R. ; HOFFMANN, G. ; ÜNAL, A.; KLUG, P. ; CHERIF, CH. ; BADAWI, S.: Technologische Lösungen zur Entwicklung von spacer fabrics mit Flächenstrukturen als Abstandshalter - Technological solutions to the development of spacer fabrics including fabric structures. In: *CD-Rom und Kurzreferateband. 8. Dresdner Textiltagung*, Dresden, 21.06. - 22.06.2006., pp. 56-59
- [22] CHERIF, CH. ; RÖDEL, H. ; DIESTEL, O. ; HOFFMANN, G. ; HERZBERG, C. ; TORUN, A.R.: Development of innovative spacer preforms for function integrated composite production. In: *CD-Rom. 7th World Textile Conference AUTEX 2007*, Tampere (Finland), 26-28.06.2007
- [23] TORUN, A.R. ; HANUSCH, J. ; DIESTEL, O. ; HOFFMANN, G. ; CHERIF, CH.: Verstärkte, gewirkte Preforms und Abstandsgewirke sowie gewebte Abstandsgewirke aus gemischten Hybridgarnen für verstärkte Kunststoffe /

- Reinforced weft-knitted preforms and spacer fabrics as well as woven spacer fabrics made of commingled hybrid yarns. In: *14. Techtexil Symposium, Frankfurt*, 12.-14.06.2007
- [24] TORUN, A.R. ; HOFFMANN, G. ; ÜNAL, A. ; CHERIF, CH.: Spacer fabrics from hybrid yarn with fabric structures as spacer. In: *CD-Rom. ICCM16, Kyoto (Japan)*, 8-13.07.2007
- [25] ABOUNAIM, M.: Process development for the manufacturing of flat knitted innovative 3D spacer fabrics for high performance composite applications. Technische Universität Dresden, Dissertation, 2011
- [26] ABOUNAIM, M. ; DIESTEL, O. ; HOFFMANN, G. ; CHERIF, CH.: High performance thermoplastic composite from flat knitted multi-layer textile preform using hybrid yarn. In: *Composites Science and Technology* 71(2011), pp. 511-519
- [27] ABOUNAIM, M. ; DIESTEL, O. ; HOFFMANN, G. ; CHERIF, CH.: Thermoplastic composites from curvilinear 3D multi-layer spacer fabrics. In: *Journal of Reinforced Plastics and Composites* 29(2010)24, pp. 3554-3565
- [28] ABOUNAIM, M. ; HOFFMANN, G. ; DIESTEL, O. ; CHERIF, CH.: Development of flat knitted spacer fabrics for composites using hybrid yarns and investigation of two-dimensional mechanical properties. In: *Textile Research Journal* 79(2009)07; pp. 596-610
- [29] TORUN, A.R. ; BADAWI, S.S. ; HOFFMANN, G. ; KLUG, P. ; CHERIF, CH.: Neue Band-Gewebe als spacer fabrics / New narrow woven spacer fabrics. In: *Band- und Flechtindustrie* 43(2006)2, pp. 27-29
- [30] BADAWI, S.S.: Development of the Weaving Machine and 3D Spacer Fabrics Structures for Lightweight Composites Materials. Technische Universität Dresden, Dissertation, 2007
- [31] JUNHOU, P. ; SHENOI R.A.: Examination of key aspects defining the performance characteristics of out-of-plane joints in FRP marine structures. In: *Composites, PartA* 1996, 27A, pp. 89-103

- [32] Picture taken during the exhibition at ICCM 16 in Kyoto Japan. Courtesy of Kado Corporation and Japan Aerospace Exploration Agency (JAXA)
- [33] RAMPANA, B. ; TIRELLI, D. ; CHERIF, Ch. ; PAUL, Ch. ; TORUN, A.R. ; DIESTEL, O. ; KUHLMANN, U.: *Tire Having A Structural Element Reinforced with a Hybrid Yarn* – WO/2009/052844
- [34] MÄDER, E. ; ROTHE, C. ; GAO, S.-L.: Commingled yarns of surface nanostructured glass and polypropylene filaments for effective composite properties. In: *Journal of Materials Science* 42 (2007) pp. 8062-8070
- [35] MÄDER, E. ; ROTHE, C. ; BRÜNIG, H. ; LEOPOLD, T.: Online spinning of commingled yarns - equipment and yarn modification by tailored fibre surfaces. In: *Key Engineering Materials* 334-335 (2007) pp. 229-232
- [36] MÄDER, E. ; ROTHE, C.: Tailoring of commingled yarns for effective composite properties. In: *Chemical Fibers International* 56 (2006) pp. 298-300
- [37] <http://www.ocvreinforcements.com/solutions/Twintex.asp>, 03.02.2011
- [38] OFFERMANN, P. ; DIESTEL, O. ; CHOI, B.-D. ; CF-PEEK Commingled yarns for textile reinforced light weight rotors – situation and development perspectives. In: *Chemical Fibers International* – Frankfurt, 52 (2002), pp. 258
- [39] CHOI, B.D.: Entwicklung von Commingling-Hybridgarnen für faserverstärkte thermoplastische Verbundwerkstoffe. Technische Universität Dresden, Dissertation, 2005
- [40] TORUN, A.R. ; HOFFMANN, G. ; MOUNTASIR, A. ; CHERIF, CH.: Effect of Twisting on Mechanical Properties of GF/PP Commingled Hybrid Yarns and UD-Composites, In: *Journal of Applied Polymer Science*, 2011, in print
- [41] LORD, P.R.; RUST, J.P.: Fibre Assembly in Friction Spinning. In: *Journal of the Textile Institute*, No.4, 1982, pp. 465-478
- [42] FEHRER, E.: Friction spinning: The State of the Art. In: *Text. Month, Sept.*, 1987, pp. 115-116
- [43] SAKAGUCHI, M. ; NAKAI, A. ; HAMADA, H. ; TAKEDA, N.: The mechanical properties of unidirectional thermoplastic composites manufactured by a

- micro-braiding technique. In: *Composites Science and Technology* Volume 60, Issue 5 (2000), pp. 717-722
- [44] TORUN, A.R. ; TANAKA, Y. ; NAKAI, A.: Effect of CF wetting properties, PP viscosity and production parameters on the impregnation quality of UD compression molded composites from micro-braided yarns, In: *Japan Material Conference*, Kyoto, 27.10.2010
- [45] GU, P. ; GREENWOOD, K.: The scope for Fabric Engineering by means of the Weave, In: *Journal of the Textile Institute* 77 (1986), pp. 88-103
- [46] CLAPHAM, C.R.J.: When a Fabric Hangs Together, In: *Bulletin of the London Mathematical Society* 12 (1980), pp. 161-164
- [47] GRÜNBAUM, B. ; SHEPHARD, G.C.: Isonemal Fabrics. In: *American Mathematical Monthly*. 95 (1988), pp. 5-30
- [48] DAWSON, R. M.: Enumeration and Identification by Elimination of Weave Families of Given Repeat Size. In: *Textile Research Journal*. 70(4) (2000), pp. 304-310
- [49] CHEN, X. ; POTIYARAJ, P.: CAD/CAM of Orthogonal and Angle-Interlock Woven Structures for Industrial Applications. In: *Textile Research Journal*. 69(9) (1999), pp. 648-655
- [50] ADVANI, S.G. ; SÖZER, E.M.: *Process Modeling in Composite Manufacturing*. Marcel Dekker, New York, 2003
- [51] OFFERMANN, P. ; WULFHORST, B. ; MÄDER, E.: Hybridgarne für neuartige Verbundwerkstoffe aus Thermoplasten. In: *Technische Textilien/Technical Textiles - Frankfurt*, 38(1995)2, pp. 55-57
- [52] BERNET, N. ; MICHAUD, V. ; BOURBAN, P.-E. ; MANSON, J.-A. E.: Commingled yarn composites for rapid processing of complex shapes. In: *Composites, Part A* 32, (2001), pp. 1613-1626
- [53] BOURBAN, P.-E. ; BERNET, N. ; ZANETTO, J.-E. ; MANSON, J.-A. E.: Material phenomena controlling rapid processing of thermoplastic composites In: *Composites, Part A* 32, (2001), pp. 1045-1057



- [54] SUBRAMANIAM, V. ; NATARAJAN, K. S.: Frictional Properties of Siro Spun Yarns. In: *Textile Research Journal* (1990), 60 (4), pp. 234-239.
- [55] RAO, Y. ; FARRIS, R.J.: A modeling and experimental study of the influence of twist on the mechanical properties of high-performance fiber yarns. In: *Journal of Applied Polymer Science* (2000), 77, pp. 1938-1949.
- [56] HADLEY, D.W. ; PINNOCK, P.R. ; WARD, I.M.: Anisotropy in oriented fibres from synthetic polymers. In: *Journal of Material Science* (1969), 4, pp. 152-165
- [57] ESHELBY, J. D.: The determination of the elastic field of an ellipsoidal inclusion and related problems. In: *Proceedings of the Royal Society* 1957, A241, pp. 376-396
- [58] ESHELBY, J. D.: The elastic field outside an ellipsoidal inclusion. In: *Proceedings of the Royal Society* 1959, A252, pp. 561-569
- [59] HYER, M.W.: *Stress Analysis of Fiber-Reinforced Composite Materials*. MyGraw-Hill, 1998
- [60] HALPIN, J.C. ; TSAI, S.W.: *Air Force Materials Laboratory Technical Report 1967*, AFML-TR-67, pp. 423
- [61] GROSSMANN, K. ; MÜHL, A.; LÖSER, M. ; CHERIF, CH. ; HOFFMANN, G. ; TORUN, A.R.: New solutions for the manufacturing of spacer preforms for thermoplastic textile-reinforced lightweight structures. In: *Production Engineering Research & Development*, pp. 589-597
- [62] MÜHL, A. ; GROSSMANN, K. ; OFFERMANN, P. ; LÖSER, M.: Neuartiges Abzugs-, Schneid und Stapelsystem für das Weben von spacer fabrics, A new take-up-motion, cutting and storing system for weaving of spacer fabrics. In: *CD-ROM 8. Dresdner Textiltagung*, 21.-22.6.2006
- [63] MÜHL, A. ; LÖSER, M. ; GROSSMANN, K. ; HOFFMANN, G. ; KLUG, P. ; CHERIF, CH.: Abzugs-, Schneid- und Stapelsystem für das Weben von Abstandsstrukturen. In: *Melliand Textilberichte* 87(2006)11/12, pp. 810-812
- [64] LIN, S. ; MODLER, KH. ; HANKE, U.: The application of mechanisms in producing textile-reinforced thermoplastic composite. In: *Journal of Mechanical Design & Research* 24 (2008), Nr. 4, pp. 380

---

## **Neue Fertigungstechnologie für 3D profilierte Preforms auf Webbasis**

Textile 3D-Halbzeuge besitzen ein großes Potenzial zur Steigerung der mechanischen Eigenschaften von Verbundwerkstoffen sowie zur Reduzierung der für ihre Herstellung notwendigen Produktionsstufen und -kosten. Die Vielfalt der webtechnisch realisierbaren Strukturen ist unendlich. Durch die Algorithmen der konventionellen Bindungsnotation lässt sich die Vielfalt der möglichen Gewebestrukturen nur begrenzt ermitteln. Die im Rahmen der Dissertation neu entwickelte Bindungsnotation erlaubt die analytische Entwicklung von Gewebestrukturen. Technologische Lösungen zur reproduzierbaren Preformherstellung mit Hybridgarnen wurden erarbeitet. Die Faltenwebtechnik ist durch die Möglichkeit der vertikalen Verbindungen auf einem Trägergewebe für die Herstellung komplexer Profile geeignet. Die Faltenwebtechnologie wurde mittels einer elektronisch gesteuerten Gewebespeichereinheit sowie einem pneumatischen Kettfadenrückzugssystem an einer Doppelgreifer-Webmaschine umgesetzt. Verschiedene spacer fabrics und 3D-Profile wurden entwickelt. Zur reproduzierbaren und schonenden Halbzeugfertigung wurde ein linearer Abzug entwickelt und umgesetzt. Durch die in die Webanlage integrierten Schneid- und Ablagesysteme wurde ein hoher Automatisierungsgrad erreicht.

## ***Advanced manufacturing technology for 3D profiled woven preforms***

*3D textile preforms offer a high potential to increase mechanical properties of composites and they can reduce the production steps and costs as well. The variety of woven structures is enormous. The algorithms based on the conventional weaving notation can only represent the possible woven structures in a limited way. Within the scope of this dissertation, a new weaving notation was developed in order to analyze the multilayer woven structures analytically. Technological solutions were developed in order to guarantee a reproducible preform production with commingled hybrid yarns. Terry weaving technique can be utilized to create vertical connections on carrier fabrics, which makes it suitable for the development of complex profiles. A double rapier weaving machine was modified with electronically controlled terry weaving and pneumatic warp yarn pull-back systems. Various spacer fabrics and 3D profiles were developed. A linear take-up system is developed to assure reproducible preform production with a minimum material damage. Integrated cutting and laying mechanisms on the take-up system provides a high level of automation.*